8-13-2015

Synthesis and Characterization of Copolyesters Based on Vanillic Acid or Syringic Acid and Dodecanedioic Acid

Michael E. Bloom

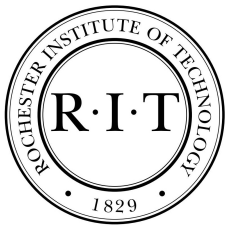

Synthesis and Characterization of Copolyesters Based on Vanillic Acid or Syringic Acid and Dodecanedioic Acid

A Thesis Submitted in Partial Fulfillment of the Requirements for the Degree of Master of Science in Materials Science & Engineering

Rochester Institute of Technology
School of Chemistry and Materials Science
College of Science
Rochester, NY 14623-5603

Michael E. Bloom

13 August 2015

Signature Page

Approved by:

Dr. Massoud J. Miri Signature_____
Associate Professor, Chemistry
Thesis Advisor

Dr. John-David R. Rocha Signature_____
Assistant Professor, Physical Chemistry

Dr. Gerald A. Takacs Signature_____
Professor, Chemistry

Dr. Thomas A. Trabold Signature_____
Associate Professor and Director, Center for Sustainable Mobility

Copyright Release

Synthesis and Characterization of Copolyesters Based on Vanillic Acid or Syringic Acid and Dodecanedioic Acid

I, Michael E. Bloom, hereby grant permission to the Wallace Memorial Library of the Rochester Institute of Technology to reproduce my thesis, in whole or in part, given that any reproduction will not be for commercial use or profit.

_____ _____

Michael E. Bloom MM/DD/YYYY

Dedication

Tara

Mom said that I was the column of support that our family leans upon...

You are my foundation.

Abstract

Incorporating renewable monomers derived from vanillic acid (VA) and syringic acid (SyA) into a polymer system will, in addition to reducing the amount of non-renewable feedstock necessary, alter the physical properties of the resultant polymer so that it can be better tailored to suit a specific need. First, a catalyst to optimize melt polymerization of 1,4-diacetoxybenzene (HQ), 4-acetoxybenzoic acid (BA), and dodecanedioic acid (DA) was determined. Acetylation of VA and SyA was necessary to produce compatible monomers. Then, two series of polymers based on HQ, BA, DA, and acetylated vanillic acid (AVA) or acetylated syringic acid (ASyA) were prepared by melt polycondensation. The polymers were characterized by proton nuclear magnetic resonance imaging (^{1}H NMR), Fourier transform infrared spectroscopy (FTIR), polymer end-group titration (PEGT), thermogravimetric analysis (TGA), differential scanning calorimetry (DSC), and gel permeation chromatography (GPC). Changes in the amount and form of methoxy moieties, from the incorporation of AVA and ASyA, altered the thermal properties of the copolyester which could be applied to the development of better tailored products. The resulting aromatic/aliphatic copolyesters are resistant to typical organic solvents.

List of Figures

1.2.1 Depiction of Lignin 8

2.2.1 System Diagram. 15

3.1.1 ^{1}H NMR Catalyst Study Composite 26

3.1.2 IR Catalyst Study Composite 27

3.1.3 GPC Catalyst Study Composite 29

3.1.4 DSC Catalyst Study Composite 31

3.1.5 TGA Catalyst Study Composite 32

3.2.1 ^{1}H NMR of AVA 33

3.2.2 ^{1}H NMR of ASyA 34

3.2.3 IR Spectrum of AVA 34

3.2.4 IR Spectrum of ASyA 35

3.2.5 ^{1}H NMR AVA Study Composite 37

3.2.6 ^{1}H NMR ASyA Study Composite 39

3.2.7 IR Spectra of AVA Series 40

3.2.8 IR Spectra of ASyA Study 40

3.2.9 GPC AVA Study Composite 41

3.2.10 GPC ASyA Study Composite 42

3.2.11 DSC AVA Study Composite 45

3.2.12 DSC ASyA Study Composite 46

3.2.13 TGA AVA Study Composite 47
3.2.14 TGA ASyA Study Composite 48

B.0.1 MWD of P-1 . . . . . B2
B.0.2 MWD of P-2 . . . . . B2
B.0.3 MWD of P-3 . . . . . B3
B.0.4 MWD of P-4 . . . . . B3
B.0.5 MWD of P-5 . . . . . B4
B.0.6 MWD of P-6 . . . . . B4
B.0.7 MWD of P-7 . . . . . B5
B.0.8 MWD of P-8 . . . . . B5
B.0.9 MWD of P-9 . . . . . B6
B.0.10 MWD of P-10 . . . . . B6
B.0.11 MWD of P-11 . . . . . B7
B.0.12 MWD of P-12 . . . . . B7

C.0.1 TGA of P-1 . . . . . C2
C.0.2 TGA of P-2 . . . . . C3
C.0.3 TGA of P-3 . . . . . C4
C.0.4 TGA of P-4 . . . . . C5
C.0.5 TGA of P-5 . . . . . C6
C.0.6 TGA of P-6 . . . . . C7
C.0.7 TGA of P-7 . . . . . C8
C.0.8 TGA of P-8 . . . . . C9
C.0.9 TGA of P-9 . . . . . C10
C.0.10 TGA of P-10 . . . . . C11
C.0.11 TGA of P-11 . . . . . C12
C.0.12 TGA of P-12 . . . . . C13

List of Schemes

1.1 Selection of Monomers. 11
1.2 General Polymerization 12
2.1 AVA Synthesis 18
2.2 ASyA Synthesis 19

List of Tables

3.1 Catalyst Study Inputs 25

3.2 ^{1}H NMR Data for Catalyst Study 27

3.3 DSC Data for Catalys Study 30

3.4 TGA Values for Catalyst Study 32

3.5 Renewable Study Inputs 36

3.6 ^{1}H NMR Data for Renewable Study 38

3.7 DSC Data for Renewable Study 43

3.8 TGA Values for Renewable Study 47

A.1 End-Group Titration Data A1

B.1 GPC Data B1

Acknowledgments

So many people helped me get to where I now stand. Any person who was part of developing or troubleshooting LaTeX2e and the various packages; this would be nearly impossible without you. Random thanks go around Gosnell to the many professors who choose not to go home at reasonable hours and who were willing to let me ask a few questions; there is nothing more confusing than not being the only person in the building, nor why you would take time to answer the questions of what is arguably a mad man. An assortment of thanks are distributed in the Chem Lounge; you kept my food cold and my level of sanity relatively consistent. Many thanks go to both of the Smiths who should have been on my committee; you were perhaps the two most helpful people on campus. A special thank you for Dr. K.S.V. for attending my proposal; without you I would have been off to a terrible start. Several thanks are also being distributed to my actual committee; especially for tolerating my ridiculous time-frame and often tangential references. Thank you Dr. Rocha, Dr. Takacs, and Dr. Trabold.

...and of course Dr. Miri; a massive thank you is in order for this wonderful opportunity.

Nicht alle, die sich wundern, sind verloren.

ᛗᛁᚲᛗᛚ·ᛗ:ᛒᚴᚢᛗ

Contents

List of Figures v

List of Schemes vii

List of Tables viii

1 Introduction 1

1.1 Reason for Research 1

1.1.1 Environmental Challenges 2

1.2 Background Concepts 3

1.2.1 Green vs. Sustainable 3

1.2.2 Condensation Polymerization 6

1.2.3 Lignin and Derivatives 7

1.2.4 Pendant Moieties and Their Effects on Crystalline Systems . . 7

1.3 Previous Research 9

1.3.1 Review of Related Literature 10

1.3.2 Preliminary Laboratory Experiments 11

1.3.3 Selected Polymerization 11

2 Experimental 13

2.1 Materials 13

2.2 General Synthesis 14

2.3 Synthesis of AVA 17
2.4 Synthesis of ASyA 18
2.5 Procedures for Characterization 19
2.5.1 General Characterization 19
2.5.2 Thermal Characterization 22

3 Results and Discussion **24**
3.1 Catalyst Study 24
3.1.1 Catalyst Study Polymer Synthesis 24
3.1.2 Catalyst Study Polymer Characterization 25
3.2 Effect of Renewable Aromatic Monomer Study 33
3.2.1 Renewable Monomer Characterization 33
3.2.2 Renewable Study Polymer Synthesis 36
3.2.3 Renewable Study Polymer Characterization 37
3.3 Solution Polymerization Experiment 49

4 Conclusions **50**

5 Suggestions for Future Work **51**

Glossary **52**

Acronyms **55**

Bibliography **58**

A PEGT Data **A1**

B GPC Data **B1**

C TGA Data **C1**

D Preliminary Series **D1**

E A Note on the Document **E1**

1. Introduction

1.1 Reason for Research

The development of a polymer fully or in part derived from natural resources was the primary driving force behind the initial research in this thesis. The incorporation of renewable monomers can create a greater demand for plant-based, and even more generally, biobased chemicals for use in plastic goods, but can also alter characteristics of the resultant material. Biobased chemicals may have similar structures to petrochemicals, yet could contain moieties that may impart steric hindrances or functionalities leading to potentially desirable characteristics. These characteristics are the crux of this thesis; by varying renewable monomers in a copolymer, melting temperature (T_m), crystallization temperature (T_c), and glass transition temperature (T_g) can be altered, resulting in specialty tailored polymers which could, in part, reduce dependency on petrochemicals.

By increasing the amount of renewable content in a polymer there would naturally be a reduction in the amount of the non-renewable content; which is generally petroleum-based. While this partially renewable polymer is not truly sustainable, it is a generally "greener" polymer. Since the structure of the renewable monomer may be different than that of the non-renewable monomer, it stands that the effects may also be different. Creating a direct substitute renewable monomer identical to the displaced petroleum monomer should have no effect, however there may not be new and desirable properties obtained from this change.

1.1.1 Environmental Challenges

Consumer and commercial demand on products puts a stress on the market which in turn puts a stress on the resources used to develop the goods and services. Plastics commonly derived from non-renewable resources are increasing in use to the point that they have become ubiquitous.[1] These plastics are the most common form of polymeric materials with which a typical consumer is familiar. Polymers are macromolecules which are formed by the repeating of smaller units, monomers. Many consumers view these products as cheap, determinant but disposable, persistent yet inferior, simultaneously safe and harmful, as well as common yet unnatural. Conflicting views create mixed opinions about the products and materials collectively known as "plastic" however that has little impact on the increasing demand for their use.

Demand for petroleum-based polymers is high and likely will increase.[1] The boom in the production of petroleum lead to an increase in the production of petrochemicals, and from the laws of supply and demand, created low-cost feedstocks that could be developed into commodity plastics. These low-cost products permeated the market to such a degree that consumers became dependent upon them. Needless to say, plastics are found in medical equipment, sanitation, emergency/disaster relief, personal protective equipment and numerous other facets of peoples' lives; it is literally everywhere. This created a large presence of these materials and a stable market that is resistant to a dramatic change. Consumers simply require these products and the market around them poses entry barriers as well as exit barriers.

As products wear, age, or otherwise outlive their functions, they generally find their ways to a metaphorical waste bin. The result is a constant need for plastics, since there is an ever present need to dispose of them and continual replacement. Plastic, or more specifically polymer, has a remarkable property: it is deceivingly robust on a chemical level; to the point that it will persist in most "waste bins" that

it lands in. Landfills are filling with plastics at alarming rates.[2] Recycling facilities can handle some of the materials, but the cost of recovery is often greater than the price of virgin-sourced material, especially taking quality and purity into consideration.[3] Most plastics cannot be composted since they are not biodegradable. Newer polymers are being developed that can biodegrade, however they are still niche and receive mixed views as they are increasingly entering the waste streams.[1,3,4]

An alternative approach to address environmental challenges is to look at the birth or beginning-of-life as opposed to the end-of-life. Materials traditionally derived from petrochemical sources can be produced from biomass sources.[5,6] However, it can sometimes be cost prohibitive to have a drop-in replacement for many of these chemicals due to the low cost of oil competing with the costs from the amount of processing necessary for biomass.[8] Yet using biomass from a waste stream used to procure familiar chemicals as well as develop newer ones while addressing the disposal of the biomass itself does have an environmental appeal. As a result, co-generation plants have been suggested as a possible means to reduce the cost in the production of plant-based chemicals and other products in what culminates in a biorefinery. Lignin and cellulose are two of the most abundant sources of biomass available; lignin, in particular, can yield many desirable chemicals which can be produced fairly easily and cheaply.[9]

1.2 Background Concepts

1.2.1 Green vs. Sustainable

Resources, both renewable and non-renewable, are crucial for the production of polymeric materials. In 2010, the United States used roughly 2.7 % of the liquid petroleum, 1.7 % of the natural gas, and 1.7 % of the total electrical energy consumed for the production of "plastics".[10] While plastics are not a major drain on oil, petroleum itself

is a non-renewable resource, has associated health concerns, and has an impact on the price of petroleum derived consumer goods. A growing consumer and governmental demand calling for alternatives to petroleum for goods and materials has lead to a "green movement."[1] The market has seen an influx of products with terms such as "green," "sustainable," and "renewable" meant to appeal to consumers who are conscious about the green movement; which is not necessarily a negative trend, but might be considered greenwashing.[11,12] Each of the terms has a specific meaning that is expanded upon in the glossary.

Creating a completely renewable polymer, or sustainable polymer, is an ideal undertaking. Coca-Cola developed PlantBottle®, a poly(ethylene terephthalate) (PET) bottle containing up to 30 % plant-based content. PET is made of the same type of polymer found in common beverage bottles, however the monomers from which it was derived for the PlantBottle® are from not petroleum-based sources.[13] While this is an example of how petroleum-based monomers can be replaced either fully or in part by renewable, plant-based feedstocks, Coca-Cola has also been accused of greenwashing,[14] which was later refuted.[15] Future polymers eschewing petrochemicals may not necessarily be limited to the main classes defined by the ever present recycling codes however the approach of having drop-in replacements might ease the transition from petroleum based to more plant based alternatives from a materials processing perspective. A large portion of plastic (81 %)[2] does not or cannot enter the recycling system, mainly due to incompatibility with other plastic, contamination, lack of infrastructure, high cost, or simple neglect.[1] Many of these polymers are often specifically tailored for a given task (e.g., coatings, thermal barriers) which can have narrow ranges of tolerances and working conditions. Creating polymers that fall into this category, which are fully or in part renewable, is important for the future.

One of the more notable contributions to the so called "green movement" is the introduction of the "Green Principles" by Anastas and Warner, listed below with a brief description of the meaning.[1,16]

1. **Prevention** It is better not to create waste than to create it.
2. **Atom Economy** Efficient use of materials; a maximum amount of the inputs are in the final product.
3. **Less Hazardous Synthesis** The employment of non-toxic or low-toxicity methods in the synthesis of chemicals.
4. **Design Safer Chemicals** The end product should also be non-toxic or have low-toxicity.
5. **Safer Solvents & Auxiliaries** Minimization and generally safer solvents should be used.
6. **Design for Energy Efficiency** Synthesis and processing should not be energy intensive.
7. **Use of Renewable Feedstocks** Raw materials should come from sources that can be maintained at a rate comparable to consumption.
8. **Reduce Derivatives** Use fewer steps and aim for fewer byproducts.
9. **Catalysis** Strive to use catalysis instead of stoichiometric reagents to drive reactions.
10. **Design for Degradation** The material should not decompose into harmful components.
11. **Real-Time Analysis for Pollution Prevention** A proactive approach, not a reactive approach, to the manufacture, processing, and disposal of materials is desirable.

12. **Inherently Safer Chemistry for Accident Prevention** Minimizing risks of fire, explosion, toxicity, etc. in the synthesis and processing of materials.

The above guidelines were set in place to facilitate the discussion of how to create a better approach to chemistry, and is referenced here to bring to attention that there are several approaches that can be taken to reach a more green end product. However, these principles are not quantitative nor are they rigorously defined, and as a result should only be used as a qualitative comparison of an improvement or regression of a process or product. A life-cycle assessment can provide more insight into the impacts that a product may have, as it is more quantitative.

Sustainability focuses on not just environmental concerns but also on economic and social impacts. Balancing the three tiers while keeping the overall goal of sustainability is the ultimate goal. The penultimate goal of an environmentally conscientious chemist is approached by Anastas and Warner, but falls short of addressing the economic and social tiers. While a thorough life-cycle assessment is outside of the scope of this thesis, economy and society do play an important role in the resultant products. Economically, producing a polymer with lignin derived chemicals that are commercially available is an important consideration that was taken. A full analysis of an industrial scale production would be necessary to address this branch of sustainability. On a social level, there is demand for green plastic which drives much of this research. Furthermore, the use of lignin for plastics does not directly impact food supply chains since it is not a major human food source.

1.2.2 Condensation Polymerization

Condensation polymerizations can be used to produce polyesters; typically a small molecule such as water is created as a byproduct, although other condensates can form depending upon the structures of the monomers. Monomers react with each other to form dimers, which in turn react to form trimer, teramers, oligomers, etc. until high

molecular weight polymer chains have formed. In order to drive the reaction forward it becomes necessary to remove the increasing amount of byproduct in accordance with Le Châtelier's Principle. This can be achieved via several methods, however a simple method is by carrying the reaction at sufficiently high temperature to permit the evaporation of the smaller molecule and flowing an inert gas to aide in its removal. This stage forms oligomers and can be referred to as Phase I. Phase II is the stage where high polymer would form by the combination of these oligomers; often such a stage could employ a reduced pressure environment. An additional side effect would be the removal of some of the ever present monomers from the reaction pot. Step-growth polymerization typically takes a high conversion and a significant amount of time to form high number average molecular weight ($\overline{M}_n$).

1.2.3 Lignin and Derivatives

Lignin (Figure 1.2.1) is a significantly important source of biomass.[17] It composes the structural components of woody plant cell walls, is generally hydrophobic, and is itself a phenolic polymer which is crosslinked.[18] As a biopolymer with desirable properties, there is a great emphasis to mimic it in the laboratory and further refine it to produce similar materials.[19,20] In addition to replicating lignin, Hatakeyama and Hatakeyama in 2012 and Miller in 2013, among many others, focused on discussing various derivatives of the material.[9,17]

1.2.4 Pendant Moieties and Their Effects on Crystalline Systems

Liquid crystalline polymers (LCPs) are polymers with interesting properties. The liquid crystalline state exudes characteristics of both solid and liquid states.[22] LCPs have regions where the polymer chains are aligned with other chains and themselves by weak bonds. Mingos concisely describes LCPs as "disordered solids or ordered liquids."[22]

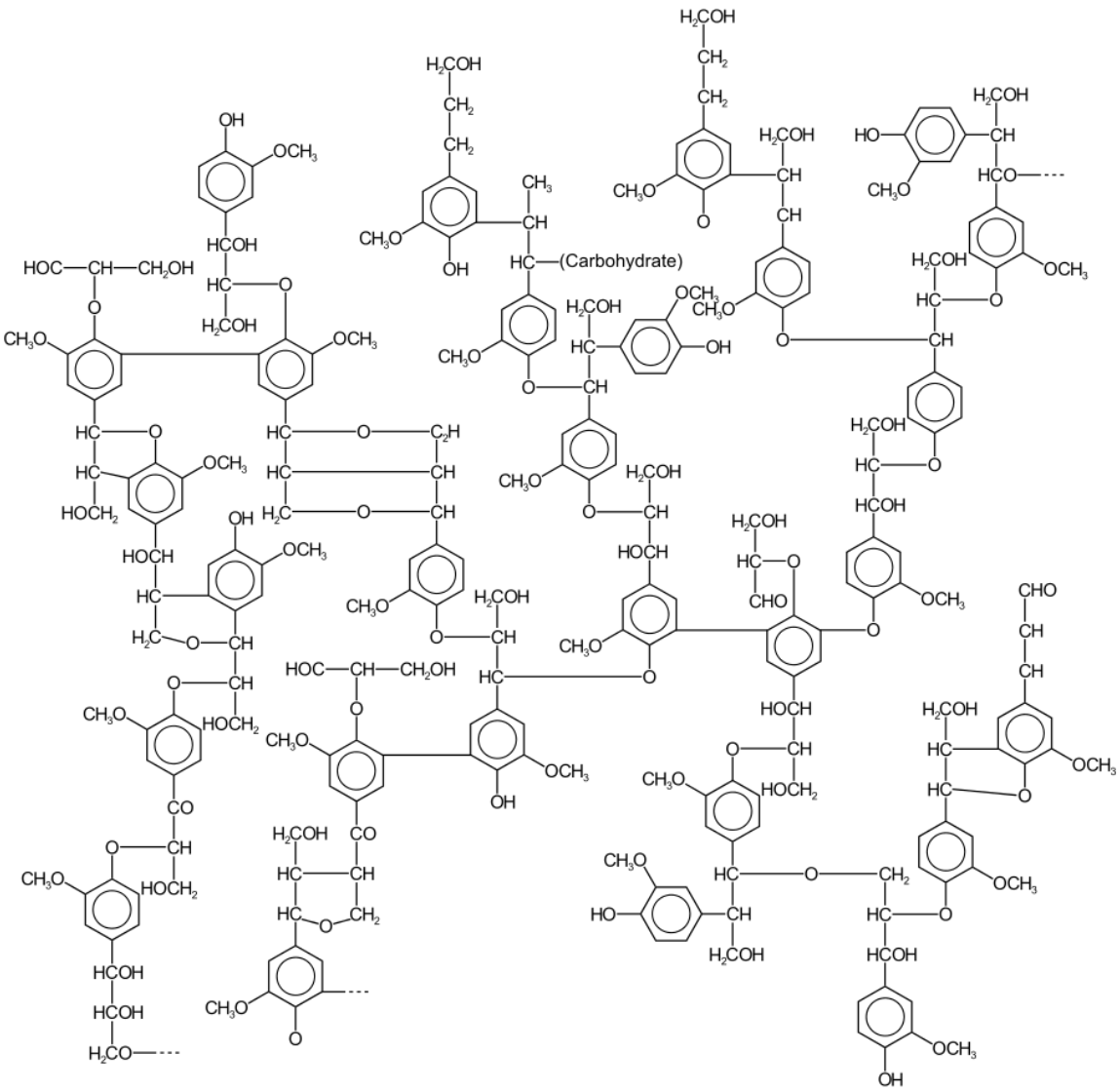

Figure 1.2.1: A depiction of lignin.[21]

Pendant groups on polymer chains can impart important effects both chemically and physically. Of particular focus to this thesis are the effects of methoxy moieties on glass transition temperature (T_g) and melting temperature (T_m). The T_g is characterized by an increase in free volume which in turn permits reptation and segmental motion of an otherwise rigid system of semi-tangled chains. Below T_g translational and rotational motions are not possible and the material exhibits glass-like properties such as brittleness and rigidity; above T_g the polymer chains are free to move about approaching behavior of a liquid. In some cases, a pendant group will impede the

movement of the polymer chain which will therefore require more energy, typically thermal, to overcome these hindrances, thus an increase in T_g; pendant groups can have an opposite effect on the T_m. Between T_g and T_m the polymer is in a rubber-like state, however it is not a true liquid where there is free movement of the molecules or polymer chains. The tangled nature of the chains and other intermolecular forces prevent the mass from behaving like a true liquid and in most thermotropic LCPs this region close to T_m is crystalline. This region between T_g and T_m is generally a soft stage where the bulk polymer can be more readily manipulated.

At T_m the material transitions to a liquid and is free to flow. Albeit the viscosity of the liquid or melt polymer can be quite high, the changes in molecular arrangement define this phase transition. Above T_m the chains are more disordered. A fully disordered state would be isotropic whereas an anisotropic LCP has some degree of ordered nature and introduce the concept of mesophases. A decrease in T_m is caused by pendant groups impeding the formation of large crystalline regions. The result of having smaller crystalline regions, or generally a more amorphous system, is that less energy is necessary to break the weak bonds holding the chains together, thus a lower T_m.

1.3 Previous Research

Much of the research on aromatic-aliphatic polyesters for this thesis was a paradigm shift for Dr. Miri's research laboratory. Miri et al. published earlier work on linear copolyesters from biodiesel based glycerol.[23] As such, considerably more literature research was performed and physical system development was necessary for a successful starting point in the experiment. Design of the reaction system, Figure 2.2.1, was only obtained after many iterations. Further notes on the preliminary observations can be found in Appendix D.

1.3.1 Review of Related Literature

Starting with papers from Wilsens et al. and Mialon et al., a general concept of developing an aromatic/aliphatic polyester from some biobased source was established.[24,25] Research by Wilsens et al. and Laurichesse and Avérous referred to alternative monomers that could be used to expand the biobased content.[26,27] From Mialon et al. and Wilsens et al., the approach of acetylating the hydroxyl groups was the preferred method employed during the polymerization series since melt transesterification produced solid polymeric material with a number average degree of polymerization ($\overline{X}_n$) between 5 and 6.[24,25]

Nagata primarily studied thermotropic LCPs, specifically copolyesters that share a strong resemblance to the base system of monomers studied in this body of research.[28] The polymer system comprised 1,4-diacetoxybenzene (HQ), 4-acetoxybenzoic acid (BA), and sebacic acid. An important observation by Nagata was the mesophase transitions that were observed with 30 mol % and greater BA content.[28] Additionally, as the BA content was increased the crystallinity decreased. Another component of the research included an environmental degradation study which showed that both crystallinity and BA content had an effect in the polymer degradation.

Wilsens et al. incorporated acetylated vanillic acid (AVA) into a polymer system to lower T_m. The predominant research performed involved 2,5-furandicarboxylic acid (2,5-FDCA), however the inclusion of AVA and BA was of interest to this research.[26] Wilsens et al. provided more insight into a HQ, BA, AVA, and suberic acid system in a related paper.[24]

Mialon et al. took a different approach to polymerization while using vanillic acid (VA) derivatives.[29] The approach was to create a homopolymer, however the properties, such as solubility, and the descriptions of issues that arose during synthesis proved insightful. Mialon et al., keeping with the approach of creating a homopolymer,

studied BA-, VA-, and syringic acid (SyA)-derived monomers.[25] Mialon et al. research focused on lignin derivatives with extended aliphatic segments.[25]

1.3.2 Preliminary Laboratory Experiments

Substantial refinement of the reactor was performed leading up to the final design as illustrated in Figure 2.2.1. Over the development of the experiment, several different chemicals were assessed to determine the monomers that would ultimately be selected to form the basis of the series. They were predominately shorter chain dicarboxylic acids, specifically succinic acid, adipic acid, suberic acid, and sebacic acid. Early attempts at polymerization yielded more amorphous products and generally undesirable properties. One trend that was noticed was that a longer aliphatic segment in the reaction produced a more stable polymer.

1.3.3 Selected Polymerization

Monomers selected for the study in this thesis are depicted in Scheme 1.1. The poly-

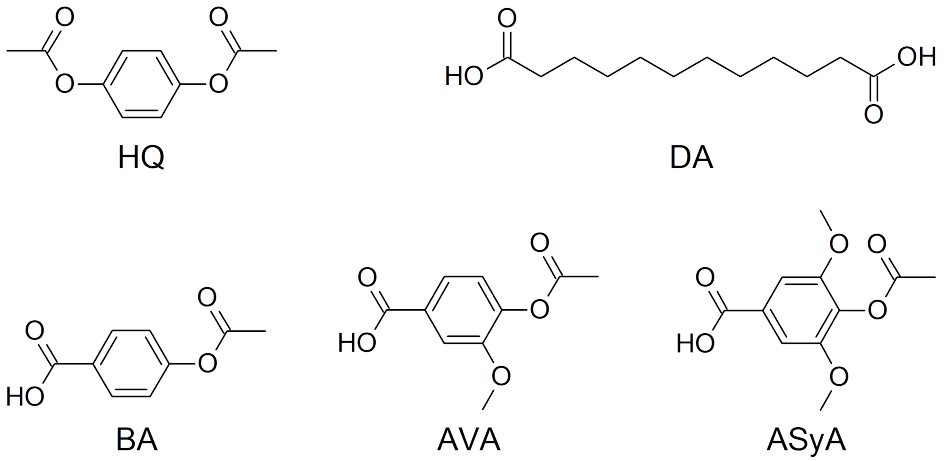

Scheme 1.1: Monomers used in these series of polymerizations include 1,4-diacetoxybenzene (HQ), dodecanedioic acid (DA), 4-acetoxybenzoic acid (BA), acetylated vanillic acid (AVA), and acetylated syringic acid (ASyA).

merization system described in Scheme 1.2 was developed to include a longer dodecanedioic acid (DA) as a result of the previous studies.

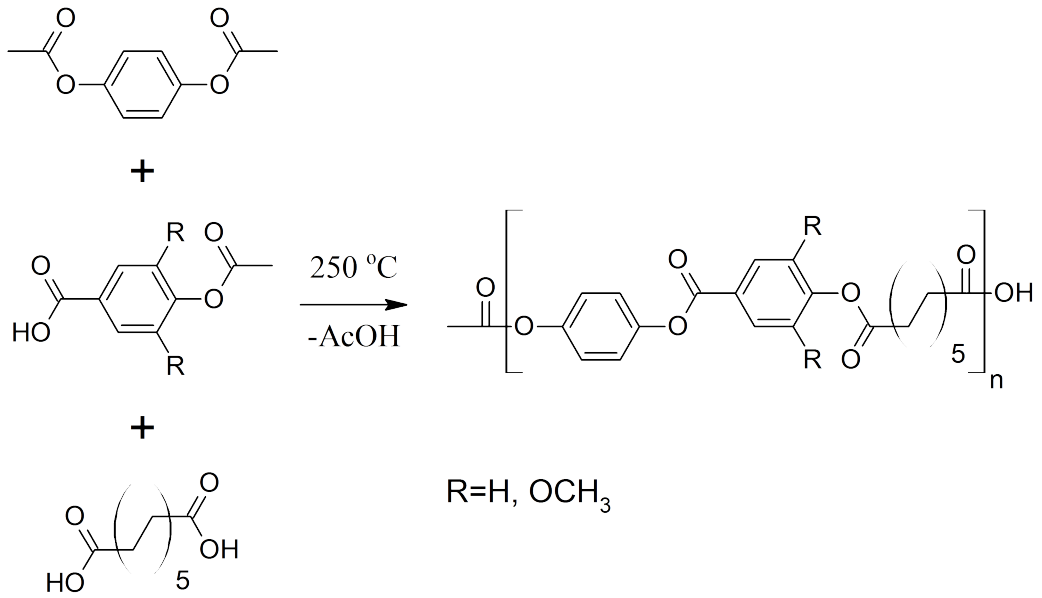

Scheme 1.2: Scheme of polymerization. Both R groups consisting of $-H$ corresponds to BA, one $-H$ and one $-O-CH_3$ corresponds to AVA, and both R groups corresponds to acetylated syringic acid (ASyA).

2. Experimental

2.1 Materials

All of the applied monomers were at the minimum 98 % purity. 1,4-diacetoxybenzene (HQ) was purchased from TCI. 4-acetoxybenzoic acid (BA) and 1,1,2,2-tetrachloroethane (TCE) were obtained from Acros Organics. Due to availability, dodecanedioic acid (DA) was acquired from TCI and Aldrich. Monohydrate *p*-toluene sulfonic acid (*p*TSA) was purchased from TCI and dried *in vacuo* prior to use. Antimony(III)oxide (Sb_2O_3) was acquired from Strem Chemicals Inc. Zinc diacetate ($Zn(OAc)_2$) was purchased from J. T. Baker®. Monomers were prepared according to Sections 2.3 and 2.4. Vanillic acid (VA) was purchased from Carbosynth. Syringic acid (SyA) was from Indofine Chemicla Co. Pyridine and acetic anhydride were supplied by Alfa Aesar. Magnesium sulfide was acquired from Fischer Chemical. Ethyl acetate, chloroform, dichloromethane (DCM), and HCl were obtained from by Macron Fine Chemicals. Methanol was acquired from Fischer Chemical. Trifluoroacetic acid (TFA) was from Oakwood Chemical. Ethanol (EtOH), 200 proof, was supplied from Koptec. Potassium hydroxide (KOH) was acquired from EM Science. Phenol was purchased from Acros Organics and Alfa Aesar. Hexafluoroisopropanol (HFIP) purchased from Apollo Scientific was sonicated with sodium trifluoroacetate (NaTFA) from Fluka as described in Section 2.5.1. Poly(methyl methacrylate) (PMMA) standard ReadyCal set Mp 500-2700000 for GPC was acquired from Sigma Aldrich. Solvents used in proton nuclear magnetic resonance imaging (^{1}H NMR) analysis, deuterated chloroform

($CDCl_3$) and deuterated trifluoroacetic acid (TFA-d), were from Cambridge Isotope Laboratories, Inc. and Acros Organics, respectively. Chemicals were used as received unless otherwise noted.

2.2 General Synthesis

Equipment used for the general polymerization procedures (Figure 2.2.1) includes a three neck flask, offset adapter, Dean-Stark apparatus with temperature maintained by a heating tape and wrapped in aluminum foil, condenser column, overhead stirrer with polished glass stir rod and glass paddle, exhaust oil bubbler, Ace Glass Trubore® bearing, straight Schlenk adapter, septum, digital temperature probe, vacuum pump system, argon system, and salt bath. A total of three saddle O-rings were used to modify the Ace Glass Trubore® bearing to ensure the vacuum seal was sufficient. The vacuum pump system consisted of a rough oil pump, a Pirani 501 vacuum gauge, one Swagelok needle valve, protective liquid nitrogen trap, an additional Swagelok needle valve and line stopcock before connection to the system via vacuum hose. Atmosphere was controlled by an argon system consisting of the gas cylinder connected to an oil bubbler and flow gauge which were then connected to the system via stopcock. Venting of pressure on the system was through a stopcock at the top of the condenser column into a clear hose to an oil bubbler for the purpose of indicating positive system pressure. An eutectic salt mixture was formed by combination of potassium nitrate (53 wt%), sodium nitrite (40 wt%), and sodium nitrate (7 wt%) and heated in a metal heating mantle to act as a heat bath.[30]

Procedure for the polymerization of each sample was modified from Wilsens et al. and Nagata.[24,28] The system was purged by alternating between reduced pressure and argon flow three times. Each charge lasted at least until the vacuum gauge registered better than 1 torr or the system was at positive pressure for the respective

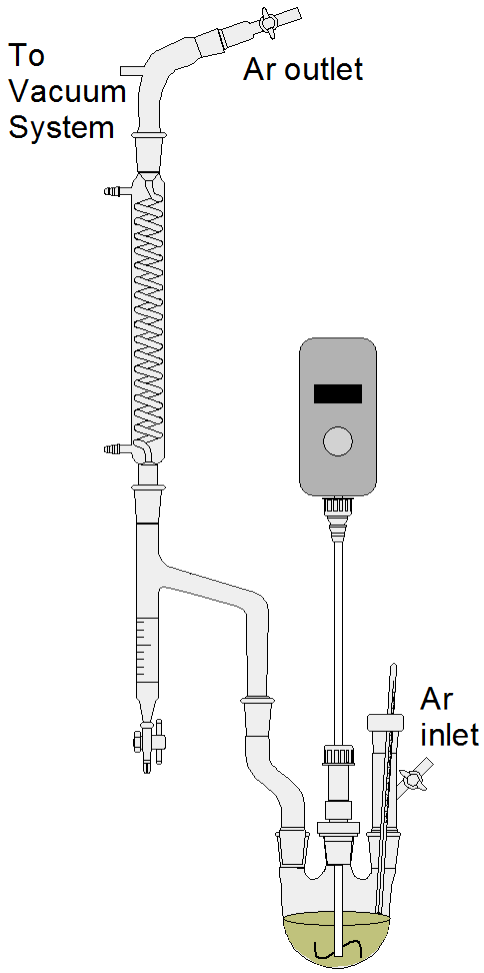

Figure 2.2.1: General diagram of system.

vacuum or argon charges. System diagnostics were performed during this time to ensure proper sealing of the reaction vessel. Any necessary adjustments were made to maintain experimental conditions. To maintain near run conditions, the overhead stirrer operated at 200 rpm during the purging process. Cooling water was flowing through the condenser column and the heating tape was set to approximately 150 °C, corresponding to slightly above the T_m of the monomers. After the third argon charge, flow was closed to the system, the septum was temporarily removed, and the mixture of monomers (Scheme 1.1) and catalyst(s) was added to the reaction vessel through the top of the Schlenk adapter. At this time, a digital temperature probe was inserted through the septum which was then replaced so the tip of the probe made contact

with the reactants. Another triple purge was performed with extra care taken to prevent loss of reactants by slowly opening the system to vacuum via needle valves and controlled increase of argon flow for the respective charges. During all charges of reduced pressure, the topmost stopcock was closed to prevent oil and extraneous gases from entering the system; it was reopened to relieve positive pressure. The general synthesis can be found in Scheme 1.2.

After the final set of purges, the salt bath (260 °C) was elevated to heat the reaction vessel. Stirring was increased to 300 rpm upon full or near full melt of the monomer blend and argon flow was temporarily halted to permit refluxing in the Schlenk adapter, ensuring any residual monomer powder was removed from the walls of the glass. The topmost stopcock was open during this time to relieve pressures that might have developed. After the walls of the Schlenk adapter were clean (i.e. the vapors refluxed to the bottom of the septum) the argon flow was reopened to maintain adequate flow of byproduct vapor into the distillation column. The reaction was monitored for distillate formation and volume during Phase I, oligomerization. After 16 h the distillate was removed and the system was switched from argon to vacuum for an additional 11 h to further polymerize, Phase II. The stirrer speed was reduced to 100 rpm at this time.

At the end of the synthesis, the system was returned to positive pressure via opening the argon system. The end product was mechanically removed from the reaction flask and placed in a 400 mL beaker. Residue, that could not be removed mechanically, was dissolved in a solution of 6:1 dichloromethane/trifluoroacetic acid (DCM/TFA) to dissolve overnight and stirred as soon as feasible.[24] Solution from the reaction vessel was added to the mechanically separated product and allowed to further dissolve. In most cases, the polymer took several days to dissolve even while stirring. After the polymer sufficiently dissolved, the polymer/DCM/TFA solution

was precipitated into a 5-fold excess of cold methanol, suction filtered, and dried *in vacuo* overnight.

Estimates of $\overline{X}_n$ were taken during the synthesis by monitoring volume of distillate and calculated using the relationship

$$\overline{X}_n = \frac{1}{1-p} \tag{2.2.1}$$

where p is the extent of reaction which is proportional to the distillate.[31,32] The relationship between $\overline{M}_n$ is

$$\overline{M}_n = \overline{M}_0 \overline{X}_n = \frac{\overline{M}_0}{1-p} \tag{2.2.2}$$

where $\overline{M}_0$ is the mean molecular weight of the chemical repeat unit (CRU).[31] While these estimates were rough, they did give an indication of what the $\overline{M}_n$ should be at a minimum.

2.3 Synthesis of AVA

Synthesis of the monomer (Scheme 2.1) used in Section 3.2.2 was a modified procedure based on Murphy et al. patent, example 12, "Synthesis of Acetyl Vanillic Acid - LN011035".[33] VA (75 g, 0.457 mol) was placed in a 1 L flask, and equal volumes (188 mL) of pyridine (2.32 mol) and dry acetic anhydride (1.99 mol) were added to the flask while stirring at room temperature (T_r). After 8 h, the solution was added to 3.5 L of distilled water and then acidified to a pH of 2 with hydrochloric acid. Organic compounds were separated via separatory funnel using 2.5 L of ethyl acetate, then dried over anhydrous magnesium sulfate overnight. The magnesium sulfate was suction filtered off and the volatile liquids were removed by rotary evaporation. Light yellow solids were obtained and dissolved in a 1:1 mixture of distilled water and

methanol which was placed in a freezer overnight to facilitate crystallization. The crystallized solids were removed via suction filtration and dried *in vacuo* for a full day. A yield of 52.4 % was obtained. Analysis of AVA from this synthesis can be found in Section 3.2.1.

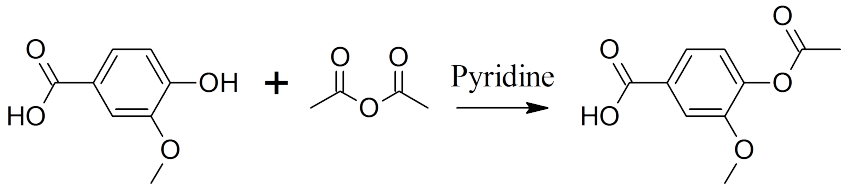

Scheme 2.1: Synthesis of AVA

2.4 Synthesis of ASyA

ASyA synthesis (Scheme 2.2) is similar to that of the synthesis of AVA from Section 2.3. The basis of the synthesis was taken from Murphy et al. patent, example 14, "Synthesis of Acetyl Syringic Acid - JLM-688-52."[33] SyA (150 g, 0.765 mol) was placed in a 3 L flask equipped with thermometer, mechanical stirrer, reflux column, and drying tube filled with Drierite. Pyridine (31 mL, 0.38 mol), dry acetic anhydride (217 mL, 2.29 mol), and dry toluene (750 mL) were added to the flask while stirring. The reaction was heated via heating mantle and allowed to reflux at 120 °C. After 8 h the solution was allowed to cool to T_r. Toluene was removed via rotary evaporation. Solids were then recrystallized, removed via suction filtration, then dried *in vacuo* for a full day. A yield of 88.4 % was obtained. Analysis of ASyA from this synthesis can be found in Section 3.2.

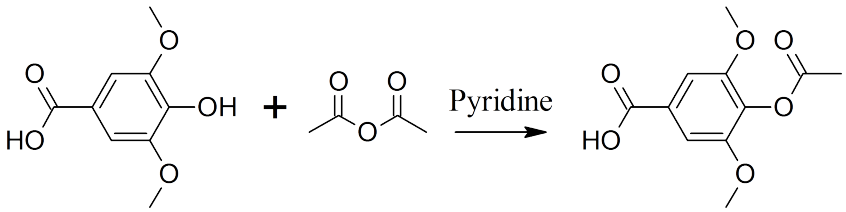

Scheme 2.2: Synthesis of ASyA

2.5 Procedures for Characterization

Characterization of each polymer sample and synthesized monomer was performed via several methods. A general characterization (Section 2.5.1) comprised of proton nuclear magnetic resonance imaging (^{1}H NMR), Fourier transform infrared spectroscopy (FTIR), polymer end-group titration (PEGT), and gel permeation chromatography (GPC) and a thermal characterization (Section 2.5.2) using differential scanning calorimetry (DSC) and thermogravimetric analysis (TGA) to adequately determine each polymer synthesized. Monomers were characterized using proton nuclear magnetic resonance imaging (^{1}H NMR) and Fourier transform infrared spectroscopy (FTIR).

2.5.1 General Characterization

Spectral analysis was the initial form of identification. ^{1}H NMR data was interpreted using Advanced Chemistry Development, Inc. (ACD/Labs) NMR Processor. FTIR data was interpreted using KnowItAll® Informatics System, Academic Edition (KnowItAll®). Plots were compiled using LibreOffice for FTIR data and ACD/Labs for ^{1}H NMR data.

^{1}H NMR

^{1}H NMR analysis was performed using a Bruker DRX-300 for monomer characterization with deuterated chloroform ($CDCl_3$) as the solvent. A Bruker Avance III 500 was

used for polymer samples with deuterated trifluoroacetic acid (TFA-d) as solvent, which was necessary due to an overlap of signals. A total of 32 scans with a 5 s delay permitted adequate resolution for identifying the monomers as well as the polymers. Spectra obtained were analyzed using ACD/Labs NMR Processor, Academic Edition.

From the spectral integration a rough estimate of $\overline{M}_n$ can be calculated.[34] The general procedure is: a) calculate the integral per proton, b) calculate the number of repeating units, n, and c) calculate $\overline{M}_n$ as per Equations 2.5.1.

$$\int \beta_{\text{per proton}} = \frac{\sum \int \beta_{\text{end groups}}}{\text{number of protons in end groups}} \tag{2.5.1a}$$

$$n = \frac{\int \beta_{\text{per proton}} \times \sum \int \beta_{RU}}{\text{number of protons in repeat units}} \tag{2.5.1b}$$

$$\overline{M}_n = FW_{\text{end groups}} + n \times FW_{RU} \tag{2.5.1c}$$

Where $\int \beta$ corresponds to the area of each signal. $\overline{FW}_{\text{end groups}}$ is the average formula weight of the end groups. Subscript RU denotes repeat units. Expanding Equation 2.5.1c to the specific system:

$$\overline{M}_n = \overline{FW}_{\text{end groups}} + \sum n_{RU} FW_{RU} \tag{2.5.2}$$

FTIR

FTIR was collected on a Biorad Excalibur FTS 3000 with Varian Resolutions Pro FT-IR analysis software. The spectra were collected as % transmittance from 4,000 to 600 cm^{-1}. A total of 16 scans were performed for each sample, and each was performed in triplicate to ensure consistent results.

PEGT

Polymer end-group titration (PEGT) was used to estimate the $\overline{M}_n$ of the polymer samples.[35,36] Samples of the polymers were accurately weighed (0.1 to 0.2 g) into 25 mL Erlenmeyer flasks. To that, 10 mL aliquots of 60:40 mixture by weight phenol:1,1,2,2-tetrachloroethane (TCE) (Ph:TCE) with phenol-red indicator was pipetted. The polymer was allowed to fully dissolve; gentle heating was provided via hot plate as necessary to allow full dissolution then the solution was cooled back to T_r in a water bath. Potassium hydroxide (KOH) pellets were sonicated in ethanol (EtOH) to produce a 0.1 M solution. Each polymer sample solution was titrated with the 0.1 M KOH in EtOH solution, via 500 µL syringe. $\overline{M}_n$ was determined by Equation 2.5.3.

$$\overline{M}_n = \frac{P_{\text{mass}}}{c(t - t_i)} \tag{2.5.3}$$

Where $\overline{M}_n$ is given in $\mathrm{g\,mol^{-1}}$. P_{mass} is the mass (mg) of the polymer sample, c is the concentration of the titer (M), and t and t_i are the volumes (mL) of titer necessary to reach end point.

GPC

Gel permeation chromatography (GPC) was used to find $\overline{M}_n$, weight average molecular weight ($\overline{M}_w$), and dispersity (Đ). 10 mM sodium trifluoroacetate (NaTFA) was sonicated in hexafluoroisopropanol (HFIP) for 1 h to ensure adequate dissolution.[37,38] Samples were prepared at $3\,\mathrm{mg\,mL^{-1}}$ in the prepared HFIP for both poly(methyl methacrylate) (PMMA) standards and test polymers. A modified Agilent 1,100 series high pressure liquid chromatography (HPLC) equipped with ZORBAX PSM 60S and PSM 1000S columns was used as a GPC. Both columns were 6.6 mm × 250 mm and could handle 5.0 µm particles. The total range of detection was 500 to 1,000,000 $\mathrm{g\,mol^{-1}}$. Calibration produces a curve calibrated from 800 to 675,000 $\mathrm{g\,mol^{-1}}$. Column tem-

perature was set at $40\,°C$ and the elluent flow at $0.5\,mL\,min^{-1}$. Agilent ChemStation and Cirrus software was used to collect data and calculate peak molecular weight (M_p), $\overline{M}_n$, $\overline{M}_w$, and Đ values.

2.5.2 Thermal Characterization

Thermal properties were measured using TA instruments. TA Universal Analysis software was used to interpret the data obtained from differential scanning calorimetry (DSC) and thermogravimetric analysis (TGA). Relevant values from the DSC include T_m, T_c, and T_g. The TGA provided temperature of 50% weight loss (T_{50}) as well as onset temperature (T_{onset}) and endset temperature (T_{endset}). Plots were compiled using LibreOffice.

DSC

Thermal properties were evaluated using a Thermal Advantage 2010 DSC. Ground polymer weighing from 5 to $15\,mg$ was placed in a sealed aluminum pan. The sample was cycled under nitrogen from T_r to $300\,°C$, held at temperature for $2\,min$, cooled to $-50\,°C$, held for $2\,min$, and repeated, with a final elevation back to T_r. First heating and cooling was at $40\,°C\,min^{-1}$ to remove thermal memory, where additional cycling was performed at $10\,°C\,min^{-1}$. Thermal values T_m, T_c, T_g, melt enthalpy (ΔH_m), and mesophase transition temperature (T_{meso}) were determined from the respective second heating and cooling scans. Subsequent cycles (not included) were performed to verify data collection. Both T_m and T_c were taken as the respective peak maxima. The T_g was based on the inflection point at the glass transition.

TGA

TGA thermograms were obtained from a TA Q500. Ground polymer weighing from 5 to $15\,mg$ was placed in a platinum boat. The sample was heated under nitrogen at

$20\,°\mathrm{C\,min^{-1}}$ from T_r to $800\,°\mathrm{C}$ and held for $3\,\mathrm{min}$. The T_{50} was taken as the temperature at the peak of the derivative weight loss curve. Plots can be found in Appendix C.

3. Results and Discussion

3.1 Catalyst Study

The catalyst study was designed to determine the best catalyst to use for the basic system of monomers: HQ, BA, and dodecanedioic acid (DA) (Scheme Scheme 1.2. An outline of the experiment can be found in Section 3.1.1. Polymers were isolated, verified, and characterized as previously described in Section 2.2.

3.1.1 Catalyst Study Polymer Synthesis

The catalyst study followed the general procedure as in Section 2.2. Each polymerization was carried out using HQ, BA, and DA with a variable catalyst. Catalysts studied were zinc diacetate ($Zn(OAc)_2$)(**P-2**), antimony(III)oxide (Sb_2O_3)(**P-3**), *p*-toluene sulfonic acid (*p*TSA)(**P-4**), combination of $Zn(OAc)_2$ and Sb_2O_3 (Zn/Sb)(**P-5**), and combination of $Zn(OAc)_2$ and *p*TSA (Zn/*p*TSA)(**P-6**). A polymer without catalyst (**P-1**) was also synthesized. Amounts of each monomer and catalyst(s) used can be found in Table 3.1.

Table 3.1: Compositions of inputs for each copolyester in the catalyst study. Parenthetical values are mol and mmol for monomers and catalyst(s), respectively. Dual catalyst systems are separated by commas and listed in the respective order of the name of the catalyst system.

Code	Catalyst	Mass/g			Mass/mg
		HQ	BA	DA	Catalyst
P-1	none	13.60 (70.0)	12.62 (70.0)	16.12 (70.0)	
P-2	$Zn(OAc)_2$	13.59 (70.0)	12.61 (70.0)	16.12 (70.0)	34.34 (156)
P-3	Sb_2O_3	13.61 (70.1)	12.62 (70.0)	16.12 (70.0)	48.10 (165)
P-4	*p*TSA	13.60 (70.0)	12.62 (70.0)	16.13 (70.1)	27.53 (160)
P-5	Zn/Sb	13.60 (70.0)	12.61 (70.0)	16.12 (70.0)	17.23 (78), 23.21 (80)
P-6	Zn/*p*TSA	13.60 (70.0)	12.62 (70.0)	16.12 (70.0)	17.49 (80), 13.89 (81)

3.1.2 Catalyst Study Polymer Characterization

The catalyst study provided insight into the reaction rates and expected outcomes for the following monomer study. The three primary catalysts, $Zn(OAc)_2$, Sb_2O_3, and *p*TSA, each had different effects on the rate of reaction. The catalysts used for **P-5** was referred to by Rogers and Long as a potential candidate for a good combination.[35] Assessing the reaction rates* and percent distillate collected in Phase I as well as Phase II, an additional catalyst combination of *p*TSA (chosen for reaction rate in Phase I) and $Zn(OAc)_2$ (for distillate formation in Phase II) was used for **P-6**.

^{1}H NMR

^{1}H NMR was performed as outlined in Section 2.5.1. As should be expected, the spectra, combined in Figure 3.1.1, were nearly identical. A peak at 3.8 ppm was present in all of the samples. This signal was not predicted nor was it present in any of the monomers. It could be the −OH end group, however that peak would be broad and in the 10.0 to 13.2 ppm range.[40] Comparison of the identified peak values corresponding to each monomer and evaluating relative amounts of each was tabulated in Table 3.2. Percentages for each monomer incorporated are roughly equal

*Rates were based on the slope of the linear portion of the plot of distillate formed versus time.

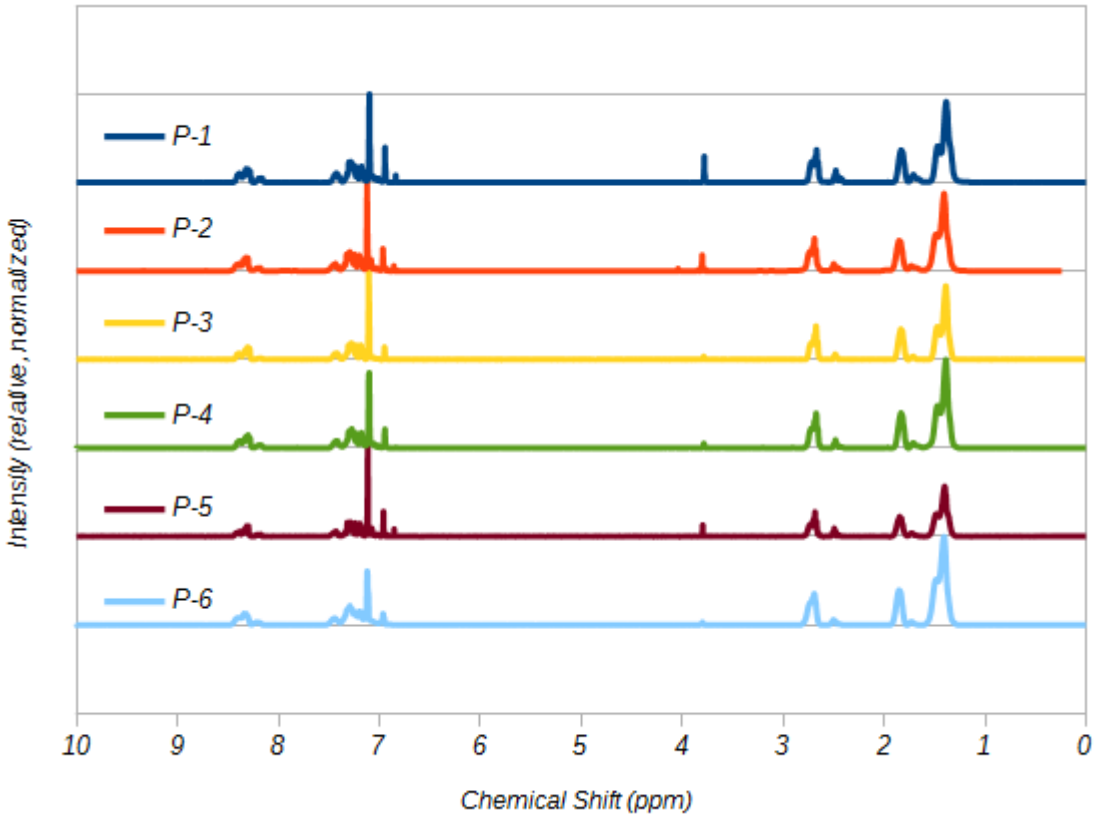

Figure 3.1.1: Composite plot of ^{1}H NMR spectra for catalyst study.

and show uniform incorporation into the polymers. These values approximated from Equation 2.5.2 for $\overline{M}_n$ were lower than the expected 10,000 g mol^{-1} region. ^{1}H NMR data showed a consistent structure for all polymer samples, with the ideal percent incorporation as 33.3 %. Table 3.2 shows fairly uniform incorporation of each monomer into the terpolymer; the greatest outlying polymers were the two with dual catalysts or no catalyst. $\overline{M}_n$ calculations produced low weights for all samples, with **P-3** being the highest (4,600 g mol^{-1}). The lowest recorded $\overline{M}_n$ was from **P-1** (1,800 g mol^{-1}); indicating that a catalyst does aide in polymerization.

Table 3.2: Data values from ^{1}H NMR for the catalyst study.

Code	HQ/%	BA/%	AVA/%	ASyA/%	DA/%	$\overline{M}_n$[a]/g mol^{-1}
P-1	32.7	35.8	0.0	0.0	31.5	1,843
P-2	33.3	33.0	0.0	0.0	33.7	2,689
P-3	34.2	32.7	0.0	0.0	33.1	4,563
P-4	33.5	32.8	0.0	0.0	33.6	3,201
P-5	35.0	32.0	0.0	0.0	33.0	2,456
P-6	36.1	31.4	0.0	0.0	32.5	3,699

[a] Calculated from Equation 2.5.2

FTIR

Analysis of FTIR was performed to identify significant structures and functional groups. The procedure and instrument are described in Section 2.5.1. As can be seen in Figure 3.1.2, all of the polymers share the same peaks and can be superimposed, thus demonstrating nearly identical moieties. Two peaks around 2,900 cm^{-1} indicate

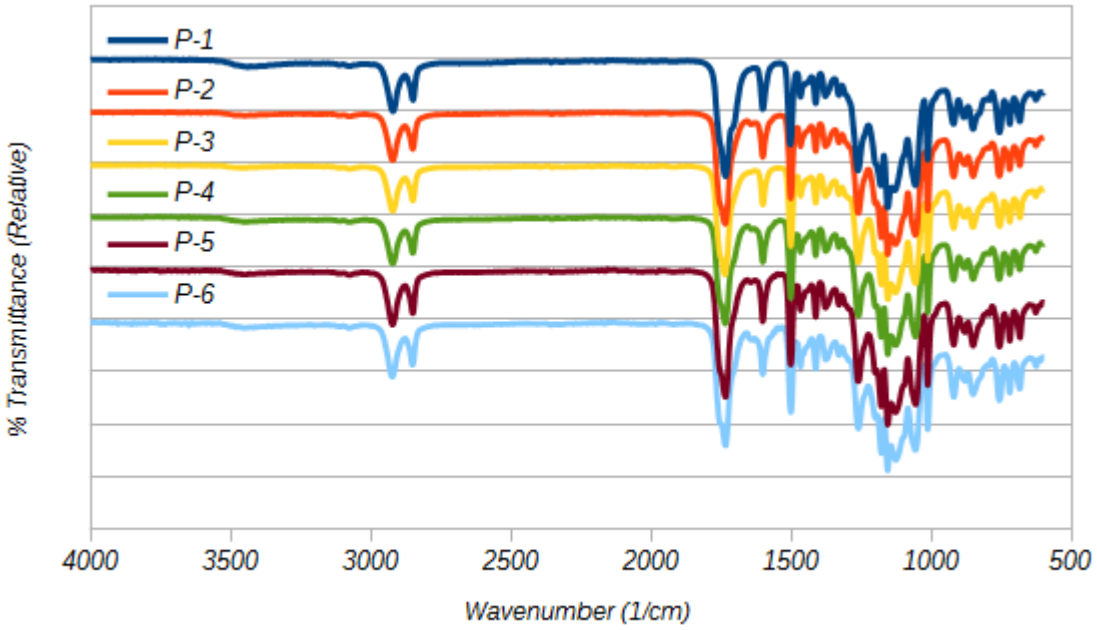

Figure 3.1.2: Composite plot of IR curves for catalyst study.

the aliphatic region corresponding to the DA and the peak near $1{,}700\,\mathrm{cm}^{-1}$ indicates an ester.

FTIR data was consistent for all catalyst study samples. Both the aliphatic region and ester region are present in all of the curves. Aromatic overtones were not as pronounced, however, they did appear as a slight peak around $3{,}075\,\mathrm{cm}^{-1}$ and weakly in the $2{,}000$ to $1{,}700\,\mathrm{cm}^{-1}$ region.

PEGT

PEGT was performed as a precautionary measure in the event GPC data could not be collected. The method was admittedly crude, as the end point was confirmed visually and without the aide of a pH meter and was subject to error from interference from the color being altered from the polymer itself in the solution. Average $\overline{M}_n$ values can be found in Appendix A.

GPC

Chromatograms GPC can be found in Figure 3.1.3. A bimodal system peak was present in all of the curves between $22\,\mathrm{min}$ and $24\,\mathrm{min}$ which is typical of the solvent. Samples **P-3**, **P-6**, and, to a lesser extent, **P-4** display a relatively sharp onset of higher molecular weights with some tailing. It is clear from the plots that **P-3** has a narrow distribution. Values found in Table B.1 show high M_p, $\overline{M}_n$, and $\overline{M}_w$ as well. Due to the generally low molecular weight of the samples overall and the range of the calibration, the values below $800\,\mathrm{g\,mol}^{-1}$ ($19.5\,\mathrm{min}$) are not an accurate representation of the true nature of the polymer. Relative comparisons and conclusions are valid, however Đ values should not be considered representative of the actual sample.

Preliminary data from the GPC was able to be obtained prior to continuation of the experiments for AVA and ASyA for the basis of choosing the catalyst for use in the subsequent studies. Comparing the $\overline{M}_n$ values from ^{1}H NMR, PEGT, and GPC, it is

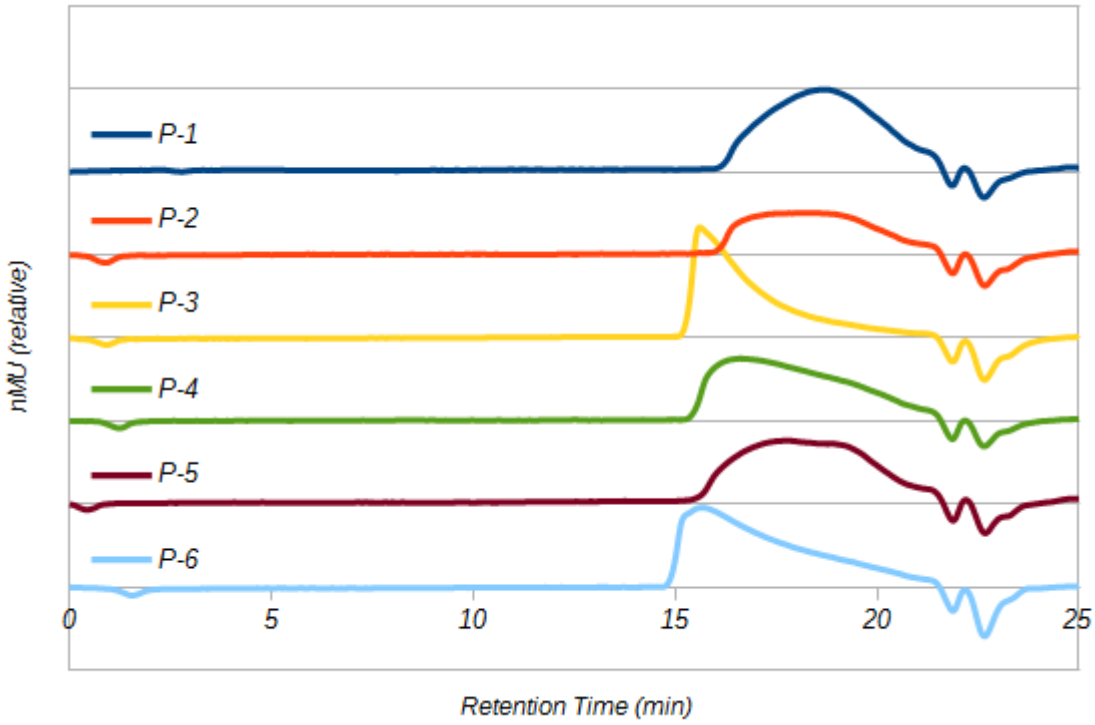

Figure 3.1.3: Composite plot of GPC chromatograms for the catalyst study.

noticeable that the values range significantly. All three methods agree that the highest $\overline{M}_n$ is **P-3**; which was the most important datum. Each of the methods employed a different solvent - TFA-d, Ph:TCE, and 10 mM NaTFA in HFIP - which could have some impact on the comparison of $\overline{M}_n$. Since each polymer in this study had a crystalline component there was a possibility that the polymer-solvent system could have an impact on the result. Equations 2.5.2 and 2.5.3 assumed a statistically even distribution of the end-groups, however there is a possibility that there were fewer terminal acetate groups, resulting in higher $\overline{M}_n$ values for the ^{1}H NMR calculation. The carboxylic acid end group is broad and variable in the ^{1}H NMR leading to the omission of the lone proton in the calculation. Due to the crudity of the PEGT method and potential for bias, the results from this component of the analysis bear little weight relative to the other two methods. PMMA has pendant groups with no aromaticity present while the synthesized polymers do have in-chain aromatic groups;

thereby affecting the hydrodynamic radius. An accurate viscosity (η) would have to be determined, since GPC is an indirect measure of molecular weights.

DSC

Composite charts for second heating and second cooling can be found in Figure 3.1.4a and 3.1.4b, respectively. It should be noted that a T_g was not observed on any of the plots. This is in agreement with the observation by Nagata.[28] Values from the thermograms are found in Table 3.3. Overall the values are near each other; **P-1** had

Table 3.3: Values for polymers in catalyst study obtained from DSC.[a]

Code	T_g/°C	$T_{m,onset}$/°C	T_m/°C	T_{meso}/°C	$T_{c,onset}$/°C	T_c/°C	T_{meso}/°C
P-1	n.o. [b]	112	136	n.o.	134	131	n.o.
P-2	n.o.	111	139	n.o.	148	139	n.o.
P-3	n.o.	131	155	217	159	155	221
P-4	n.o.	111	141	200	129	126	198
P-5	n.o.	115	147	n.o.	143	136	n.o.
P-6	n.o.	105	136	n.o.	120	117	n.o.

[a] All values are taken from the second heating or cooling curve.
[b] Not observed.

a slightly higher T_m and T_c compared to the other polymers. This is attributed to the slight increase in $\overline{M}_n$. Due to the shorter chain lengths, there is a greater impact of the $\overline{M}_n$ on thermal properties. Additionally, a T_{meso} was observed in **P-1** similar to Nagata. DSC analysis showed no T_g which was in agreement with observations in Nagata.[28] Since the samples generally had lower molecular weights, there can be some impact on T_m. While this effect was not expected to be dramatic, **P-3** with the highest $\overline{M}_n$ also has the highest T_m. Double melting and crystallization peaks are present in several of the curves in Figures 3.1.4a and 3.1.4b, respectively; potentially indicating different crystal domains through co-crystallization or phase separation, similar to what was seen in Cho et al..[41]

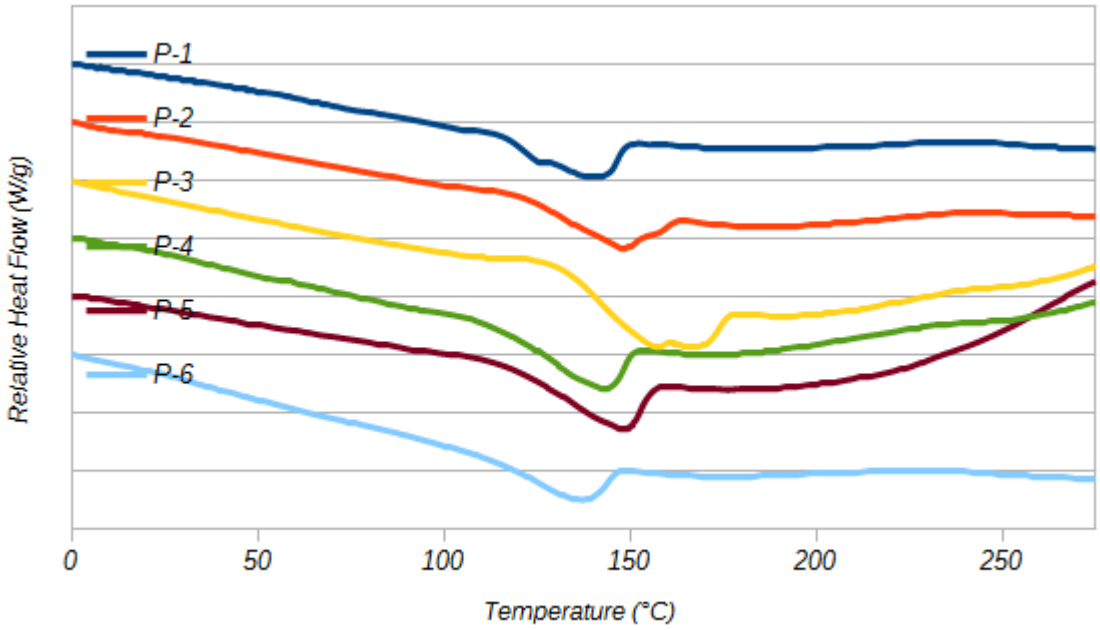

(a) Heating curves.

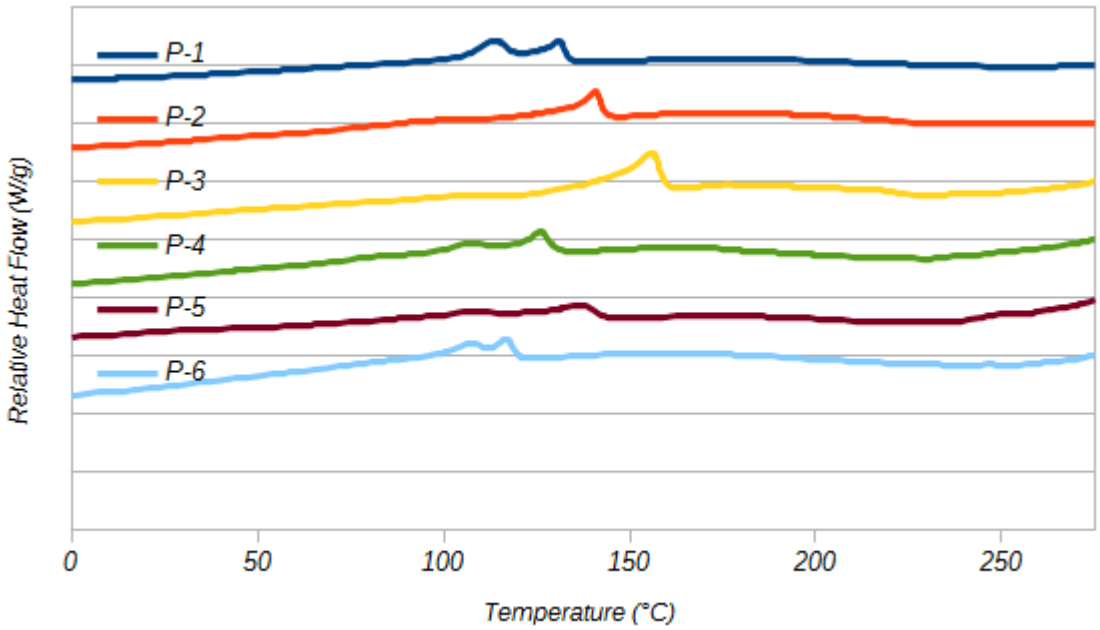

(b) Cooling curves.

Figure 3.1.4: Composite plot of (a) heating curves and (b) cooling curves for catalyst study. Exotherm up.

TGA

TGA was administered as described in Section 2.5.2. Weight percent curves (Figure 3.1.5) show excellent overlap, indicating consistently pure material to nearly 450 °C, between the different catalysts studied. Values for Figure 3.1.5 are located in

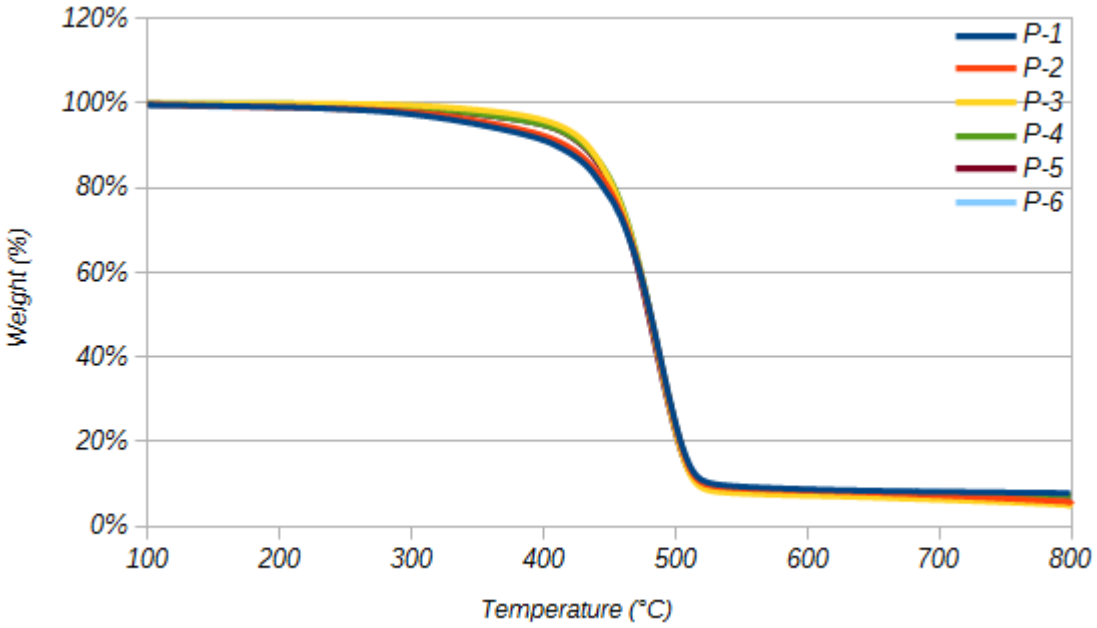

Figure 3.1.5: Composite plot of TGA weight percent curves.

Table 3.4: Values for polymers in catalyst study obtained from TGA.

Code	T_{onset}/°C	T_{50}/°C	T_{endset}/°C	Weight Loss/%
P-1	448	489	510	90.5
P-2	448	488	509	91.6
P-3	447	486	509	92.8
P-4	446	487	510	92.7
P-5	445	484	509	92.7
P-6	446	483	508	91.7

Table 3.4. Some spreading does appear beginning near 300 °C, which could indicate a range of molecular weights present. This is in agreement with ^{1}H NMR and GPC findings.

3.2 Effect of Renewable Aromatic Monomer Study

3.2.1 Renewable Monomer Characterization

AVA was characterized as described in Section 2.5.1. ASyA was characterized as described in Section 2.5.1.

^{1}H NMR

Analysis of the ^{1}H NMR spectrum (Figure 3.2.1) closely agrees with the predicted values for AVA. From the clean baseline and lack of extraneous peak inclusions, the

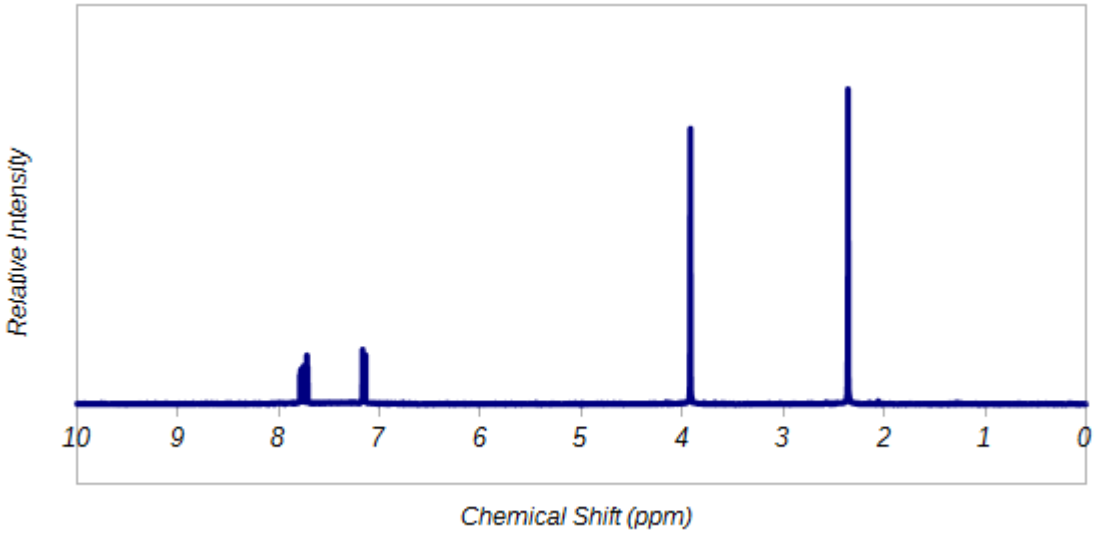

Figure 3.2.1: ^{1}H NMR of AVA.

sample was determined to be adequately pure.

^{1}H-NMR (300 MHz, $CDCl_3$): δ 2.36 (s, 4 H), 3.92 (s, 4 H), 7.15 (d, $J = 8.10$ MHz, 1 H), 7.72 (d, $J = 1.88$ MHz, 1 H), 7.77 (dd, $J = 8.10, 1.88$ MHz, 1 H)

Analysis of the ^{1}H NMR spectrum (Figure 3.2.2) closely agrees with the predicted values for ASyA.

^{1}H-NMR (300 MHz, $CDCl_3$): δ 2.38 (s, 2 H), 3.90 (s, 4 H), 7.40 (s, 1 H)

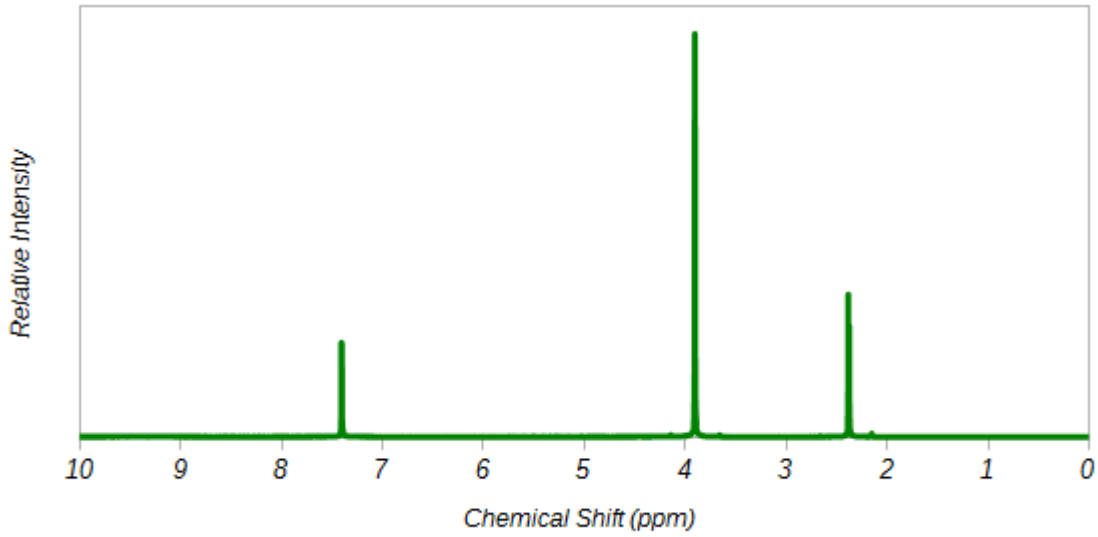

Figure 3.2.2: ^{1}H NMR of ASyA.

FTIR

The spectrum of AVA (see Figure 3.2.3) was obtained as per the procedure described in 2.5.1. There are clear aromatic overtones around 2,500 to 2,000 cm^{-1}. Peaks at

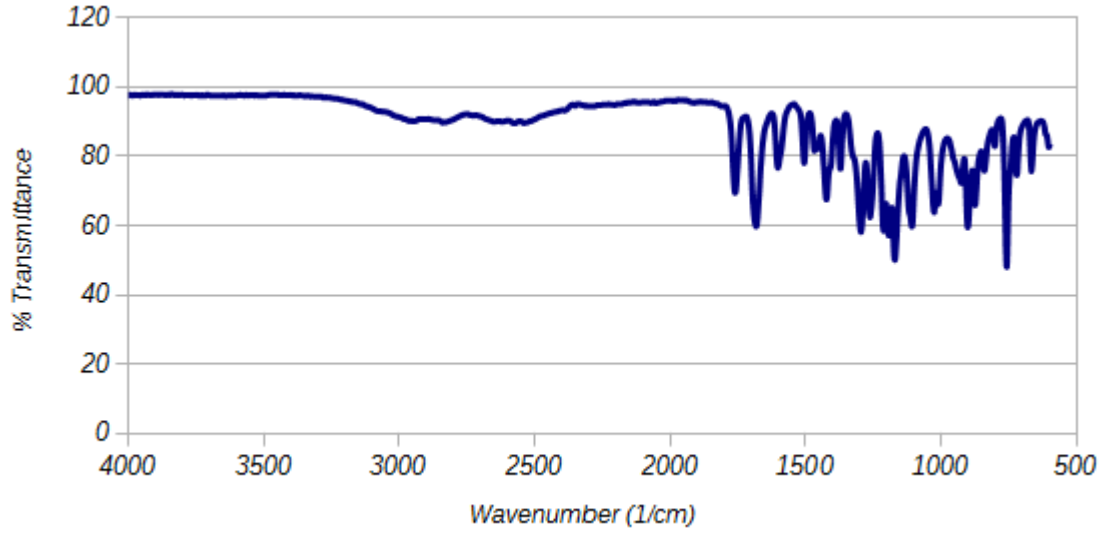

Figure 3.2.3: FTIR spectrum of AVA.

1,761 cm^{-1} and 1,684 cm^{-1} in the carbonyl region indicate the presence of ester func-

tional groups. Aromatic overtones from 2,300 to 1,900 cm^{-1} are present, as well as a broad phenolic carbo-acid stretch around 3,000 cm^{-1}, indicating an aromatic system. Additional peaks of the phenolic carbo-acid at 1,603 cm^{-1}, 1,424 cm^{-1}, 1,263 cm^{-1} and 903 cm^{-1} denote ethers. The presence of a broad stretch around 2,500 cm^{-1} could be indicative of primary amine salts resultant from residual pyridine. Comparison of the sample to ^{1}H NMR data indicates that the amine salts are in trace amounts and should have no impact on the reaction.

The spectrum of ASyA (see Figure 3.2.4) was obtained, as per the procedure described in Section 2.5.1. There are aromatic overtones around 2,400 to 2,000 cm^{-1}.

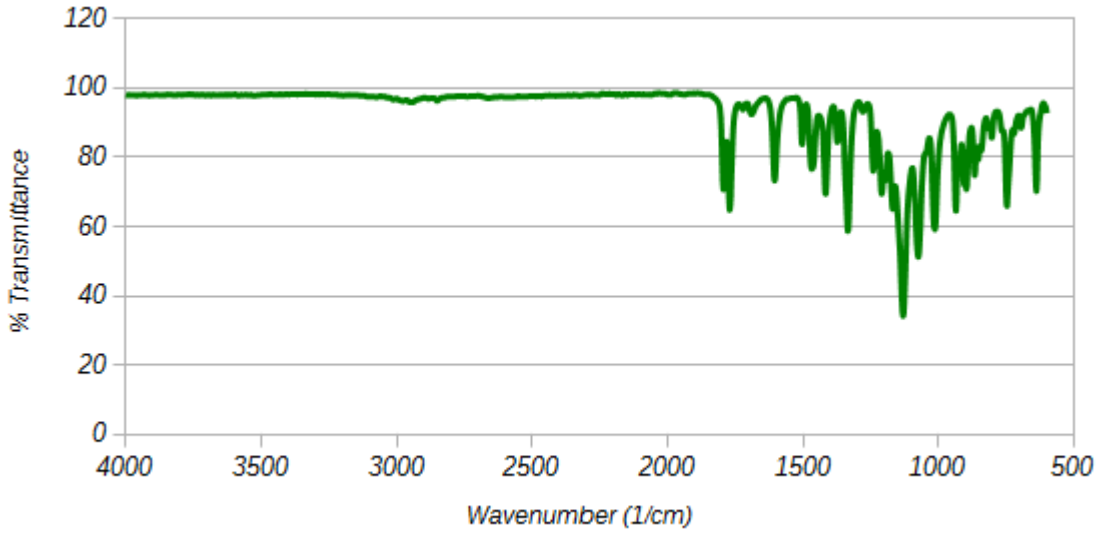

Figure 3.2.4: FTIR spectrum of ASyA.

Peaks at 1,794 cm^{-1} and 1,771 cm^{-1} in the carbonyl region indicate the presence of ester functional groups. Aromatic overtones from 2,400 to 1,900 cm^{-1} are present, as well as a weak broad phenolic carbo-acid stretch around 3,000 cm^{-1} demonstrating an aromatic system. Additional peaks of the phenolic carbo-acid at 1,605 cm^{-1} and 1,335 cm^{-1} denote ethers. The peak at 1,130 cm^{-1} appears to indicate an ester.

3.2.2 Renewable Study Polymer Synthesis

The AVA study consisted of an incremental increase in the amount of AVA monomer relative to BA. Ratios studied were 2:1 (**P-7**), 1:1 (**P-8**), and 1:2 (**P-9**) BA:AVA, which are further outlined in Table 3.5. AVA and BA are identical with the exception of a methoxy functional group adjacent to the acetoxy functional group, as can be seen in Scheme 1.1. Incremental increases in the amount of AVA incorporated into the polymer resulted in an increase in methyoxy groups along the polymer chain.

The ASyA study is nearly identical to the AVA study with the exception of an additional methoxy group. Ratios studied were the same as above; 2:1 (**P-10**), 1:1 (**P-11**), and 1:2 (**P-12**) BA:ASyA, which are further outlined in Table 3.5. ASyA and BA are identical with the exception of two methoxy functional groups adjacent to the acetoxy functional group, as can be seen in Scheme 1.1. The second methoxy functional group was thought to have a more dramatic effect on thermal properties (e.g., T_g)[25] or to stabilize chain formation during polymerization relative to the AVA.

Table 3.5: Compositions of inputs for each copolyester in the AVA and ASyA studies. Parenthetical values are mol and mmol for monomers and catalyst, respectively.

Code	Mass/g				Mass/mg
	HQ	BA	AVA	DA	Sb_2O_3
P-7	13.59 (70.0)	8.41 (46.7)	4.91 (23.3)	16.12 (70.0)	47.40 (163)
P-8	13.59 (70.0)	6.31 (35.0)	7.36 (35.0)	16.12 (70.0)	47.04 (161)
P-9	13.59 (70.0)	4.21 (23.3)	9.81 (46.7)	16.12 (70.0)	46.00 (158)
P-10	13.59 (70.0)	8.41 (46.7)	5.61 (26.7)	16.12 (70.0)	46.72 (160)
P-11	13.60 (70.0)	6.31 (35.0)	8.41 (40.0)	16.12 (70.0)	46.87 (161)
P-12	13.59 (70.0)	4.21 (23.3)	11.21 (53.3)	16.12 (70.0)	46.68 (160)

3.2.3 Renewable Study Polymer Characterization

^{1}H NMR

Figure 3.2.5 depicts the comparison of the ^{1}H NMR spectra of polymers in the AVA study. The increase in the signal around 3.9 ppm indicates an increase in the methoxy

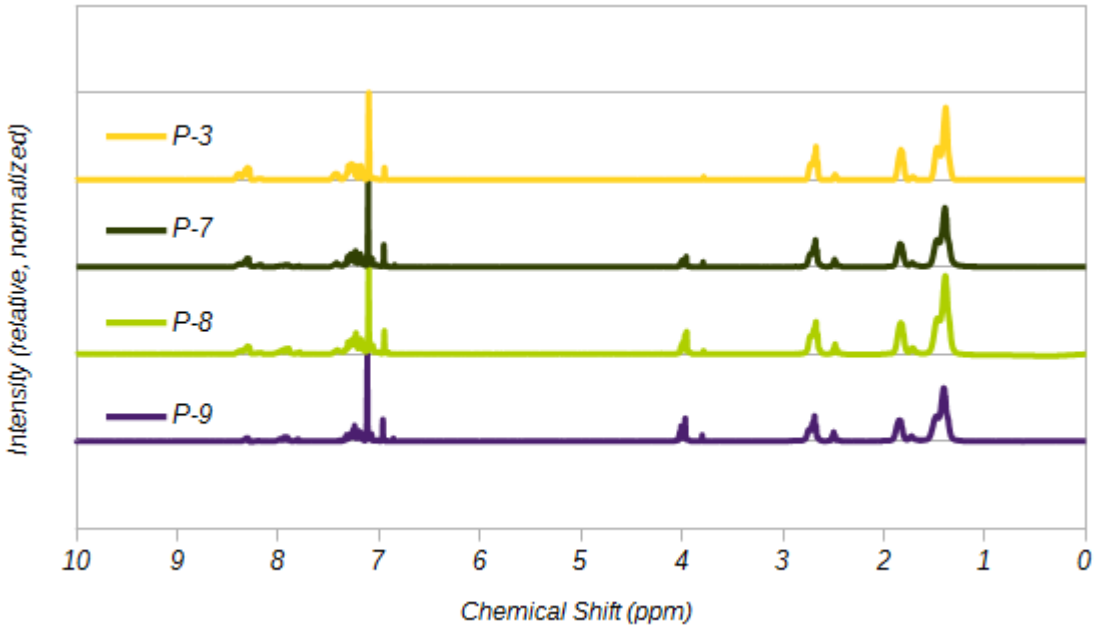

Figure 3.2.5: Composite plot of ^{1}H NMR spectra for AVA study.

substituent. Values from Table 3.6 show a slight decrease in HQ incorporation, however the relative incorporation of BA to AVA was skewed to more favorable incorporation of BA. As was expected, there was a decrease in $\overline{M}_n$, as determined by end groups. Figure 3.2.6 shows a similar trend to the results from the AVA study. The increase in the signal around 3.9 ppm is more pronounced due to double the number of methoxy groups present. Incorporation of monomers was significantly improved over that of AVA as tabulated in Table 3.6. A clear decrease in $\overline{M}_n$ is present likely due to the increase in steric hindrances or other factors retarding the reaction.

Table 3.6: Data values from ^{1}H NMR for renewable study.

Code	HQ/%	BA/%	AVA/%	ASyA/%	DA/%	$\overline{M}_n$[a]/g mol^{-1}
P-7	32.1	23.5	8.2	0.0	36.2	2,311
P-8	30.3	17.8	15.8	0.0	36.1	2,534
P-9	27.2	13.6	20.8	0.0	38.4	2,120
P-10	33.2	22.1	0.0	11.3	33.4	2,548
P-11	34.2	16.0	0.0	16.8	33.0	2,266
P-12	33.3	11.0	0.0	23.6	32.2	1,026

[a] Calculated from Equation 2.5.2

While expected, the percent incorporated, as reported in Table 3.6, showed less than ideal incorporation of AVA into the tetrapolymer system. The monomer most impacted by the presence of AVA appeared to be the HQ, although the BA to AVA ratio was also less than favorable. One reason considered early in the study was the asymmetry of the AVA molecule, as shown in Scheme 1.1, creating a less than favorable reaction site on the acetate end. However, the values are skewed to the reverse, possibly indicating that the acetate was more active, bonding to the DA and leaving fewer sites for the HQ to react.

Peaks corresponding to methoxy on the ^{1}H NMR plots were far more developed in ASyA polymers due to double the moieties present for each unit of renewable. Amounts of each incorporated monomer found in Table 3.6 show that ASyA had improved reactivity relative to AVA. One reason for this might be the symmetry of the molecule allowing for a more uniform, and therefore approachable, reaction site. Overall the incorporation of each monomer was near ideal.

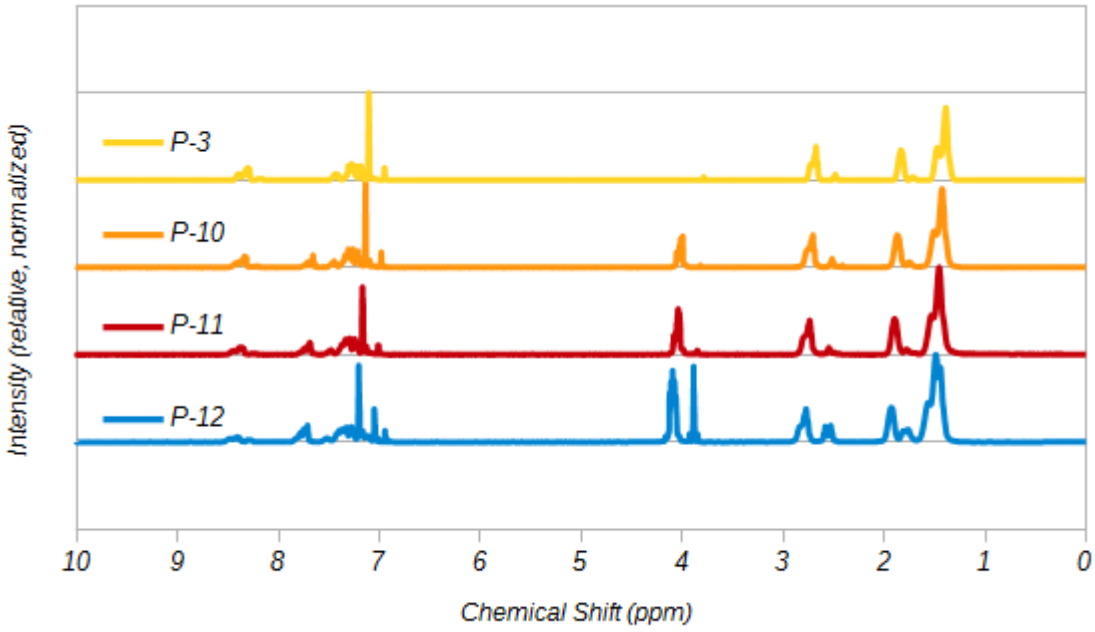

Figure 3.2.6: Composite plot of ^{1}H NMR spectra for the ASyA study.

FTIR

FTIR data (Figure 3.2.7) for the AVA series appears to be consistent with not only itself, but with **P-3**. This follows since the methoxy moieties will not be displayed as a dramatic signal due to how similar they are relative to the other components within the polymers. FTIR data (Figure 3.2.8) for the ASyA series also appears to be consistent with not only itself but with **P-3**, which is similar to spectra of the AVA polymers. However, a peak near $1{,}100\,\mathrm{cm}^{-1}$ corresponding to an ether, which is present in all polymers, does show an increase as each sample increases in amount of methoxy.

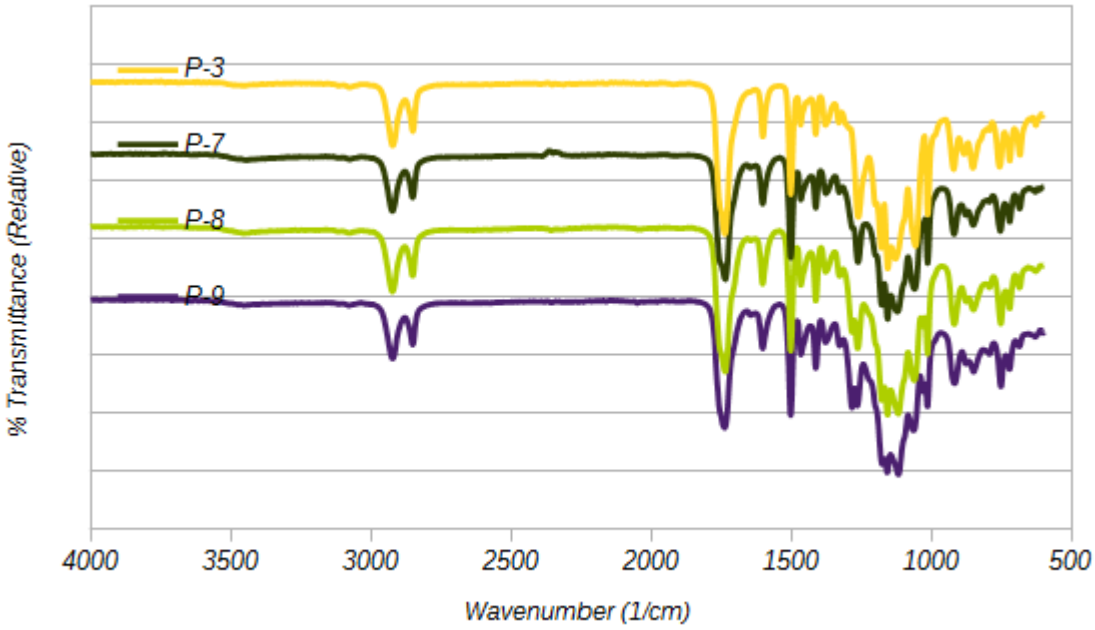

Figure 3.2.7: FTIR spectra of AVA series.

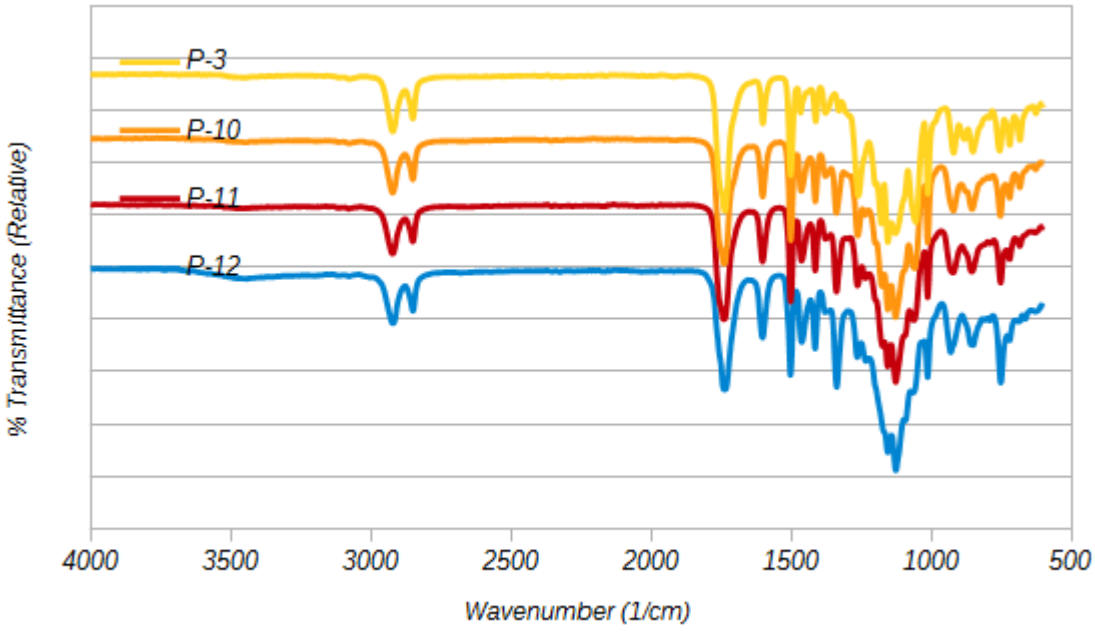

Figure 3.2.8: FTIR spectra of ASyA study.

PEGT

Average $\overline{M}_n$ values can be found in Appendix A. PEGT while offering minimal information, appeared to show a decrease in $\overline{M}_n$, as was expected from increasing the variety of species of monomers in the copolymer. An apparent decrease in $\overline{M}_n$ is observed, which is confirmed by GPC.

GPC

A plot of GPC chromatograms for AVA can be found in Figure 3.2.9. The sharp onset

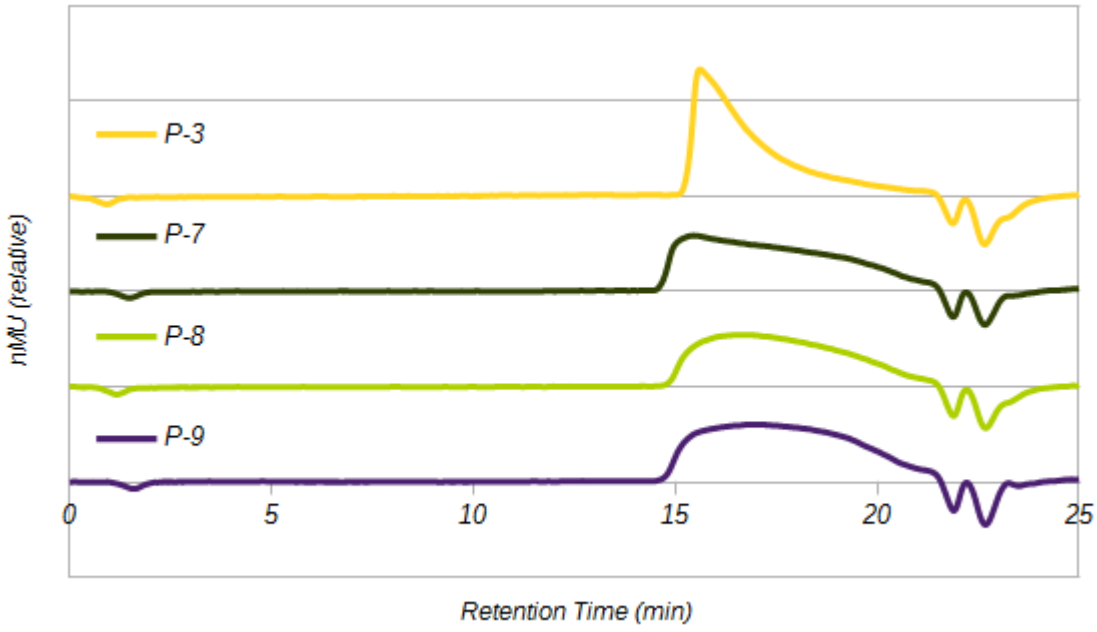

Figure 3.2.9: Composite plot of GPC chromatograms for AVA study.

of **P-3** is muted, but tailing is still present. Increasing the AVA content decreases the M_p and $\overline{M}_w$ while the $\overline{M}_n$ remains near consistent. Values from the GPC, found in Table B.1, showed a decrease in $\overline{M}_n$ and a more erratic Đ, which was broader than the majority of the samples from the catalyst study. Plots of retention time showed broadening toward lower molecular weights, indicating a reduction of the formation of high polymer.

A plot of GPC chromatograms for ASyA can be found in Figure 3.2.10. Although

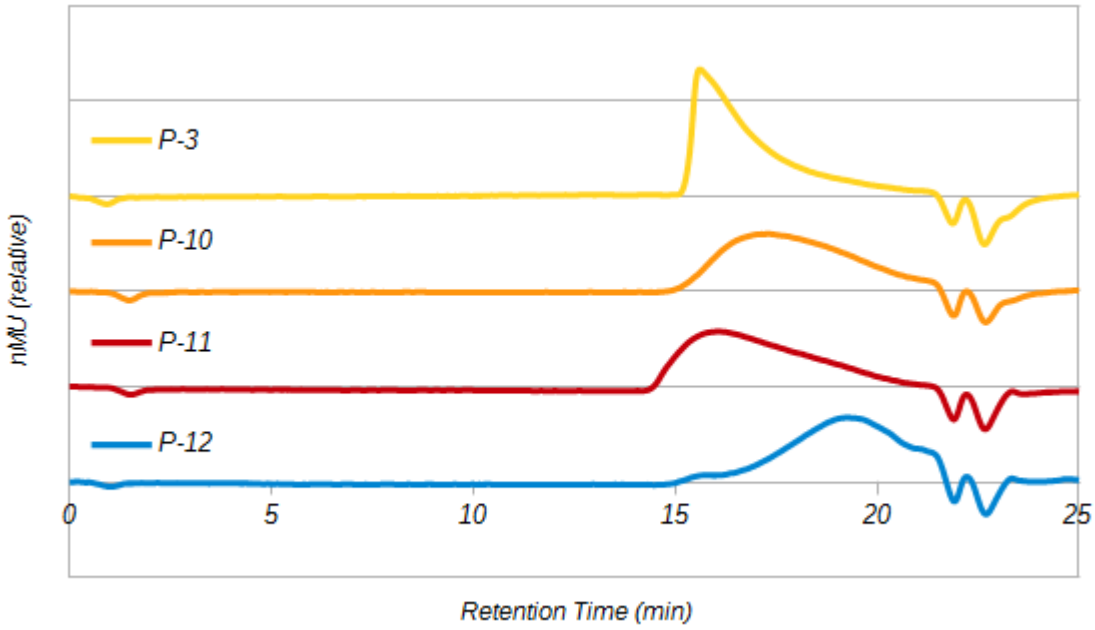

Figure 3.2.10: Composite plot of GPC chromatograms for ASyA study.

broadest, **P-11** had the greatest M_p, $\overline{M}_n$, and $\overline{M}_w$ of the renewable study. Tailing was still present in all of the samples, however **P-12** showed the worst characteristics with a majority of the curve falling outside of the calibrated region and even below the column limits.

DSC

A noticeable T_g is present in the polymer samples **P-7**, **P-8**, and **P-9**. The general trend of increasing T_g was observed from Figure 3.2.11b as expected from the increasing number of methoxy groups acting as points of steric hindrance with regard to the rotation of the chain.[31] Values from Table 3.7, which were from the inflection point at T_g, indicated a decrease. Melting and crystallization temperatures (T_m and T_c respectively) show decreases as expected with the exception of **P-8** having a slight increase in T_m. Again the methoxy pendant groups play a significant role, however

Table 3.7: Values for polymers in renewable study obtained from DSC.[a]

Code	T_g/°C	$T_{m,onset}$/°C	T_m/°C	T_{meso}/°C	$T_{c,onset}$/°C	T_c/°C	T_{meso}/°C
P-7	40	108	130	183	107	97	178
P-8	36	108	135	180	104	95	172
P-9	37	107	128	n.o.	97	89	137
P-10	43	118	136	n.o.	112	107	n.o.
P-11	37	99	120	n.o.	109	102	n.o.
P-12	15	77	107	n.o.	86	77	n.o.

[a] All values are taken from the second heating or cooling curve.
[b] Not observed.

here they prevent formation of closely packed chains. The chains thereby require less energy to break the intramolecular forces holding them together and can more readily enter a state with less energy. Values from heating and cooling thermograms (3.2.11a and 3.2.11b, respectively) are found in Table 3.7. A T_g was markedly present in the polymers containing AVA. Relative to the T_m of **P-3**, a decrease is clearly present with an increase in heat of melting as the amount of renewable monomer increases. This general trend was predicted due to the increasing number of methoxy groups causing the polymer chains to become less tightly bound. A smaller percentage of crystallinity was anticipated as AVA was increased. Another startling observation was present on the cooling curve with the partially renewable polymers: an apparent T_{meso} in **P-7** and **P-8**. Since the proper instrumentation was not readily available for full analysis of the samples with regard to behavior at the state in question the observations can only be speculative. Nagata observed similar properties which were describes as a nematic mesophase transition.[28] Without the necessary tools, anything beyond an assignment of an apparent mesophase is beyond the scope of this thesis.

With ASyA, there were more pronounced trends and magnitudes due predominately to double the methoxy groups present relative to the respective counter polymer. Values from heating and cooling thermograms (3.2.12a and3.2.12b, respectively) are in Table 3.7. Thermal analysis offered a more dramatic change as compared to

AVA polymers. A visible increase in T_g is observed, as well as a reduction in T_m. **P-12** shows a significantly lower T_m which could be attributed to such a low $\overline{M}_n$. Unlike the AVA polymers, no strong T_{meso} was observed. Since the $\overline{M}_n$ of **P-12** was so low, and the weight can have an impact on the thermal properties at such values, the thermal data may be considered as an outlier. Values of T_g appear to decrease in Table 3.7, however they increase in Figure 3.2.12a. The broadness of the T_g region, as well as shallowness or stray inflections could shift the calculated value. Observing what could effectively be termed T_{endset}, an increase in T_g could be realized.

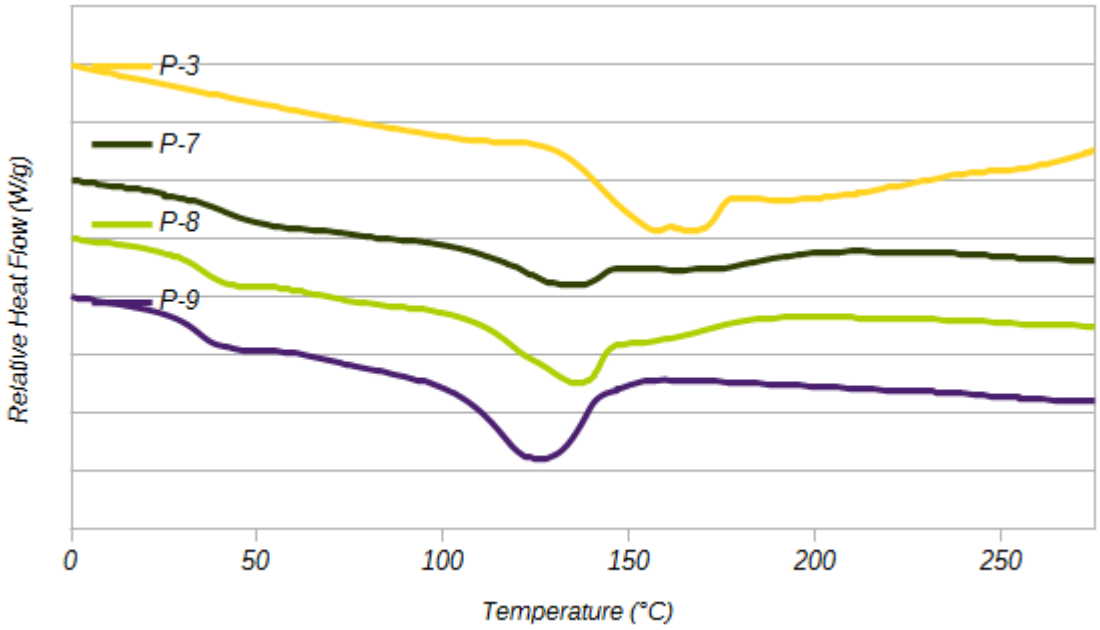

(a) Heating curves.

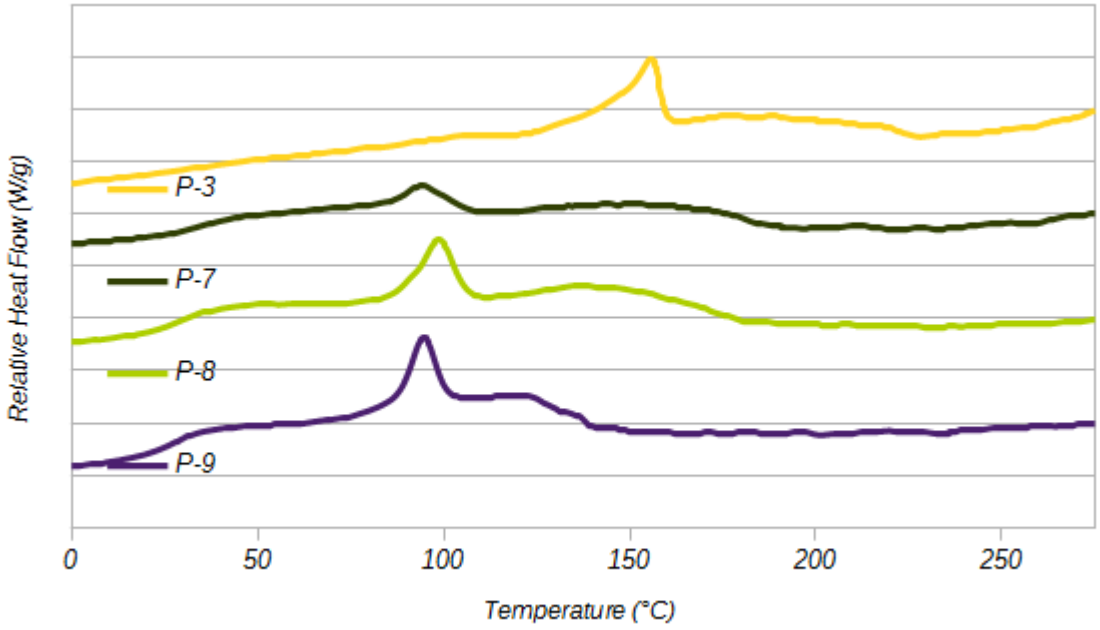

(b) Cooling curves.

Figure 3.2.11: Composite plot of (a) heating curves and (b) cooling curves for AVA study. Exotherm up.

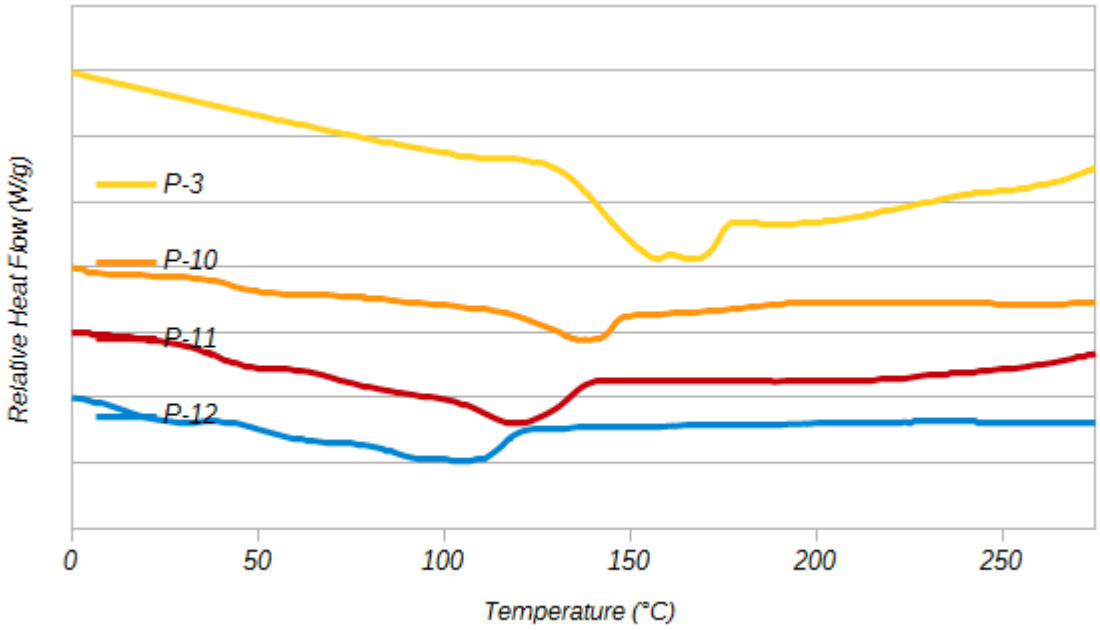

(a) Heating curves.

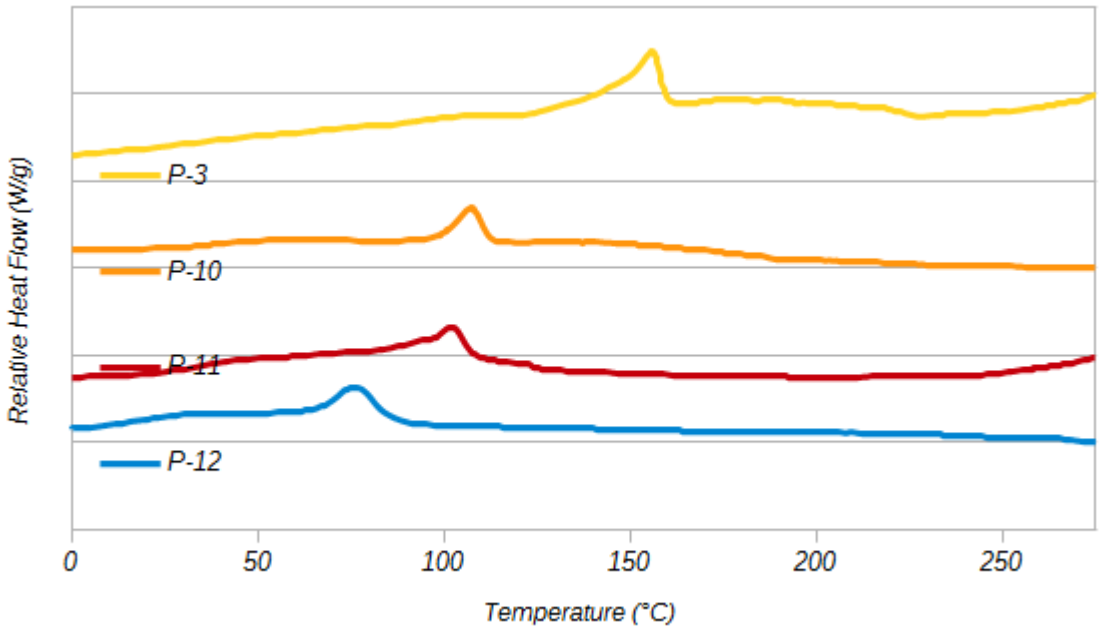

(b) Cooling curves.

Figure 3.2.12: Composite plot of (a) heating curves and (b) cooling curves for ASyA study. Exotherm up.

TGA

Figure 3.2.13 shows overlaid weight percent curves from **P-3** and the three AVA polymers. A gradual decrease in T_{onset} and T_{50} were observed as the amount of AVA

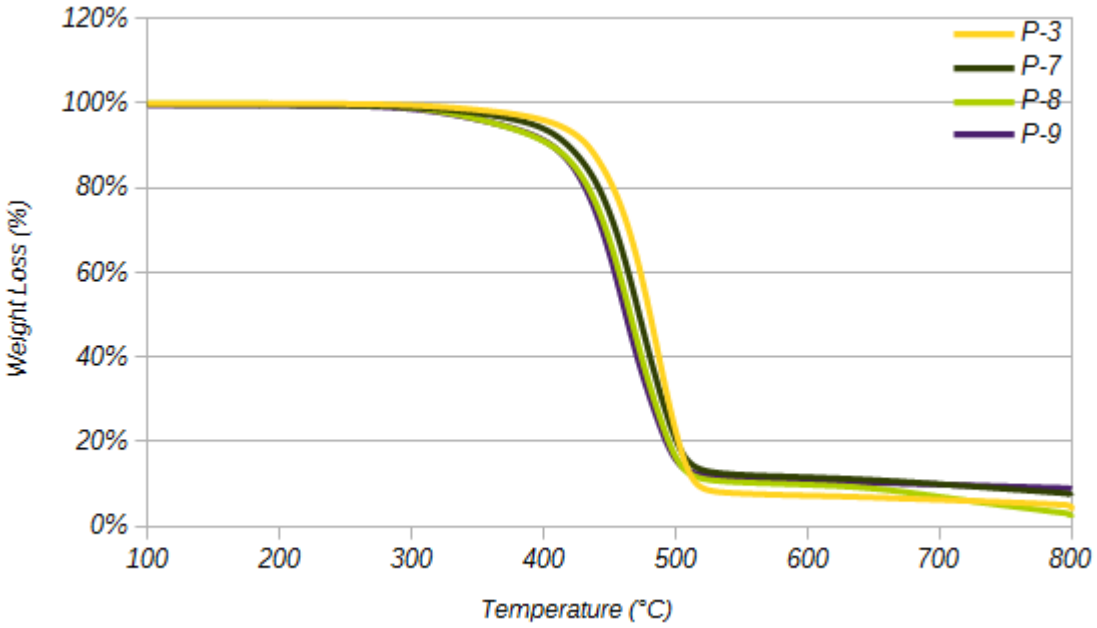

Figure 3.2.13: Composite plot of TGA weight percent curves.

was increased, however there was a slight increase in the amount of residue remaining after degradation. Values from Figure 3.2.13 are found in Table 3.8. A drawback of

Table 3.8: Values for polymers in renewable study obtained from TGA.

Code	T_{onset}/°C	T_{50}/°C	T_{endset}/°C	Weight Loss/%
P-7	432	473	503	88.5
P-8	424	467	498	90.0
P-9	421	461	494	89.6
P-10	432	468	495	92.8
P-11	422	457	484	90.4
P-12	429	464	485	87.1

the increase in renewable content was a reduction in thermal stability, as was seen through TGA. An overall reduction in temperatures of degradation, T_{onset}, T_{50}, and

T_{endset}, all were present in the AVA series. Likely, the methoxy groups are breaking off earlier than the main backbone of the polymer chain. Slight shouldering was seen in the derivative weight loss curves in Appendix C, however the presence extends to the catalyst study polymers, lessening the likelihood that early loss of methoxy is the primary factor in the reduction in T_{onset}. Furthermore, the mass of the methoxy present is significantly less than the relative mass of the polymer, and no double peak is present as might be indicative of the methoxy acting sacrificially or as a plasticizer, similar to observations by Yang et al..[42]

Figure 3.2.14 shows overlaid weight percent curves from **P-3** and the three ASyA polymers. Due to a greater number of methoxy groups present, the changes are more

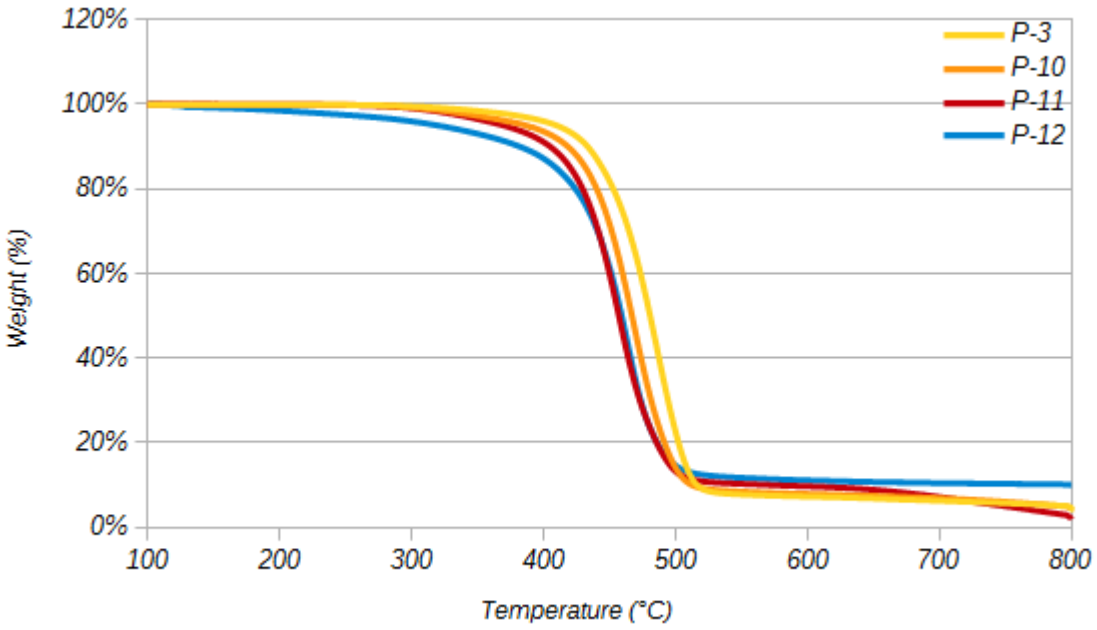

Figure 3.2.14: Composite plot of TGA weight percent curves.

pronounced. The gradual decrease in T_{onset} and T_{50} as the amount of ASyA was increased produces earlier degradation as compared to the cognate AVA polymer. The slight increase in post-degradation residue was also observed. Values from Figure 3.2.14 are found in Table 3.8. Degradation of the polymers as measured by TGA

showed a slightly off of predicted behavior; **P-12** has a higher T_{50} and T_{endset} than **P-11**. Upon further examination of the TGA curve, it was noticed that there was a gradual decay of **P-12**, which would be expected if there was a broad low $\overline{M}_n$.

3.3 Solution Polymerization Experiment

One possible solution to the hindrances, e.g., high viscosity of the product, caused as the reaction progresses is solution polymerization. Hot dimethyl sulfoxide (DMSO), HFIP, trifluoroacetic acid (TFA), and Ph:TCE can dissolve the polymer.[28] Of these, DMSO was selected for a trial solution polymerization due to it being the only non-halogen in the set and having a slightly higher boiling point. The trial was microscale and appeared to proceed, however the yield was insufficient and the solids quickly dissolved in a water/methanol rinse during filtration, leading to a conjecture that there was an unintended side reaction. Despite this poor attempt, there may be a possibility that a solution reaction could provide a better route for synthesis by allowing better movement and thereby contact of the reactive sites.

4. Conclusions

Acetylated vanillic acid (AVA) and acetylated syringic acid (ASyA), two inexpensive raw materials found in bagasse, were both incorporated into a copolymer system in lieu of 4-acetoxybenzoic acid (BA). Dodecanedioic acid (DA) was applied as an aliphatic renewable monomer. Results from FTIR and ^{1}H NMR confirmed an increasing amount of methoxy constituents in the polymer system with the increase in aromatic renewable monomers present. The polymer remained semi-crystalline even with the incorporation of over 50 % renewable content between either AVA or ASyA and DA. Systematic incorporation of the renewable aromatic monomers yielded a direct reduction in T_m. Even the polymers with contents of renewable aromatic monomers in excess of BA showed marked melting peaks. A change in glass transition temperature (T_g) with increase in contents of AVA or ASyA was not as pronounced as to make definitive conclusions. However, T_{endset} of the T_g displayed an increase and the overall region is broader. Furthermore, the DSC plot of sample of the copolymer with the highest ASyA content (**P-12**) showed a relatively low T_g which could stem from an exceptionally low molecular weight of the sample itself. Samples appeared to be thermally stable according to TGA. Some samples included a large high molecular weight fraction, however major tailings were observed, denoting a significant amount of lower molecular weight polymer. This high contents of low molecular weight polymer is most likely due to degradation of the polymers over the relatively long polymerization times (27 h) applied. Although not fully sustainable, due to the non-renewable content, these polymers are a step toward greener polymers.

5. Suggestions for Future Work

It is highly advisable to shorten the overall polymerization time, since longer exposure of the polymer under the high temperature appears to cause degradation of the polymer and cause a lower molecular weight fraction and broadening of the molecular weight distribution (MWD). One way the time can be shortened is to switch to Phase II (reduced pressure) once the formation of distillate reaches a plateau. Furthermore, the time for Phase II can be shortened when the polymer reaches a high viscosity and stirring becomes inefficient, even if a portion of the product can still be stirred. Since HQ and BA were not naturally sourced nor are they considered renewable resources, it is advised to either find a replacement or new synthetic route to produce them. While the BA is offset by the inclusion of either AVA and ASyA, it was still necessary for synthesis to achieve sufficient crystallinity. The observation that *p*TSA had a superior reaction rate out of the catalysts employed could provide a starting point for future research in reaction performance. Halogenated solvents were necessary for dissolution of the samples; alternative solvents would further push the green aspect of these polymers.

Glossary

amorphous irregular arrangement of molecules; no long-range order;[43] not crystalline, has no sharp T_m[44]

anisotropic properties are dependent upon orientation or direction;[43] see isotropic

biobased composed or derived in whole or in part of biological products issued from the biomass; not necessarily environmentally friendly nor biocompatible nor biodegradable;[45] see also plant-based

biodegradable qualifier for a substance that is susceptible to biodegradation[46]

biodegradation degradation due to enzymatic activities of cells[47]

biomacromolecule a large molecule formed by any living organism[48]

biomass materials from living organisms[49]

biopolymer a polymer made of one type of biomacromolecule[50]

biorefinery facility designed to process biomass into usable products and energy[51]

co-generation facility designed to produce electricity as well as heat

condensation polymerization combining of monomers such that a small molecule is formed as a byproduct of the reaction[44]

crystalline ordered structure; relatively long-range systematic arrangement

drop-in replacement direct substitution of one material for another

feedstock bulk source of material

green modifier denoting consideration of the concepts outlined in green chemistry

green chemistry design, processing, and use of chemicals in such a manner that there is a reduction or elimination of harm to life and the environment in general[52]

green movement societal trend to promote environmentally friendly practices

greenwashing marketing claims, often unsubstantiated, of a product, process, or system having environmentally friendly characteristics

isotropic properties are uniform or consistent in all directions;[43] see anisotropic

life-cycle assessment a method to quantitatively assess the impacts of a product from beginning-of-life to end-of-life by looking at environmental consequences

mesophase equilibrium state of a liquid crystalline system where there is less order then a pure crystal and less mobility than an isotropic liquid[43]

macromolecule large molecule[43]

monomer the basic chemical unit repeated to form a polymer[43]

non-renewable describing a resource that cannot be replenished

petrochemical chemical obtained from petroleum; see petroleum-based

petroleum-based derived from petroleum or other fossil resources; chemicals are refined from crude oil

plant-based derived from plant matter; chemicals are extracted from vegetative material or portions of the plant are used in bulk

plastic colloquial term for predominately polymeric materials; has ability to be flow processed[53]

polymer substance composed of macromolecules;[54] long covalently bonded chains of atoms[43]

renewable describing a resource that can be replenished

step-growth polymerization polymerization in which all species, both monomers and chains, can react to form higher order polymer;[43] see also condensation polymerization

sustainability developments that meet the needs of the present without sacrificing the ability of future generations to meet their needs;[55] self sufficient or able to maintain its own equilibrium such that it does not reach an unintended terminus

sustainable a process or practice that adheres to the concept of sustainability

Acronyms

Đ dispersity

^{1}H NMR proton nuclear magnetic resonance imaging

2,5-FDCA 2,5-furandicarboxylic acid

ACD/Labs Advanced Chemistry Development, Inc.

ASyA acetylated syringic acid

AVA acetylated vanillic acid

BA 4-acetoxybenzoic acid

$CDCl_3$ deuterated chloroform

CRU chemical repeat unit

DA dodecanedioic acid

DCM/TFA dichloromethane/trifluoroacetic acid

DMSO dimethyl sulfoxide

DSC differential scanning calorimetry

EtOH ethanol

FTIR Fourier transform infrared spectroscopy

GPC gel permeation chromatography

ΔH_m melt enthalpy

HFIP hexafluoroisopropanol

HPLC high pressure liquid chromatography

HQ 1,4-diacetoxybenzene

KnowItAll® KnowItAll® Informatics System, Academic Edition

KOH potassium hydroxide

LCP liquid crystalline polymer

$\overline{M}_n$ number average molecular weight

M_p peak molecular weight

$\overline{M}_w$ weight average molecular weight

NaTFA sodium trifluoroacetate

PEGT polymer end-group titration

PET poly(ethylene terephthalate)

Ph:TCE 60:40 mixture by weight phenol:TCE

PMMA poly(methyl methacrylate)

***p*TSA** *p*-toluene sulfonic acid

Sb_2O_3 antimony(III)oxide

SyA syringic acid

T_{50} temperature of 50% weight loss

T_c crystallization temperature

T_{endset} endset temperature

T_g glass transition temperature

T_m melting temperature

T_{meso} mesophase transition temperature

T_{onset} onset temperature

T_r room temperature

TCE 1,1,2,2-tetrachloroethane

TFA trifluoroacetic acid

TFA-*d* deuterated trifluoroacetic acid

TGA thermogravimetric analysis

VA vanillic acid

$\overline{X}_n$ number average degree of polymerization

Zn/*p*TSA combination of $Zn(OAc)_2$ and pTSA

Zn/Sb combination of $Zn(OAc)_2$ and Sb_2O_3

Zn(OAc)$_2$ zinc diacetate

Bibliography

[1] Tolinski, M. *Plastics and Sustainability: Towards a Peaceful Coexistence between Bio-based and Fossil Fuel-based Plastics*; John Wiley & Sons, 2011.

[2] US EPA, OSWER, O. o. R. C.; Recovery, Plastics, Common Wastes & Materials. `http://www.epa.gov/wastes/conserve/materials/plastics.htm`.

[3] Al-Salem, S. M.; Lettieri, P.; Baeyens, J. *Waste Management* **2009**, *29*, 2625–43.

[4] Körner, I.; Redemann, K.; Stegmann, R. *Waste management (New York, N.Y.)* **2005**, *25*, 409–15.

[5] Scott, J. L.; Unali, G. In *Materials for a Sustainable Future*; Letcher, T. M., Scott, J. L., Eds.; Royal Society of Chemistry, 2012; Chapter 10, pp 279–324.

[6] Werpy, T.; Petersen, G. *Top Value Added Chemicals from Biomass Volume I: Results of Screening for Potential Candidates from Sugars and Synthesis Gas*; 2004.

[7] Hakeem, K. R.; Jawaid, M.; Alothman, O. Y. *Agricultural Biomass Based Potential Materials*; Springer, 2015.

[8] Ref. 7, p. 391.

[9] Miller, S. A. *ACS Macro Letters* **2013**, *2*, 550–554.

[10] How much oil is used to make plastic? - FAQ - U.S. Energy Information Administration (EIA). `http://www.eia.gov/tools/faqs/faq.cfm?id=34&t=6`.

[11] Vert, M.; Doi, Y.; Hellwich, K.-H.; Hess, M.; Hodge, P.; Kubisa, P.; Rinaudo, M.; Schué, F. *Pure and Applied Chemistry* **2012**, *84*, 377–410.

[12] GreenBlue, *Labeling for Package Recovery*; 2011.

[13] PlantBottle: The Coca-Cola Company. `http://www.coca-colacompany.com/plantbottle-technology/`.

[14] Zara, C. Coca-Cola Company (KO) Busted For 'Greenwashing': PlantBottle Marketing Exaggerated Environmental Benefits, Says Consumer Report. 2013; `http://www.ibtimes.com/coca-cola-company-ko-busted-greenwashing-plantbottle-marketing-exaggerated-environmental-benefits`.

[15] Zara, C. Coca-Cola Company (KO) Responds To 'Greenwashing' Charge: Criticism Of PlantBottle Is 'Half-Empty'. 2013; `http://www.ibtimes.com/coca-cola-company-ko-responds-greenwashing-charge-criticism-plantbottle-half-empty-1403284`.

[16] Anastas, P. T.; Warner, J. C. *Green Chemistry: Theory and Practice*; Oxford University Press, 2000.

[17] Hatakeyama, H.; Hatakeyama, T. *Advances in Polymer Science*; 2012; pp 1–34.

[18] Lebo, S. E. J.; Gargulak, J. D.; McNally, T. J. *Kirk-Othmer Encyclopedia of Chemical Technology*; John Wiley & Sons, Inc.: Hoboken, NJ, USA, 2000.

[19] Fahlman, B. D. *Materials Chemistry*, 2nd ed.; Springer, 2011.

[20] Gross, R. A.; Kalra, B. *Science* **2002**, *297*, 803–807.

[21] Commons, W. Lignin Structure. 2007; `https://commons.wikimedia.org/wiki/File:Lignin_structure.svg#/media/File:Lignin_structure.svg`.

[22] Mingos, D. M. P. In *Structure and Bonding*; Mingos, D. M. P., Ed.; Springer Berlin Heidelberg, 1999; Vol. 94.

[23] Miri, M. J.; Nori, K. E.; Andrew, R. M.; Ge, C. *Renewable and Sustainable Polymers*; American Chemical Society, 2011; Vol. 1063; Chapter 2, pp 11–35.

[24] Wilsens, C. H. R. M.; Verhoeven, J. M. G. A.; Noordover, B. A. J.; Hansen, M. R.; Auhl, D.; Rastogi, S. *Macromolecules* **2014**, *47*, 3306–3316.

[25] Mialon, L.; Vanderhenst, R.; Pemba, A. G.; Miller, S. A. *Macromolecular Rapid Communications* **2011**,

[26] Wilsens, C. H. R. M.; Noordover, B. A. J.; Rastogi, S. *Polymer* **2014**, *55*, 2432–2439.

[27] Laurichesse, S.; Avérous, L. *Progress in Polymer Science* **2014**, *39*, 1266–1290.

[28] Nagata, M. *High Performance Polymers* **2001**, *13*, S265–S274.

[29] Mialon, L.; Pemba, A. G.; Miller, S. A. *Green Chemistry* **2010**, *12*, 1704.

[30] Thiyagarajan, S.; Vogelzang, W.; J. I. Knoop, R.; Frissen, A. E.; van Haveren, J.; van Es, D. S. *Green Chemistry* **2014**, *16*, 1957–1966.

[31] Painter, P. C.; Coleman, M. M. *Fundamentals of Polymer Science: An Introductory Text*, 2nd ed.; CRC Press, 1998.

[32] Odian, G. *Principles of Polymerization*, 4th ed.; John Wiley & Sons, Inc.: Hoboken, New Jersey, 2004.

[33] Murphy, J. L.; Dalsin, J. L.; Lyman, A. N.; Vollenweider, L. L.; Broussard, J. L.; Winterbottom, N.; Koepsel, J. T. Mono-layer thin film adhesive compounds and methods of synthesis and use. 2014; `https://www.google.com/patents/US20140030944`.

[34] Sigma-Aldrich Quality Control Team, *Material Matters* **2006**, *1.1*.

[35] Rogers, M. E., Long, T. E., Eds. *Synthetic Methods in Step-Growth Polymers*; John Wiley & Sons: Hoboken, NJ, USA, 2003; pp 69–74.

[36] Pohl, H. A. *Analytical Chemistry* **1954**, *26*, 1614–1616.

[37] Agilent PL HFIPgel GPC Columns. 2013.

[38] Japu, C.; de Ilarduya, A. M.; Alla, A.; Muñoz Guerra, S. *Polymer* **2013**, *54*, 1573–1582.

[39] Robert, S. M.; Francis, W. X.; David, K. J. *Spectrometric Identification of Organic Compounds*, 7th ed.; Wiley, 2005.

[40] Ref. 39, p. 153.

[41] Cho, K.; Li, F.; Choi, J. *Polymer* **1999**, *40*, 1719–1729.

[42] Yang, X.; Clénet, J.; Xu, H.; Odelius, K.; Hakkarainen, M. *Macromolecules* **2015**, A–J.

[43] Case Western Reserve University, Glossary. 2004; `http://plc.cwru.edu/tutorial/enhanced/files/glossary/glossary.htm`.

[44] Harper, C. A. In *Modern Plastics Handbook*; Harper, C. A., Ed.; McGraw-Hill, 2000.

[45] Ref. 11, entry 16.

[46] Ref. 11, entries 20, 21.

[47] Ref. 11, entries 22, 23.

[48] Ref. 11, entry 28.

[49] Ref. 11, entry 29.

[50] Ref. 11, entry 32.

[51] Kamm, B. Definition and technical status of Biorefineries. 2008.

[52] Ref. 11, entry 154.

[53] Ref. 11, entry 89.

[54] Ref. 11, entry 90.

[55] Ref. 11, entry 159.

A. PEGT Data

Table A.1: Data values from end group titrations for the determination of $\overline{M}_n$.

Code	$\overline{M}_n$[a] / g mol^{-1}	Notes
P-1	2,700	
P-2	2,000	Polymer brown in solution[b]
P-3	4,900	
P-4	3,000	
P-5	1,600	
P-6	1,300	
P-7	2,800	Polymer brown in solution[b]
P-8	2,400	
P-9	1,600	Polymer brown in solution[b]
P-10	2,500	
P-11	2,600	
P-12	1,600	Polymer brown in solution[b]

[a] Calculated from Equation 2.5.3

[b] Color change was determined by visual observations relative to a standard. Hues caused by the solution of the polymers altered the saturation of the end point.

B. GPC Data

Table B.1: Values for polymers in catalyst, AVA, and ASyA studies obtained from GPC.

Code	M_p/g mol^{-1}	$\overline{M}_n$/g mol^{-1}	$\overline{M}_w$/g mol^{-1}	Đ	
P-1	990	720	1,300	1.8	[a]
P-2	1,400	840	2,000	2.4	
P-3	10,300	1,800	4,400	2.5	
P-4	3,900	970	2,300	2.4	
P-5	1,600	860	1,800	2.1	
P-6	9,500	1,300	4,300	3.3	
P-7	12,500	1,100	4,500	4.0	
P-8	3,800	1,200	3,200	2.7	
P-9	2,600	1,000	3,100	3.0	
P-10	2,300	930	2,200	2.4	
P-11	6,400	1,400	4,500	3.3	
P-12	690	510	1,200	2.4	

Column limits ranged from 1,000,000 to 500 g mol^{-1}. Values outside of that range are projected based on the calibration data of the PMMA standards.

[a] Value as calculated by instrument. Due to low M_p and greater error associated with much of the distribution lying outside of the calibrated region the Đ is reported with little confidence.

The following are plots of the MWDs of each polymer sample, **P-1** through **P-12**. Data collected from GPC was converted to MWD via the calibration curve generated from the Cirrus calibration data and plotted in LibreOffice. Due to the significant tailing for most of the polymers reported, values in Table B.1 cannat be deemed reliable. Comparisons of the distribution curves, however, provide an indication of the relative MWDs and are sufficient enough to draw conclusions.

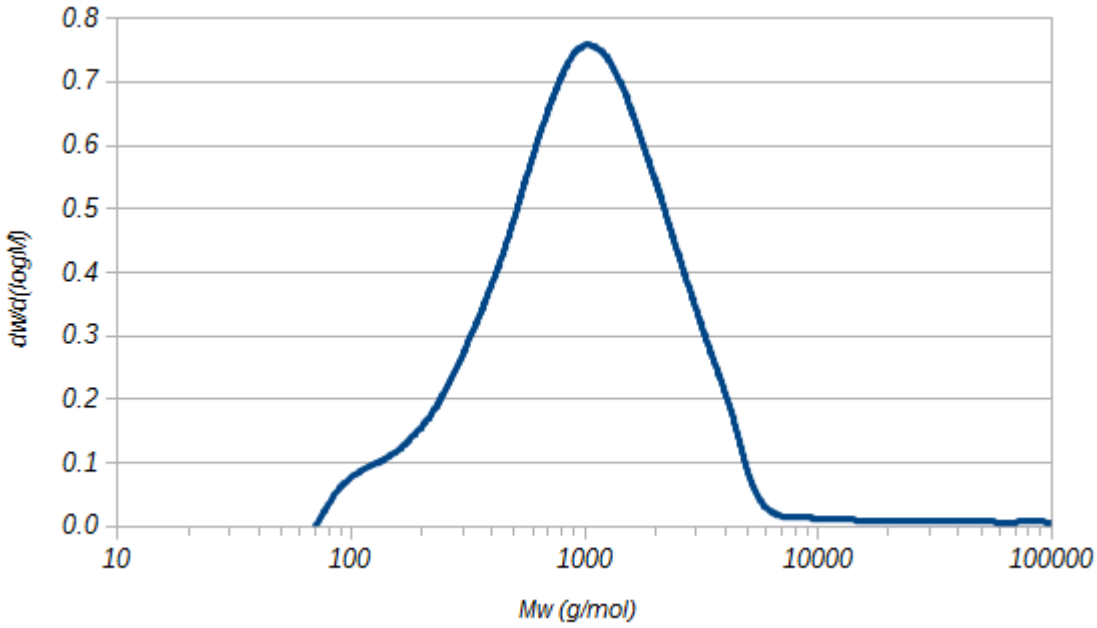

Figure B.0.1: MWD for **P-1**.

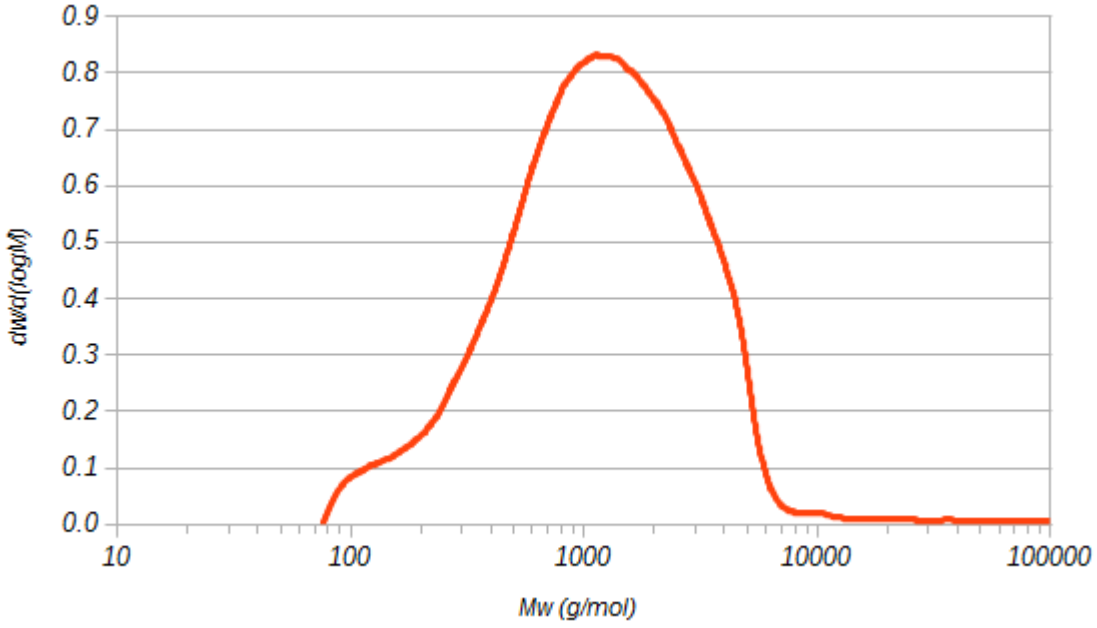

Figure B.0.2: MWD for **P-2**.

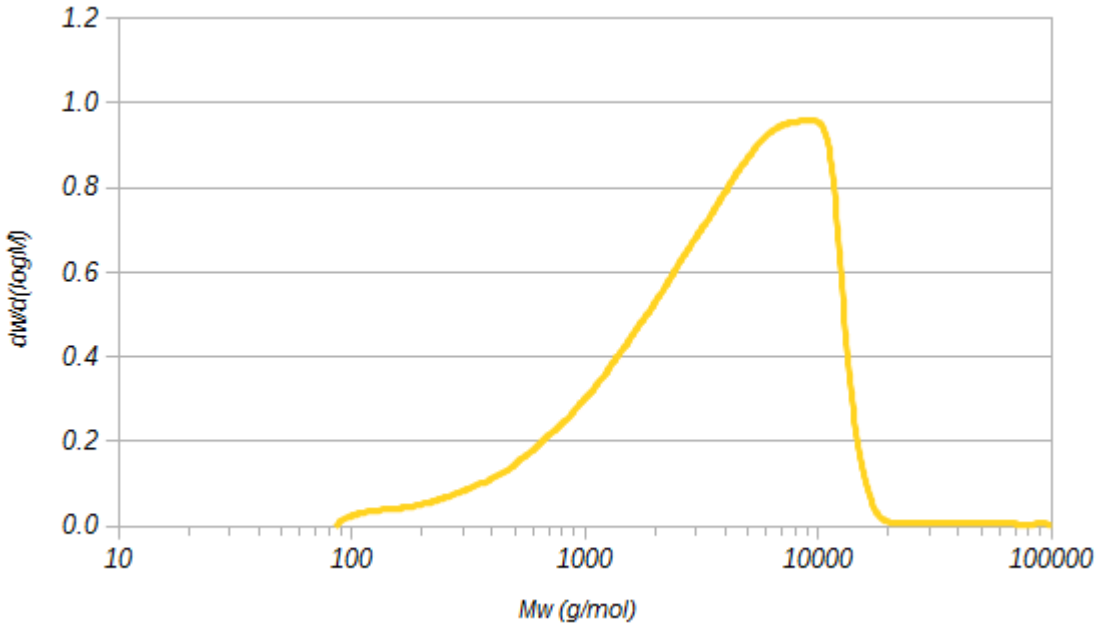

Figure B.0.3: MWD for **P-3**.

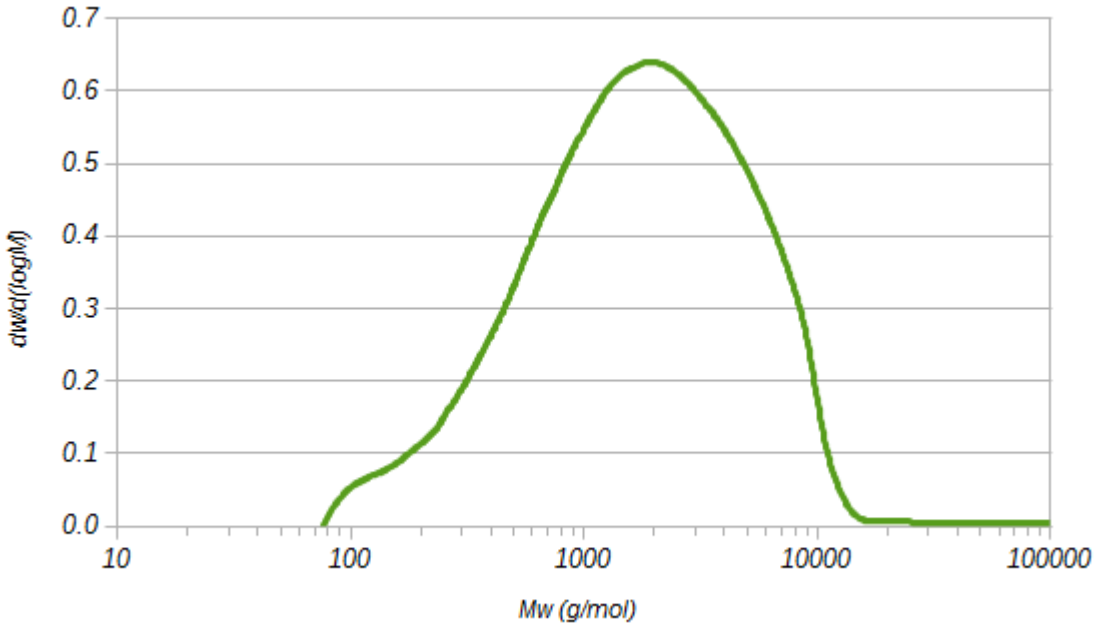

Figure B.0.4: MWD for **P-4**.

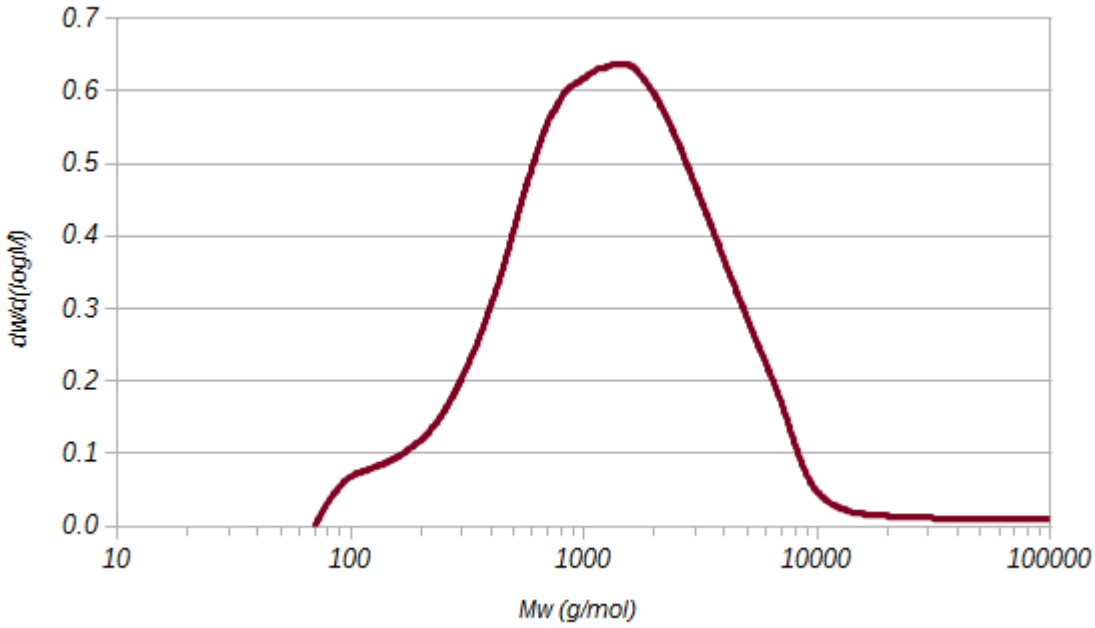

Figure B.0.5: MWD for **P-5**.

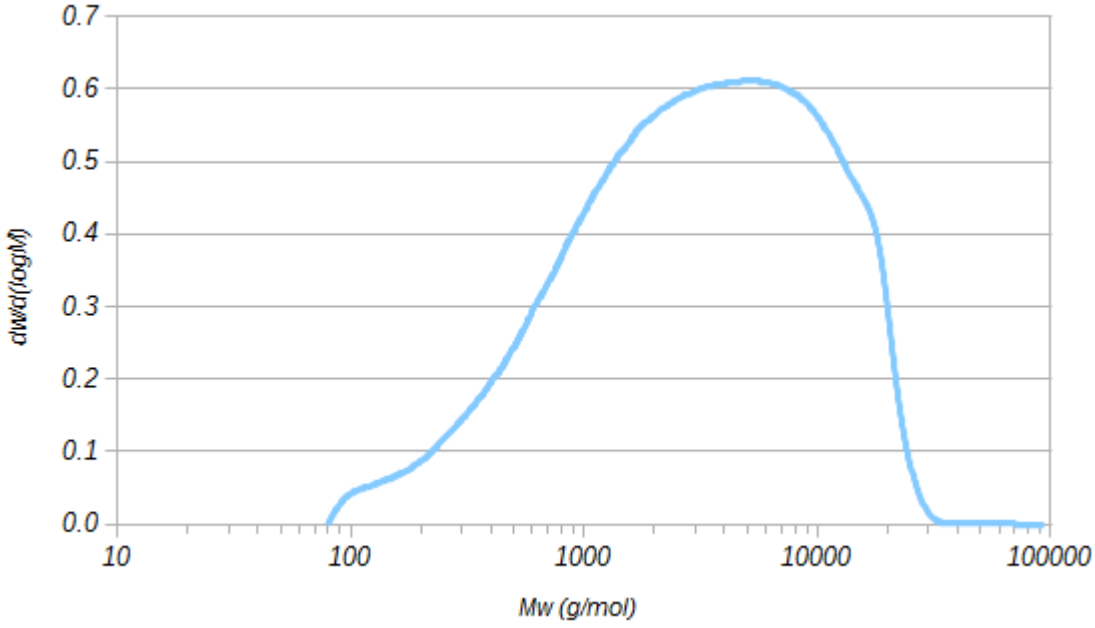

Figure B.0.6: MWD for **P-6**.

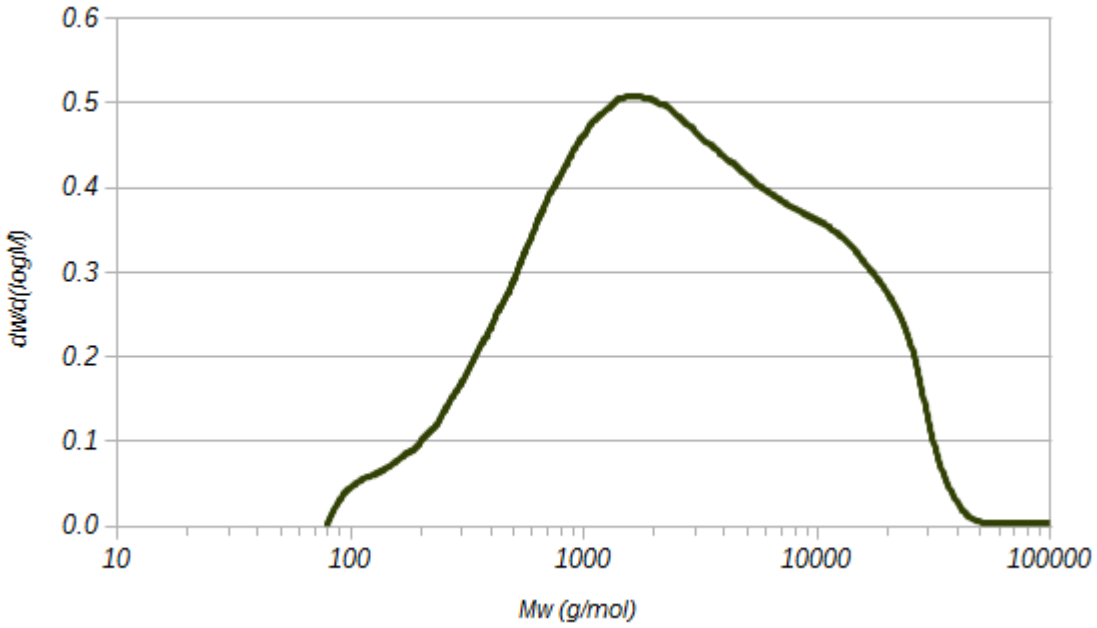

Figure B.0.7: MWD for **P-7**.

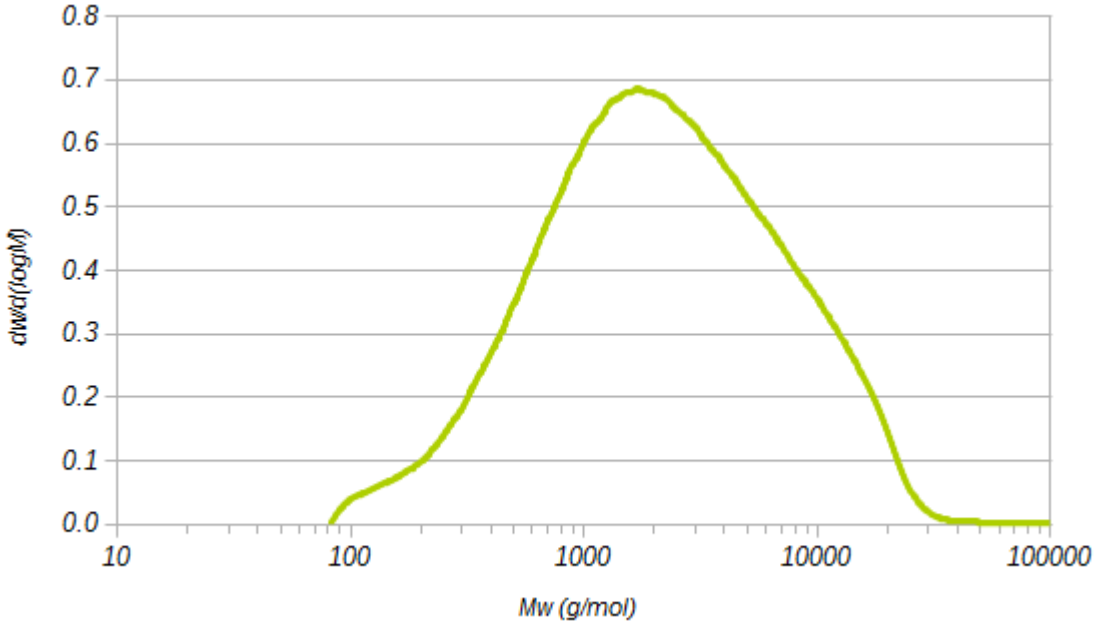

Figure B.0.8: MWD for **P-8**.

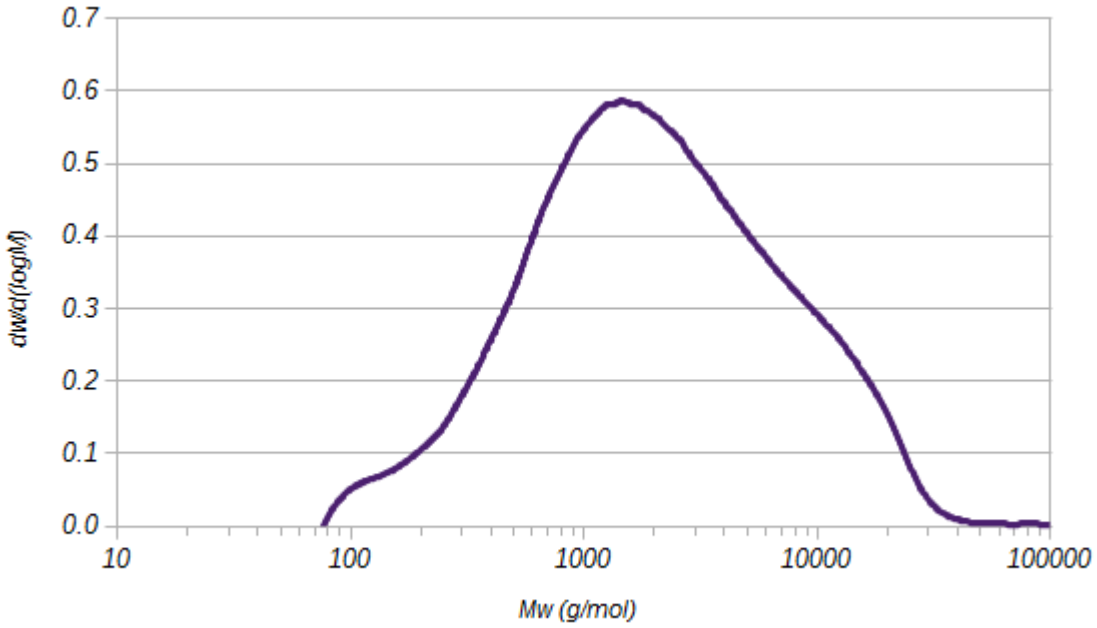

Figure B.0.9: MWD for **P-9**.

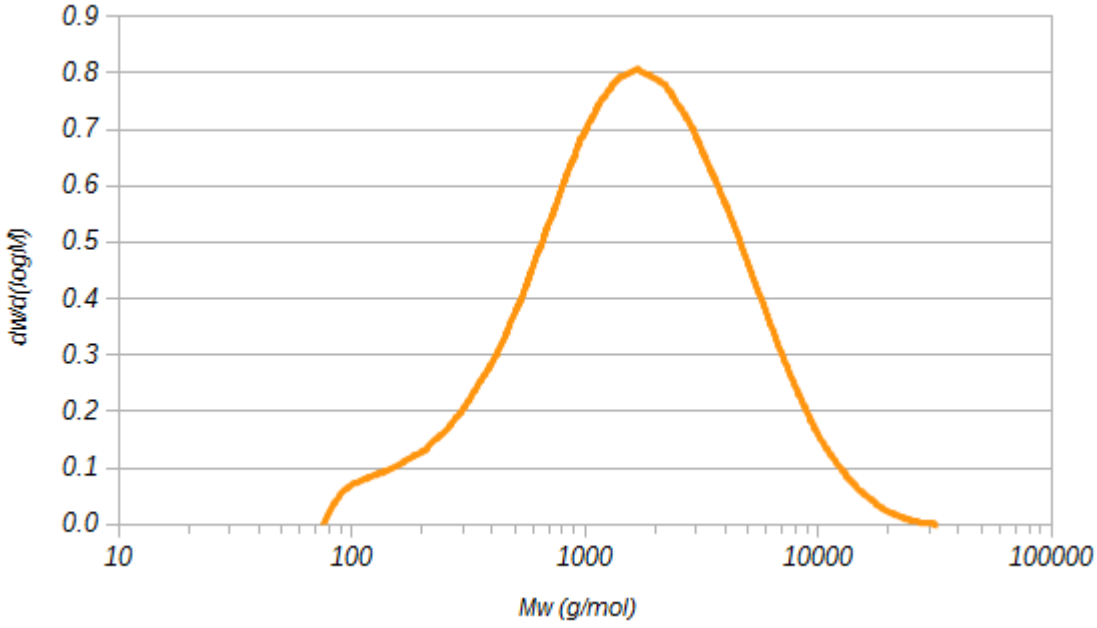

Figure B.0.10: MWD for **P-10**.

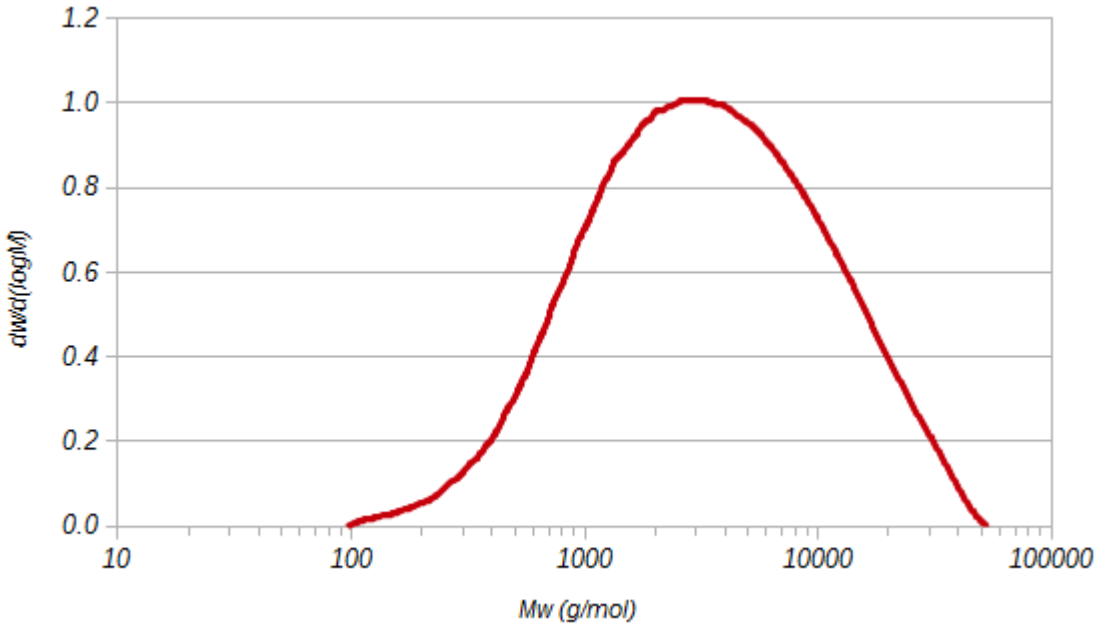

Figure B.0.11: MWD for **P-11**.

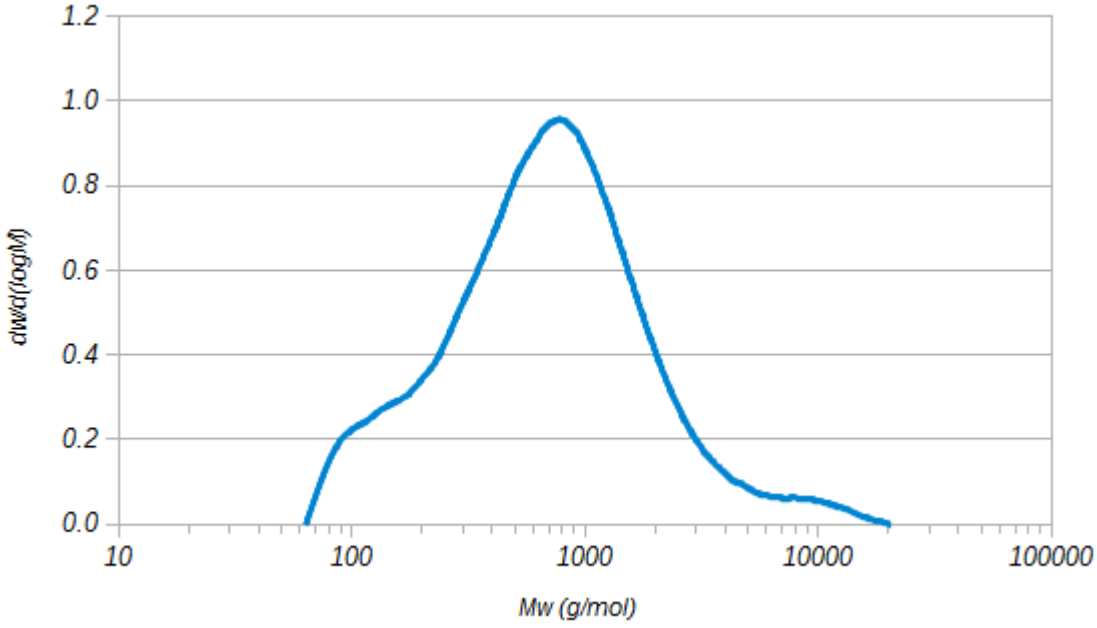

Figure B.0.12: MWD for **P-12**.

C. TGA Data

The following are isolated plots of the weight percent (%) of each polymer sample, **P-1** through **P-12** with the accompanying derivative percent weight loss ($\%\,^{\circ}C^{-1}$) for comparison.

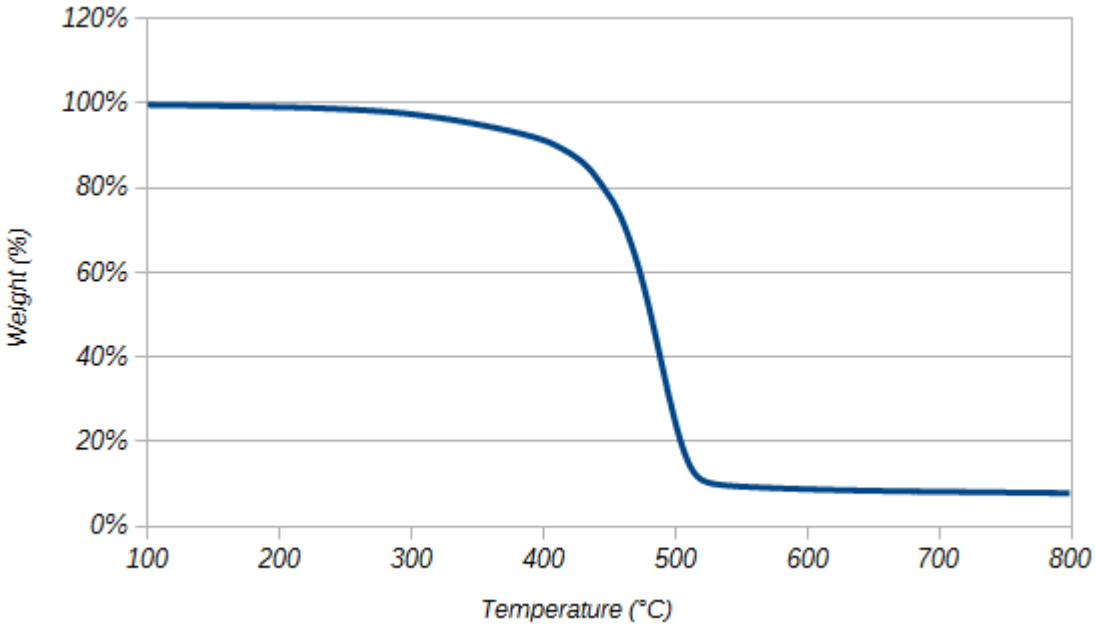

(a) Weight loss.

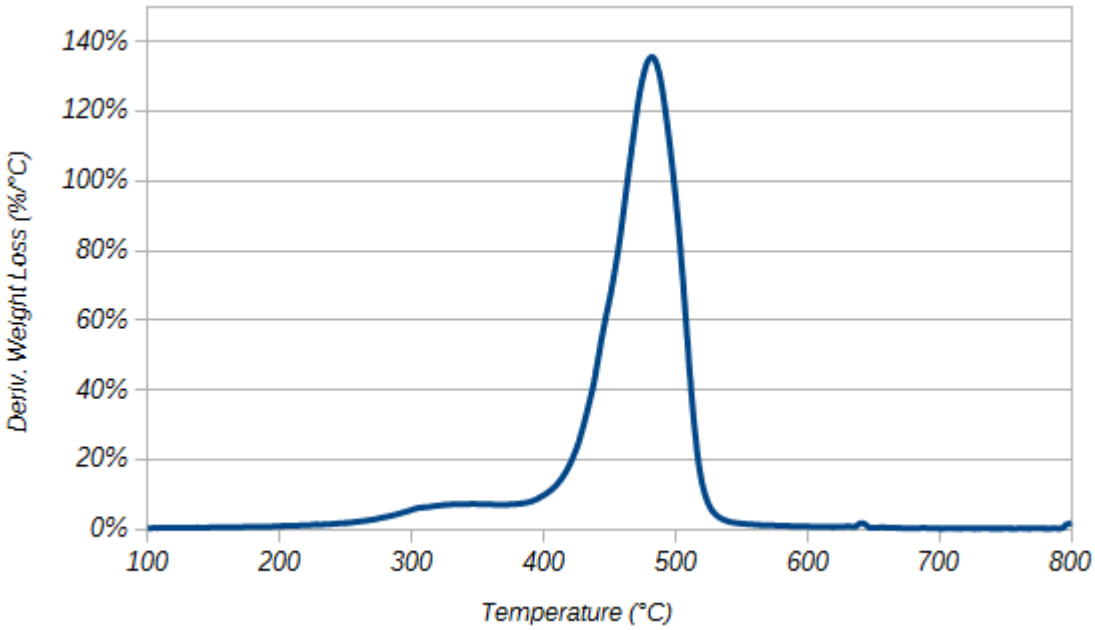

(b) Derivative weight loss.

Figure C.0.1: TGA plots of (a) weight percent and (b) derivative weight loss for **P-1**.

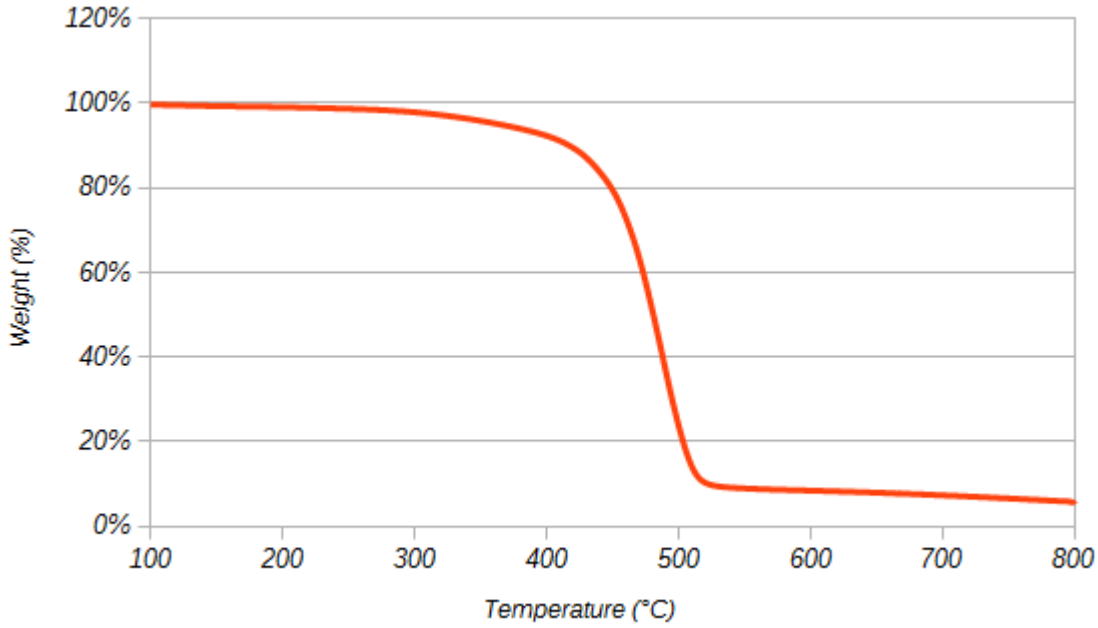

(a) Weight loss.

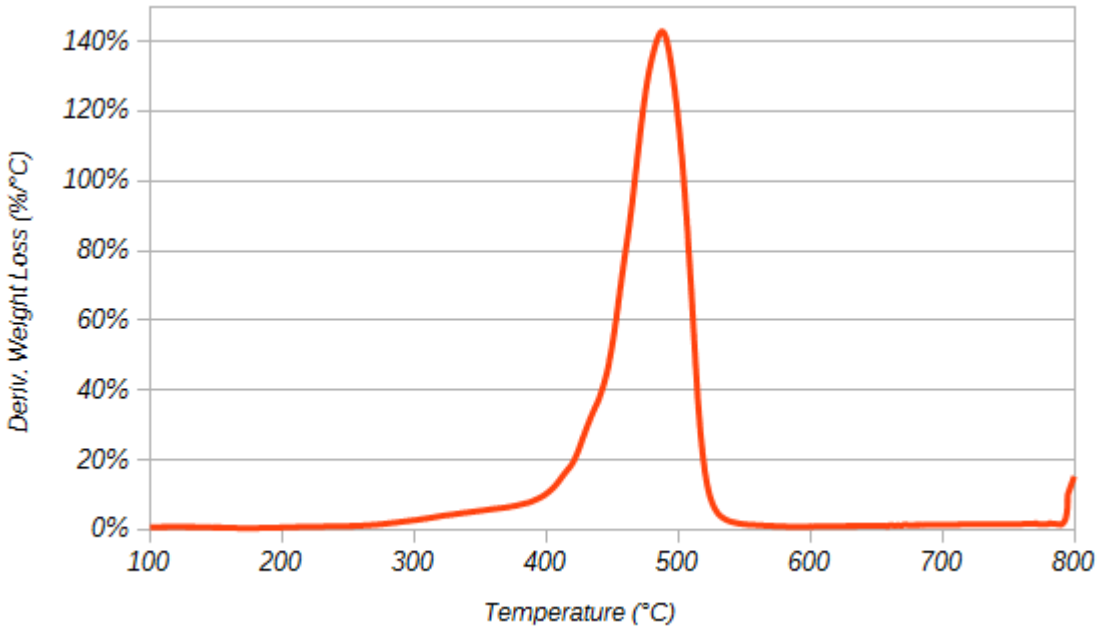

(b) Derivative weight loss.

Figure C.0.2: TGA plots of (a) weight percent and (b) derivative weight loss for **P-2**.

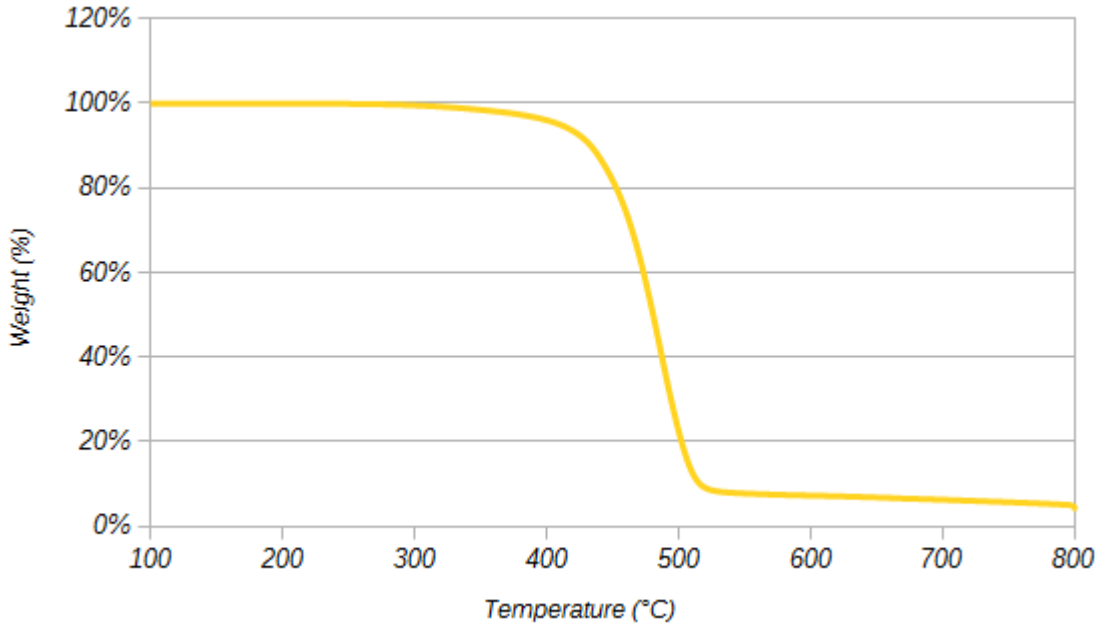

(a) Weight loss.

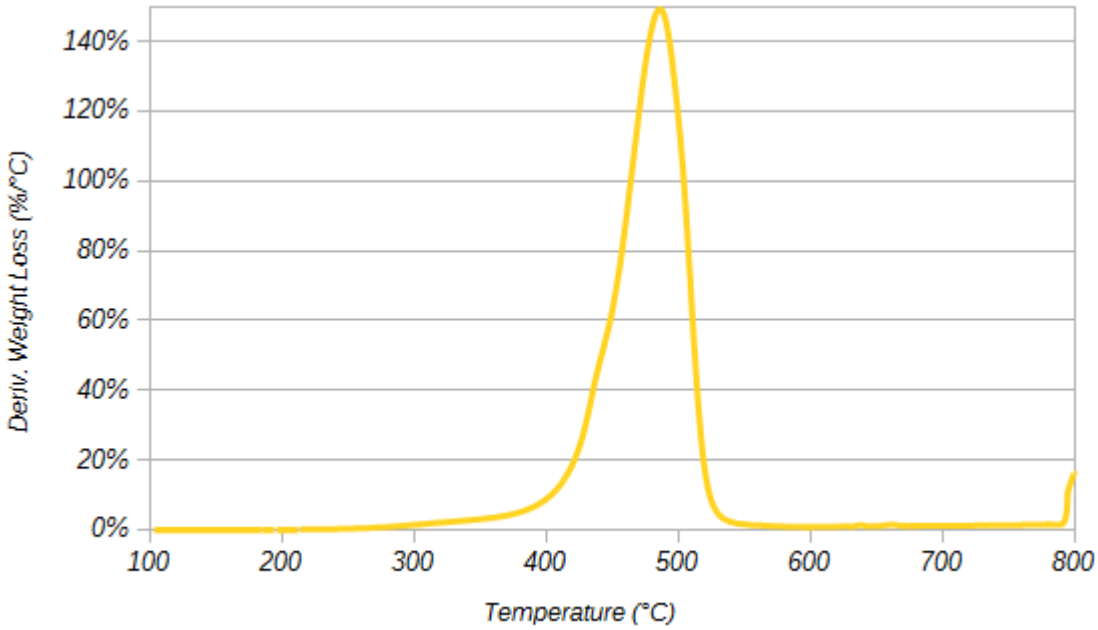

(b) Derivative weight loss.

Figure C.0.3: TGA plots of (a) weight percent and (b) derivative weight loss for **P-3**.

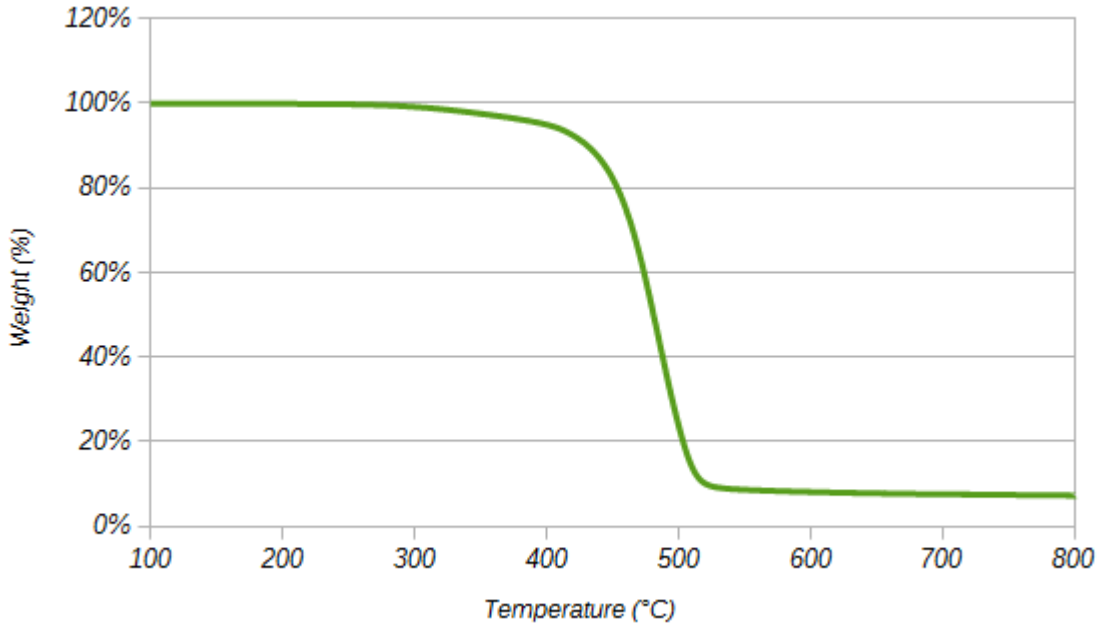

(a) Weight loss.

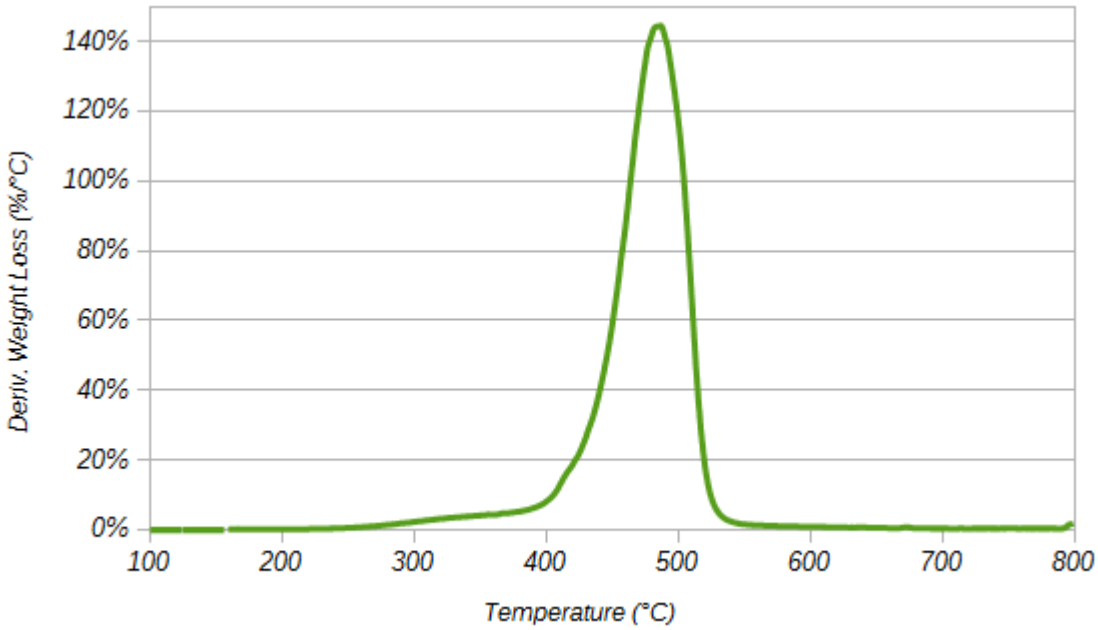

(b) Derivative weight loss.

Figure C.0.4: TGA plots of (a) weight percent and (b) derivative weight loss for **P-4**.

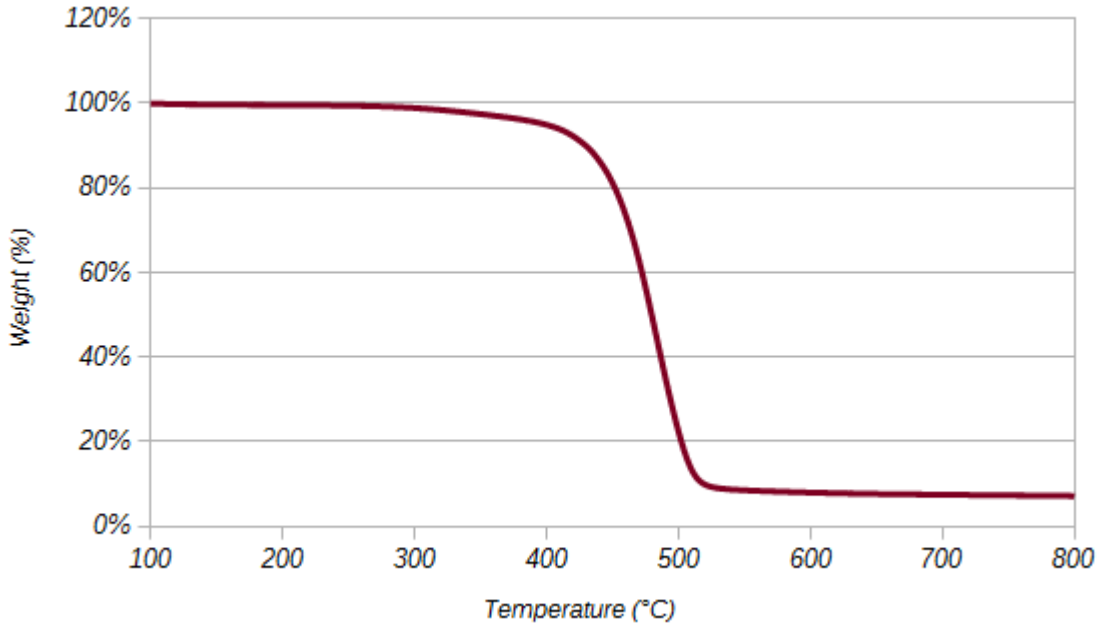

(a) Weight loss.

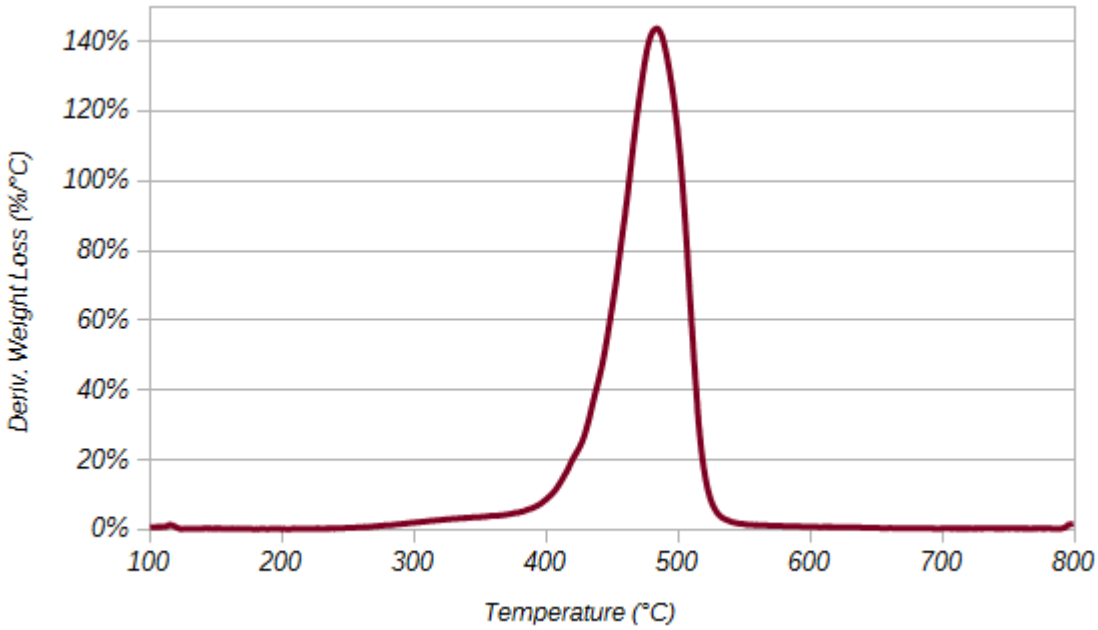

(b) Derivative weight loss.

Figure C.0.5: TGA plots of (a) weight percent and (b) derivative weight loss for **P-5**.

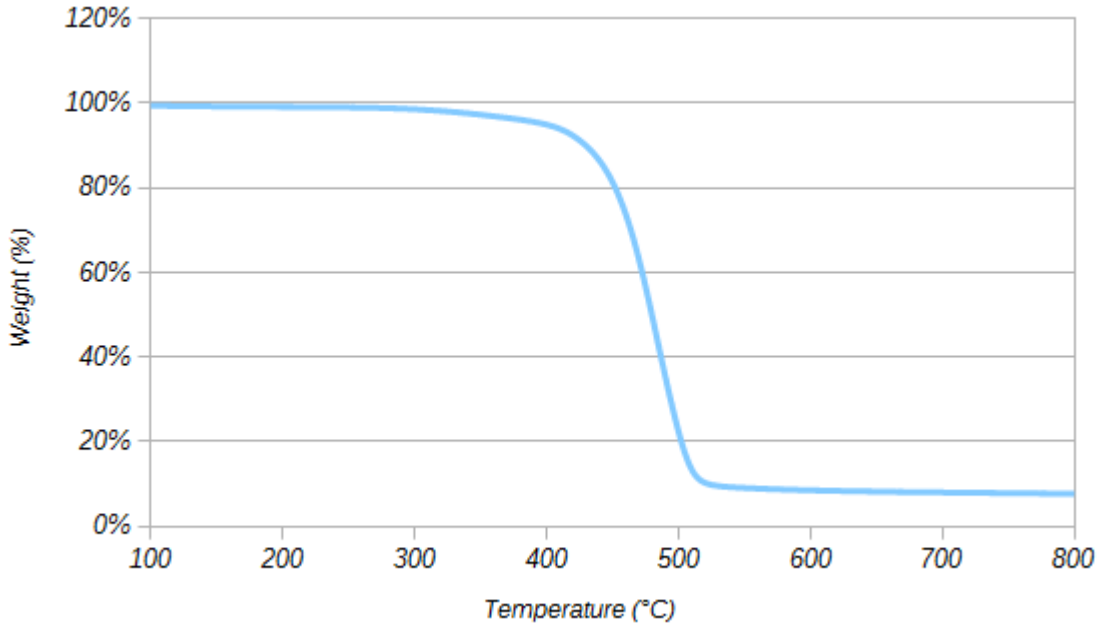

(a) Weight loss.

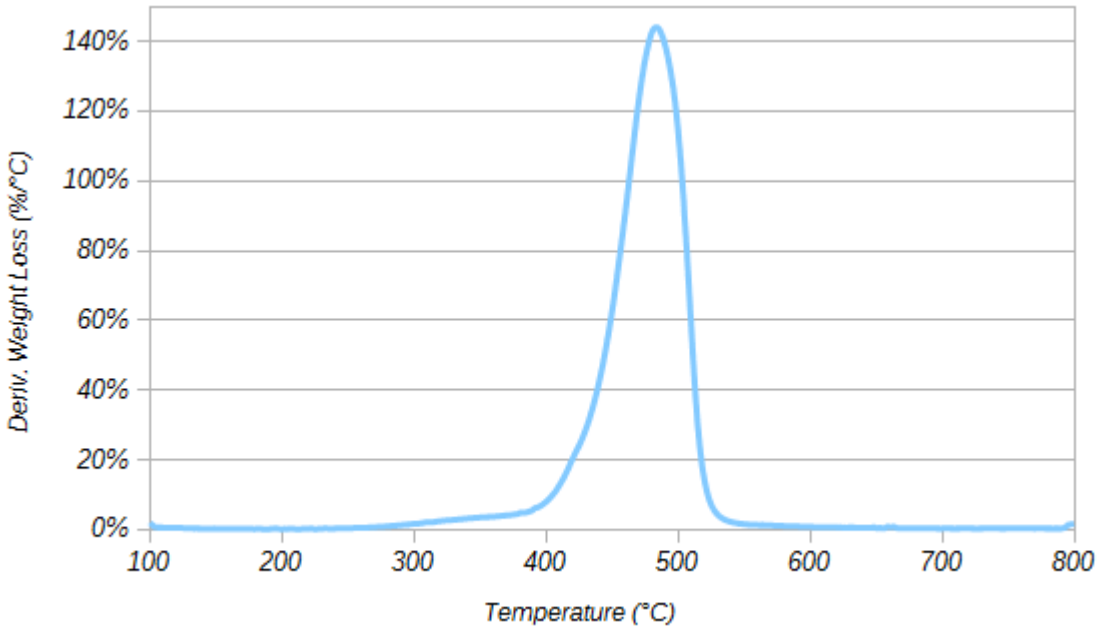

(b) Derivative weight loss.

Figure C.0.6: TGA plots of (a) weight percent and (b) derivative weight loss for **P-6**.

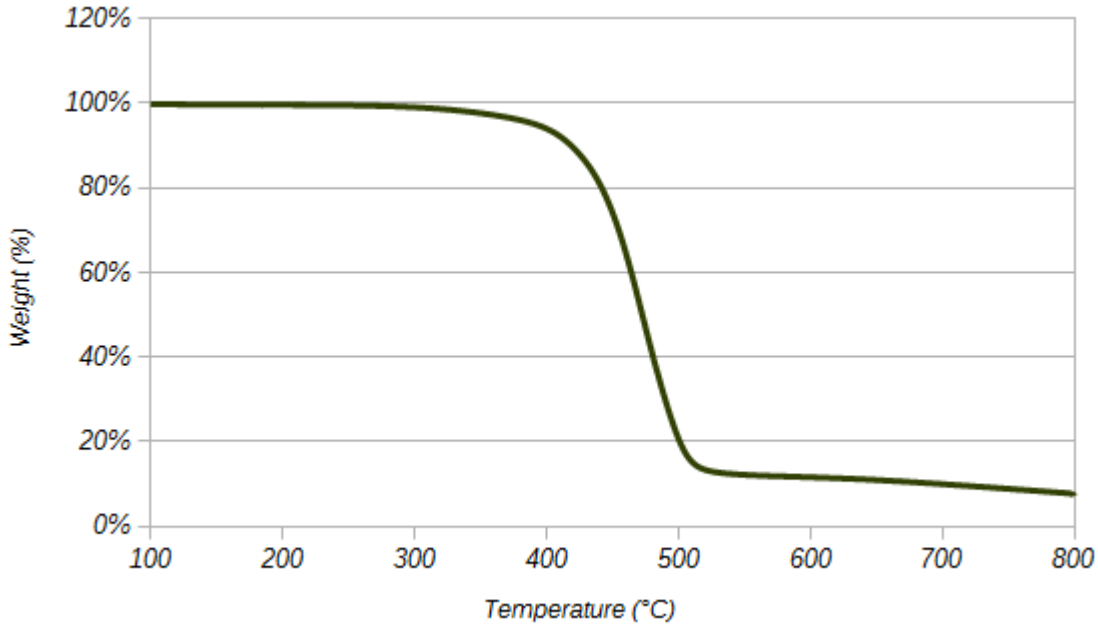

(a) Weight loss.

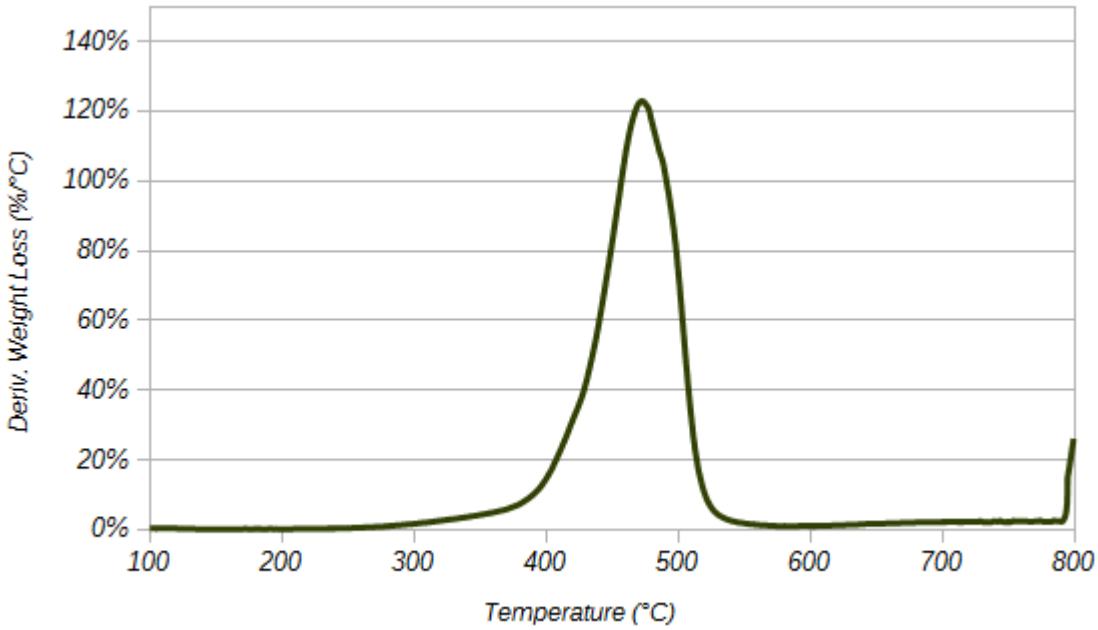

(b) Derivative weight loss.

Figure C.0.7: TGA plots of (a) weight percent and (b) derivative weight loss for **P-7**.

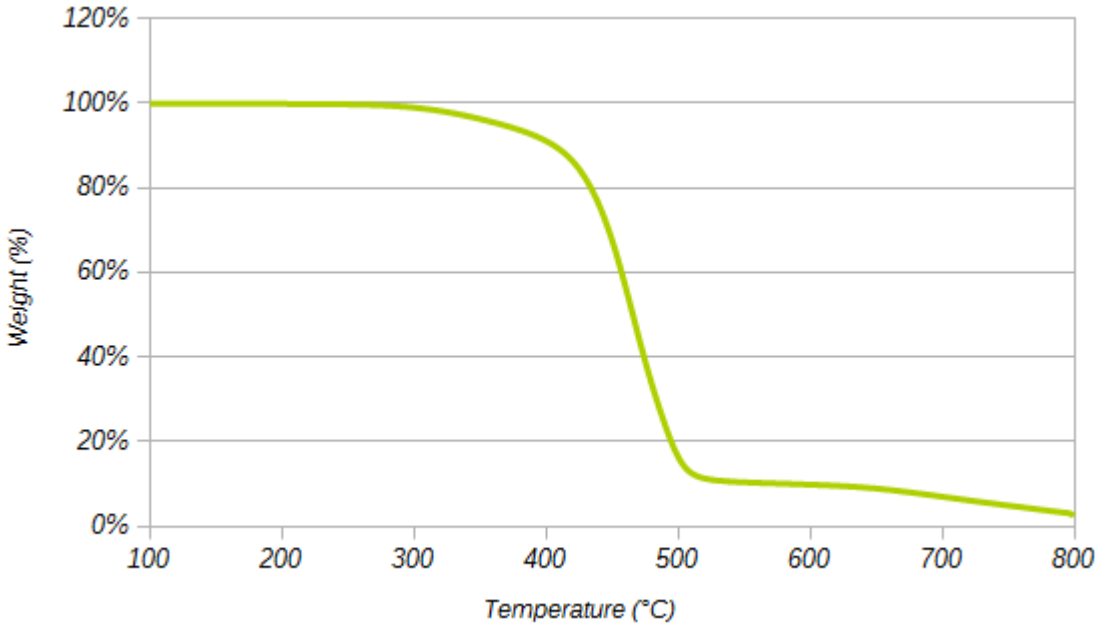

(a) Weight loss.

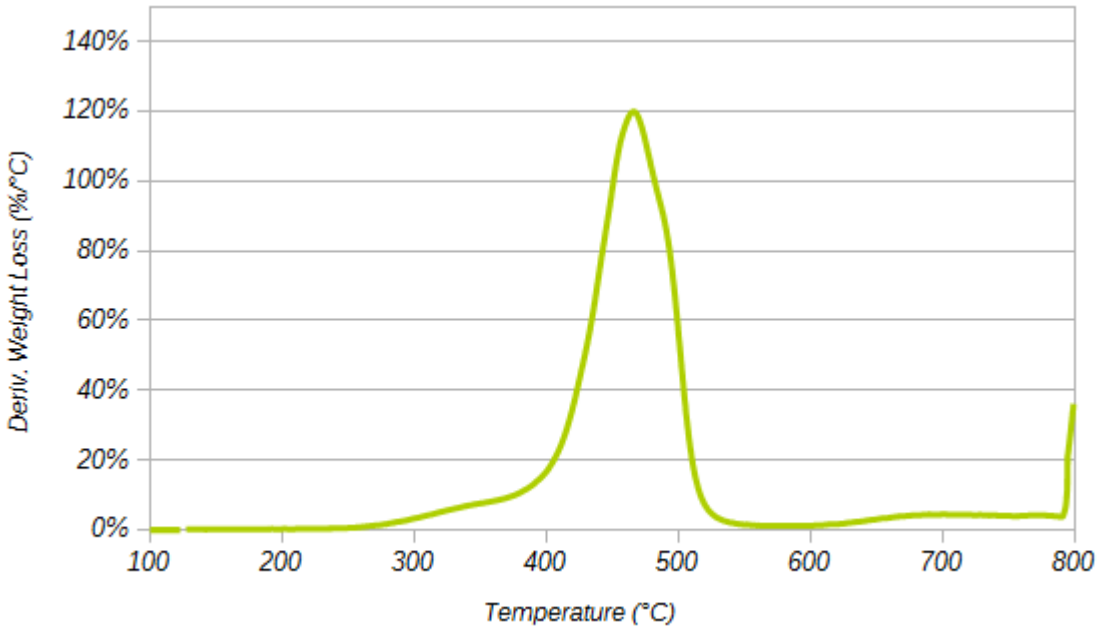

(b) Derivative weight loss.

Figure C.0.8: TGA plots of (a) weight percent and (b) derivative weight loss for **P-8**.

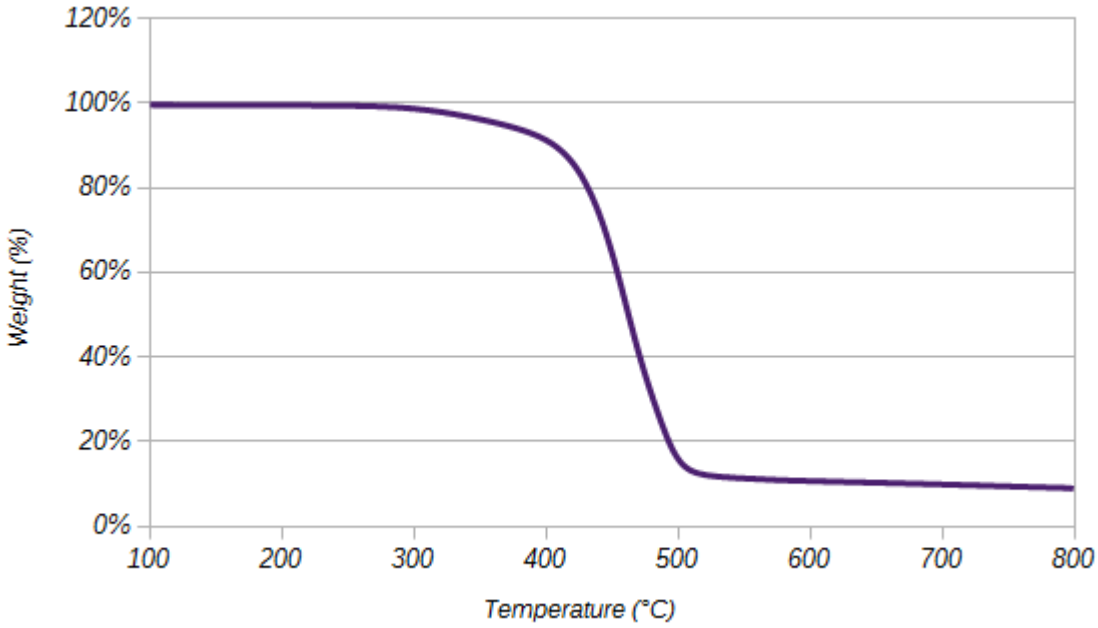

(a) Weight loss.

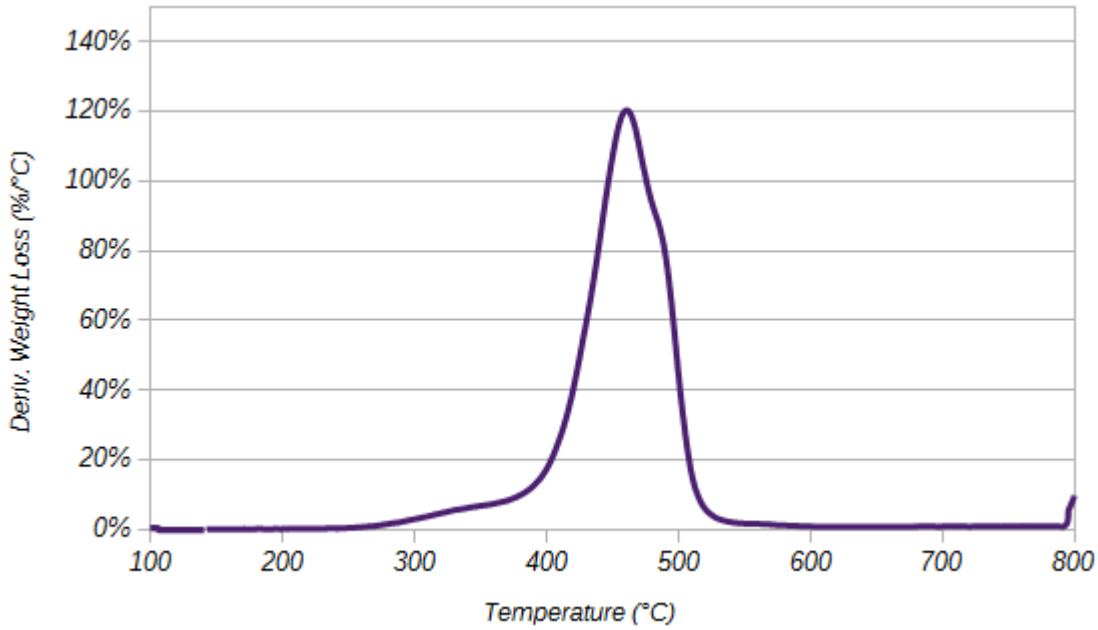

(b) Derivative weight loss.

Figure C.0.9: TGA plots of (a) weight percent and (b) derivative weight loss for **P-9**.

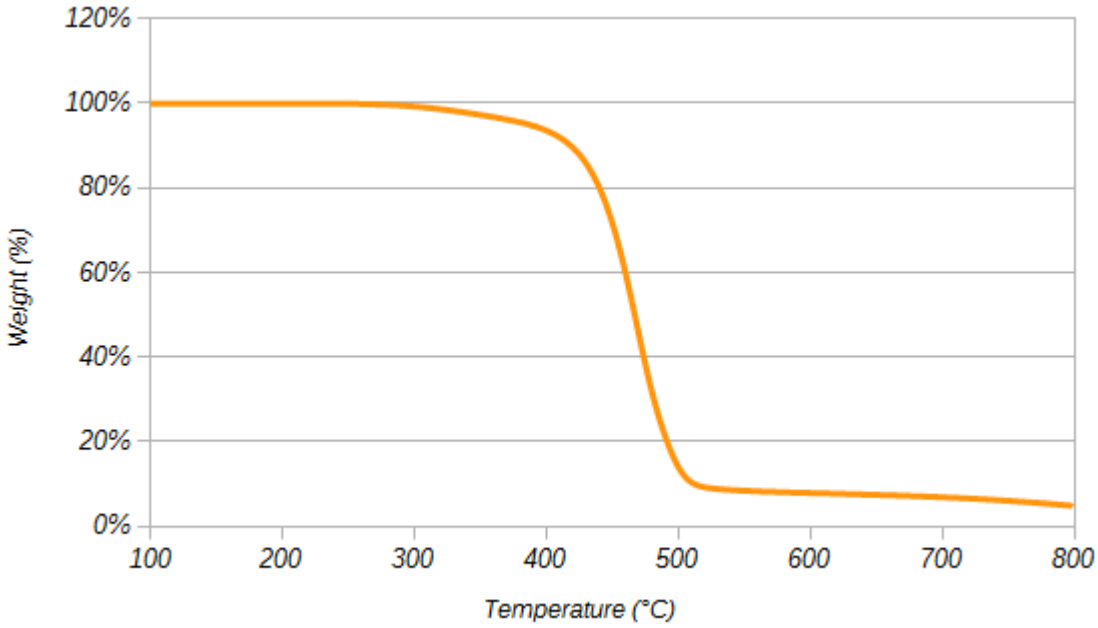

(a) Weight loss.

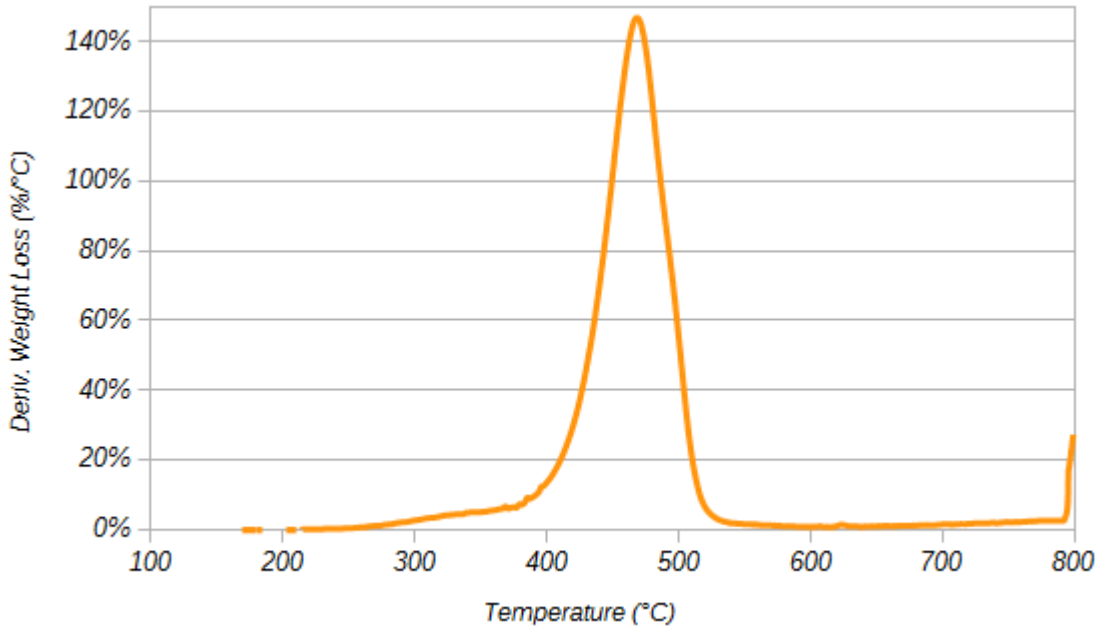

(b) Derivative weight loss.

Figure C.0.10: TGA plots of (a) weight percent and (b) derivative weight loss for **P-10**.

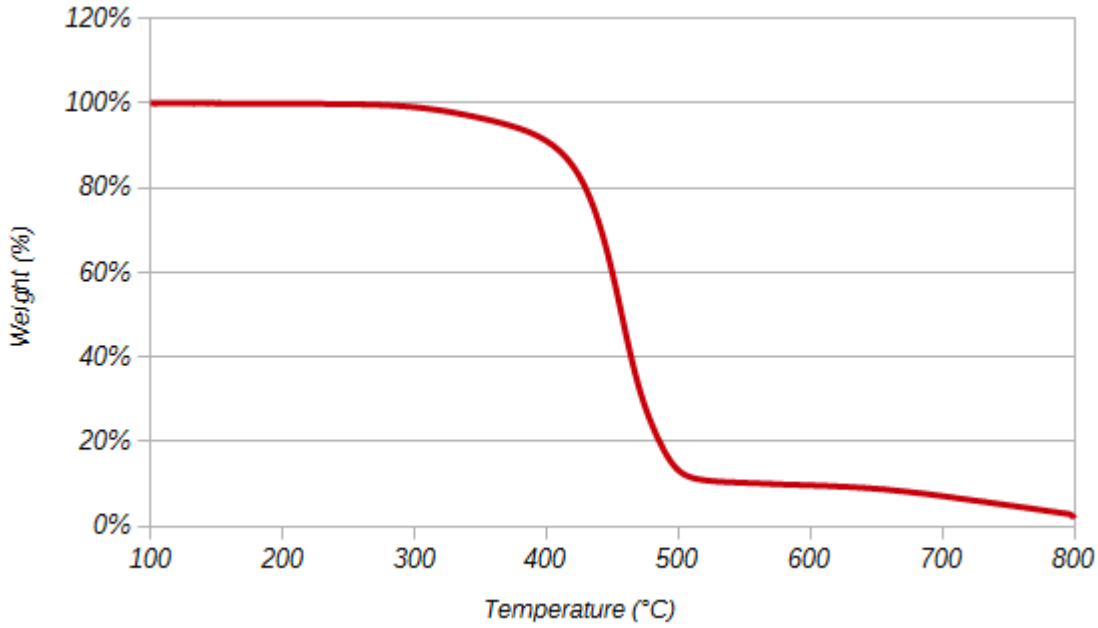

(a) Weight loss.

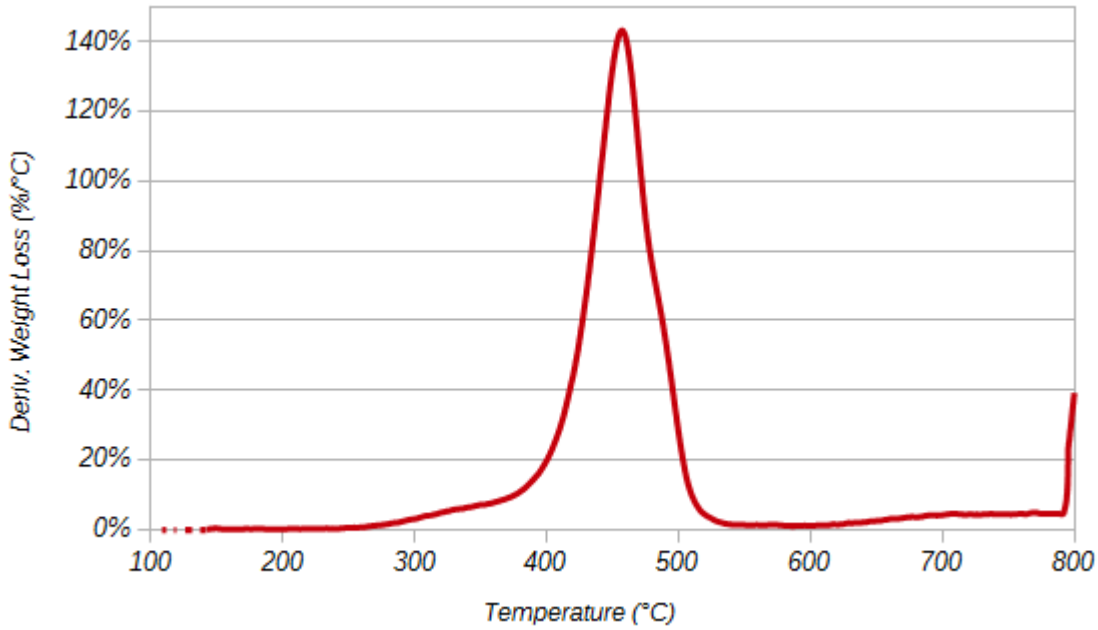

(b) Derivative weight loss.

Figure C.0.11: TGA plots of (a) weight percent and (b) derivative weight loss for **P-11**.

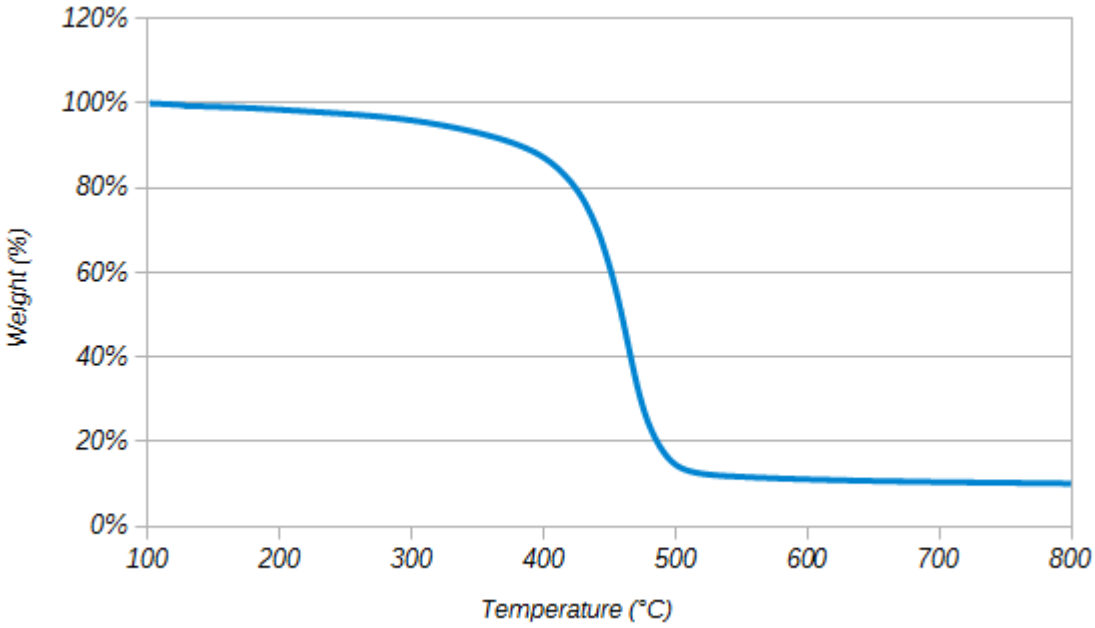

(a) Weight loss.

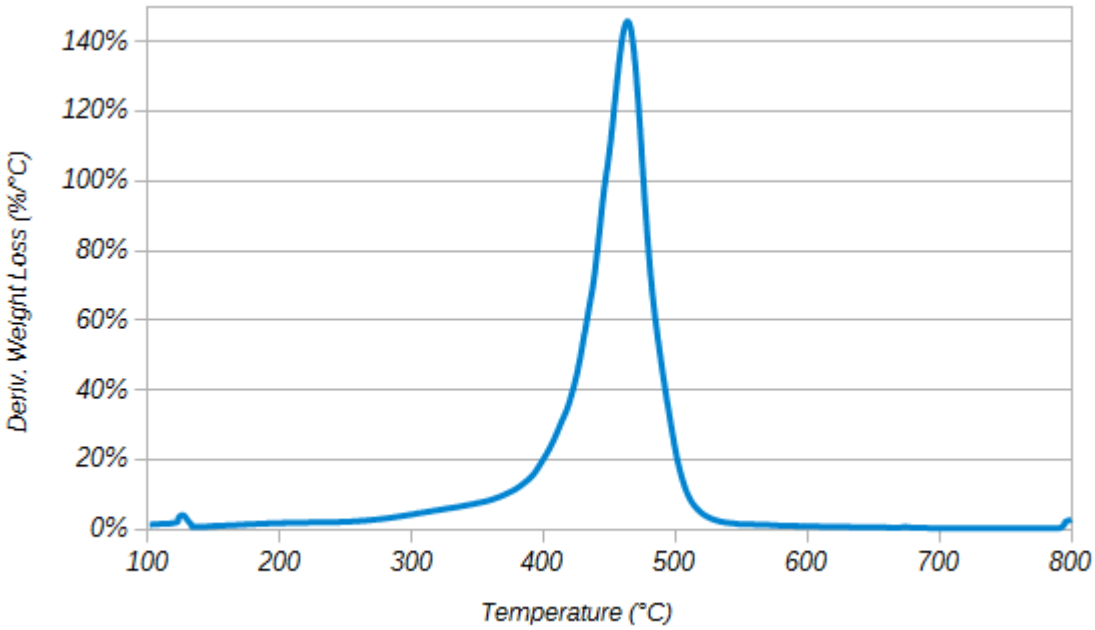

(b) Derivative weight loss.

Figure C.0.12: TGA plots of (a) weight percent and (b) derivative weight loss for **P-12**.

D. Preliminary Series

Early polymerization attempts were performed with a slightly different method while trying to optimize the system as well as other reaction conditions. These early polymers provided insight and some added benefit to the understanding of the optimization of the overall result. From these early studies, several observations became apparent: (a) increasing the temperature increased reaction rate, (b) increasing inert gas flow increased reaction rate, (c) stirring became increasing difficult if not impossible as the reaction approached end, and (d) longer times resulted in more distillate recovered .

Shorter times for Phase I were used in some of the early trials, similar to Nagata.[28] Longer Phase I times were attempted as well to push the reaction forward and maximize the distillate collected. After a period distillate ceased to produce linearly and effectively flat-lined. Longer Phase I would allow the incremental collection of the distillate during this period. The alternative method to drive distillate collection was through heat or flow, as mentioned above. Both of these could have thermally degraded the monomers or increased the likelihood of losses to evaporation or mechanical removal. As such, increasing the time was chosen as the preferred method to optimize Phase I.

Phase II witnessed the increase in toughness of the protopolymer which resulted in damaging of numerous PTFE stirrer paddles before the transition to glass. Additionally, the overhead stirrer struggled to maintain speed, if it was able to rotate at all. Several cases of the early polymerizations involved the polymer melt clinging to

the stir rod and not effectively mixing. At the point the polymer was unable to be stirred, or the stirrer could not function, there was little point in continuing the reaction, so they were terminated. Several cases resulted in both Phases being completed in a single day, but varied widely in times.

To ensure a consistent series, both Phases were set to a defined length of time to ensure there was less error due to misinterpreting the end of distillate formation or the point at which the stirrer cannot function effectively. Each reaction would have the given time window to run to whatever stage of completion as was possible before termination.

With the standard procedure established, the procedure was enacted as described in the main matter of this thesis. Judgments from the results of the catalyst study of the main theory indicated **P-3** to be the ideal choice for the basis of the renewable study, however comparing the data from that method with the data from previous trials, some noticeable outliers were observed. During Phase I the prepolymer formed and was susceptible to degradation due to the high temperature. Since some of the earlier runs were at lower temperatures and shorter times this degradation was reduced. Of the early polymerizations with the shorter Phase I that were able to be characterized via GPC, it was noticed that the overall chromatograms were shifted left and narrower, indicating higher molecular weight and lower distributions. With the observation that a shorter phase I produced higher quality polymers, it was also noted that the trend of increasing T_g for polymers containing renewable aromatic monomer was observed. Essentially, the optimization of the catalyst to drive the reaction further through to completion countermanded the effects of the incorporated renewable monomers.

E. A Note on the Document

Several aspects of this document are worth mentioning. First, regarding the document itself, this thesis was created in LaTeX 2_ε. The significance of this should become apparent once the reader realizes the shear number of cross references scattered throughout this body of work; especially in the PDF with the full benefit of clickable hyperlinks. Second, there are some ill-defined terms found in the literature that may be confusing or have several alternate definitions. Third, due to the large number of acronyms used in the research it is easy to become lost in a jumble of seemingly incoherent letters. There is a glossary and a list of acronyms included in this thesis for help with de-jumbling the mess. Fourth, citations are deceivingly complicated; managing them was only possible through Mendeley and LaTeX 2_ε. Finally, as mentioned in the first point, there are hyperlinks in the PDF that make it far easier to access the information referred to in the citations, as well as in the acronyms and glossary terms.

As for some of the content and background, data analysis was computed using free software as available, including ACD/Labs program suite, KnowItAll®, and TA Universal Analysis. Google Drive and many of the tools offered through Google were used to organize the notes and data, sync files, and crunch some of the 'smaller' numbers. For the sake of uniformity and computation of larger data sets, plots were compiled using LibreOffice Calc.